JEAN-CHARLES BOISSET

THE ORIGIN OF BLOOD STEM CELLS

The origin of blood stem cells

~

Jean-Charles Boisset

ISBN: 978-94-6182-183-6

Printing: Off Page, www.offpage.nl

Printing of this thesis was kindly supported by: J.E. Jurriaanse Stichting, B.D. Bioscience, and the Erasmus University Rotterdam.

Cover represents an intra-aortic hematopoietic cluster attached to the endothelium in an E10 mouse embryo, imaged by scanning elctron microscopy (in collaboration with Mieke Mommaas-Kienhuis and Jos Onderwater, Leiden University Medical Center).

The origin of blood stem cells

Thesis

To obtain the degree of Doctor from the Erasmus University Rotterdam by command of the rector magnificus Prof.dr. H.G. Schmidt and in accordance with the decision of the Doctorate Board

The public defence shall be held on
Thrusday 25 October 2012 at 9:30 hrs

by

Jean-Charles Boisset
born in Montauban, France

Doctoral Committee

Promotor
Prof. Elaine Dzierzak

Co-promotor
Dr. Catherine Robin

Other members
Prof. Frank Grosveld, Dr. Niels Galjart and Dr. Thierry Jaffredo

Table of contents

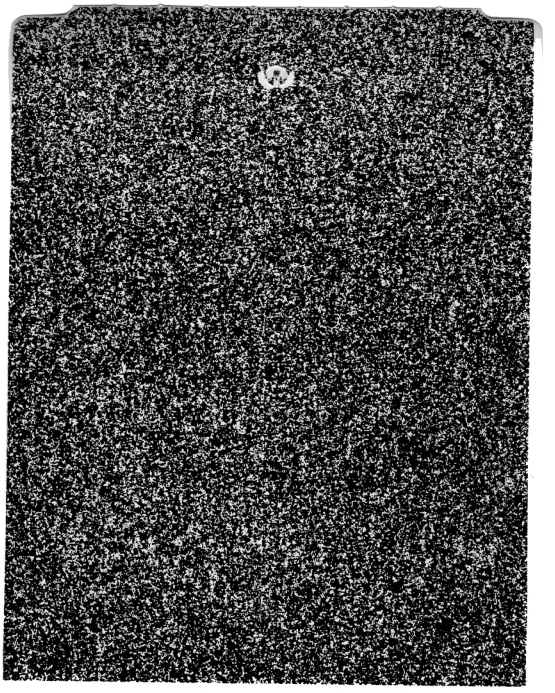

Chapter 1 – Introduction

Part of this chapter was published in Stem Cell Research (2012) 8, 1–13
Review by J-C. Boisset & C. Robin

The concept of hematopoietic stem cells

The development of cell biology research coincides with the advance of microscopes in the 19th century. It was finally possible to directly observe the various blood cell types and to witness their proliferation and differentiation (Mazzarello, 1999). On the basis of his observations, the German pathologist Franz E.C. Neumann (1834–1918) suggested that the site of blood formation was the bone marrow (BM). He also proposed the pioneer theory in which one cell might be at the origin of all blood cell lineages. The Russian scientist Alexander A. Maximow (1874–1928) also developed and introduced the theory of a common cell for the complete blood-building system or hematopoiesis (Maximow, 1909). The concept of Hematopoietic Stem Cells (HSCs), although very controversial at the time, was born and has led to the beginning of stem cell research (Ramalho-Santos and Willenbring, 2007).

Ernest A. McCulloch and James E. Till provided the first experimental proof of the stem cell theory by performing the transplantation of BM cells into irradiated mice (Becker et al., 1963; Till and Ea, 1961). These cells gave rise to erythroid-myeloid multilineage colonies in the spleen of the transplanted animals, the number of colonies being proportional to the number of injected cells. Such experiments demonstrated the multilineage potential of single BM cells (so-called CFU-S, Colony-Forming Unit in the Spleen) (Siminovitch et al., 1963). However, because these cells only have limited self-renewing capabilities, they are not considered to be true stem cells, which according to the definition must be both multipotent and self-renewing. E. Donnall Thomas performed the first successful stem cell transplantation on identical human twins in 1957 (Thomas et al., 1957). This demonstrated formally that intravenous injection of BM cells allows long-term repopulation with the production of new blood cells. The oncologist Georges Mathé also performed transplantations on Yugoslavian nuclear workers whose BMs were damaged by irradiation (Mathé et al., 1959). Later on, he successfully cured a patient with leukemia (pre-treated by irradiation) after allogenic BM transplantation (Mathé et al., 1963). For nearly 50 years, such transplantations have been performed to treat patients with blood-related disorders. Adult HSCs can now be highly enriched with a combination of several surface markers. However, no unique HSC marker has so far been identified, as is the case for most stem cell categories. Thus, a functional test is required to prove that genuine HSCs are present in a cell population. In vivo transplantation is the gold standard experimental procedure to prove retrospectively that the cells are multipotent and self-renewing, by

analyzing at long-term the multilineage HSC progeny in primary and secondary recipients.

Nevertheless, HSCs residing in the BM during the entire life of an individual are not initially generated there. They are produced and expanded during embryonic development before colonizing the BM prior to birth (starting at embryonic day (E)17 in mice) (Christensen et al., 2004). Thus, studying HSC development in the embryo is a powerful tool and a reliable model to decipher the complex characteristics and regulation of HSCs.

The journey of a hematopoietic stem cell: From embryo to adult

HSCs are at the foundation of the entire adult blood system. The multipotency property allows single HSCs to differentiate and proliferate into more committed progenitors and precursors that will then produce all mature cells from the erythroid, myeloid and lymphoid lineages. Given the fast turnover in mature blood cells, only HSCs, which are by definition able to self-renew while keeping their multilineage properties, can sustain blood production during the entire life of an organism.

Embryonic hematopoiesis has been studied in various animal models (e.g. amphibian, avian, rodent), but the focus of this chapter will mainly be on the mouse embryonic model. The first hematopoietic cells produced in the embryo are differentiated cells that are most likely needed at the time for proper oxygenation and protection of the developing embryo. The initial site of hematopoietic production is the yolk sac (YS) (Ferkowicz and Yoder, 2005; Moore and Metcalf, 1970; Palis et al., 1999). Starting at E7.25 of mouse development, this extra-embryonic tissue, composed of both visceral endoderm and mesoderm, transiently produces large nucleated erythrocytes termed erythroblasts (Fig. 1A) (Palis et al., 1999), as well as some macrophages and megakaryocytes (Xu et al., 2001). A layer of endothelial cells will surround these first blood cells to form specialized structures called blood islands (Ferkowicz and Yoder, 2005; Haar and Ackerman, 1971). Some evidence (reviewed later) led to the idea that both cell types (hematopoietic and endothelial) are generated from a common mesodermal precursor known as the hemangioblast (Choi et al., 1998; Eichmann et al., 1997; Ferkowicz and Yoder, 2005; Huber et al., 2004; Shalaby et al., 1995). Mature cells can easily be identified directly under the microscope by specific morphological criteria, or by analysis of surface marker expression using, for example, immunohistochemistry. On the other hand, hematopoietic progenitors are identified retrospectively in a short-term *in vitro* assay (clonogenic assay). In this culture system, different types

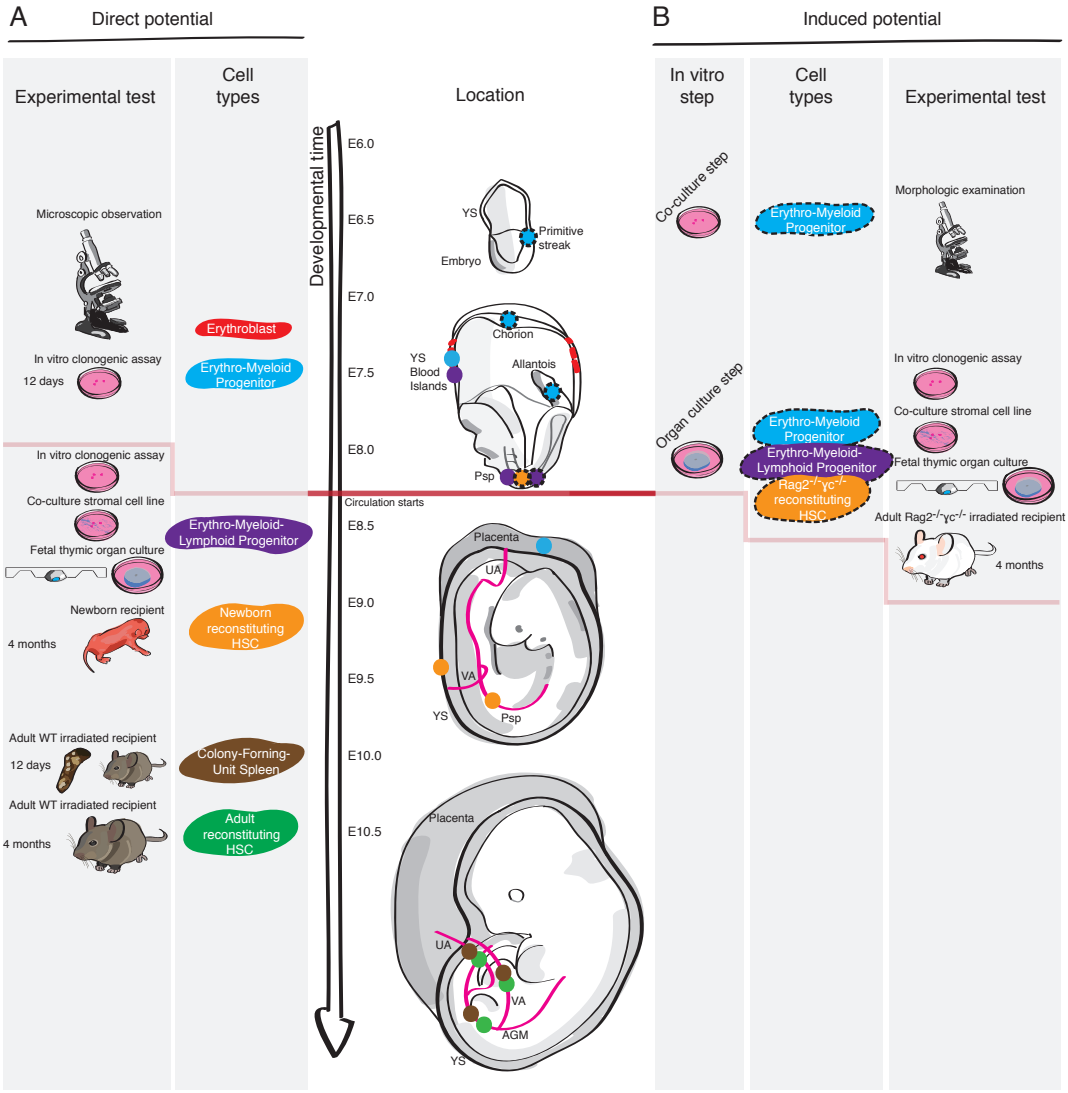

Figure 1
First sites of hematopoietic stem/progenitor cell (HSPC) appearance during mouse embryonic development (from E6.0 to E10.5). Different types of hematopoietic cells have been found in different anatomical sites throughout development. However, it is important to note that the time points and sites of appearance of HSPCs differ according to the experimental approach used. The hematopoietic potential of the embryonic tissues has been tested (A) directly on freshly isolated tissues or (B) after an *in vitro* culture step (needed to reveal a hematopoietic potential undetectable in fresh tissues). The first time points of appearance of the different HSPCs are indicated in the different anatomical sites as well as the *in vitro* and *in vivo* assays used to identify these cells. HSC: hematopoietic stem cells, YS: yolk sac, UA: umbilical artery, VA: vitelline artery, P-Sp: para-aortic splanchnopleura, E: embryonic day post-coitus, WT: wild-type.

of lineage-restricted progenitors (erythroid, granulocytic, macrophagic and/or megakaryocytic) are able to form colonies that are identified and quantified based on specific criteria (e.g. colony cell composition, size, color). By using such assay, it was shown that beginning at E7.5-E8, erythroid-myeloid progenitors start to appear in the YS (Moore and Metcalf, 1970; Palis et al., 1999) and in the chorion and allantois (which later fuse to form the placenta and the umbilical cord) (Alvarez-Silva et al., 2003; Corbel et al., 2007; McGrath et al., 2011; Palis et al., 1999; Zeigler et al., 2006). In addition, it is possible to identify erythroid-myeloid progenitors earlier in E6.75 embryos if the cells are first co-cultured on OP9 stromal cell lines before to be tested in clonogenic assay (Furuta et al., 2006) (Fig. 1B). Slightly later, at E8.5, erythroid–myeloid–lymphoid progenitors are found in the YS and the Para-aortic Splanchnopleura (P-Sp, region formed by the dorsal aorta, omphalomesenteric (or vitelline) artery, gut and splanchnopleura) (Godin et al., 1995). Indeed, B progenitors were identified after co-culture of the different tissues on S-17 stromal cell line, while T progenitors were identified in a fetal thymic organ culture assay (where the cells are placed in contact with fetal thymus lobes in a hanging drop) (Fig. 1A). Culturing of YS and P-Sp before the establishment of circulation showed that while myeloid and lymphoid progenitors were found in the P-Sp, only myeloid progenitors were present in the YS. Because these tissues are tested before circulation it proves that such progenitors are generated de novo in these tissues (at least after culture) (Fig. 1B) (Cumano et al., 1996). However, low lymphoid potential could be obtained from the YS, when YS-YS graft and subsequent embryo culture were performed before the circulation started (Sugiyama et al., 2007). In addition, isolation and culture of YS cells from E9 *ncx1*$^{-/-}$ embryos (which lack a heart beat and thus circulation) on OP9 or OP9-Dl1 stromal cell lines, followed by transplantation into immunodeficient (NOD/*scid*/IL-2R^{null} or NOG) neonates, showed that the YS contain B and T progenitors (Yoshimoto et al., 2011; Yoshimoto et al., 2012). Thus, both P-Sp and YS seem to be endowed with lymphoid potential. Then at E10, CFU-S are detected in the YS and the intra-embryonic Aorta-Gonad-Mesonephros region (AGM, region corresponding to the earlier P-Sp) (Medvinsky et al., 1993) (Fig. 1A).

The first adult-type HSCs are only detected at mid-gestation. HSCs in adult can be highly purified (Osawa et al., 1996; Purton and Scadden, 2007). However, HSCs found in the embryo are more difficult to enrich thus far (Taoudi et al., 2005). Indeed, many markers currently used to isolate adult HSCs do not apply for embryonic HSCs. Moreover, surface marker expression on HSCs varies during development (McKinney-Freeman et al., 2009; Robin et al., 2011) and also between animal strains and species. For example, the SLAM marker CD150, which allows high enrichment of HSCs in the adult BM (Kiel et al., 2005) and fetal liver (Kim et al., 2006), is not a marker of

AGM HSCs (McKinney-Freeman et al., 2009). The lineage antibody panel (Lin) has been designed and used routinely to deplete mature cells from the erythroid, lymphoid and myeloid lineages (Muller-Sieburg et al., 1986), and is notably used in combination with the positive markers c-kit and Sca-1 (LSK) to purify HSCs. Such depletion does not apply to purifying embryonic HSCs. Indeed, Mac-1 (CD11b), a marker classically expressed by macrophages/monocytes in adults, is also expressed by a fraction of AGM HSCs (Sanchez et al., 1996). Moreover, HSCs and endothelial cells share many surface markers, reflecting their close developmental relationship (Garcia-Porrero et al., 1998). Therefore, depletion based on endothelial marker expression cannot be used to enrich in embryonic HSCs. The only reliable method used to identify HSCs is to perform a long-term *in vivo* assay. The multilineage repopulation and self-renewal abilities of the cells are tested after transplantation into primary and secondary adult wild-type irradiated recipients. Using this standard assay, HSCs were first detected in the AGM region starting at E10.5 (Fig. 1A) (Medvinsky and Dzierzak, 1996; Muller et al., 1994). More precisely, HSCs are restricted to the aorta, as shown by the subdissection of the AGM region to separate the aorta from the urogenital ridges before performing transplantation (de Bruijn et al., 2000). HSC activity in the AGM is transient and stops after E12. Interestingly, HSCs are also found at E10.5 in two other major vessels, the vitelline and umbilical arteries (de Bruijn et al., 2000) (Fig. 1A and Fig. 2). Slightly later (E11–11.5), HSCs are also detected in other major highly vascularized hematopoietic sites: the YS, placenta and fetal liver (Gekas et al., 2005; Kumaravelu et al., 2002; Ottersbach and Dzierzak, 2005). Only very few HSCs (~4–11 cells, as calculated by limiting dilution and transplantation into irradiated adult recipients) are present in the complete mouse conceptus at E11. By E12, the number of HSCs multiplies by at least 14 times, mainly in the placenta and fetal liver (Gekas et al., 2005; Kumaravelu et al., 2002) (Fig. 2). The fetal liver becomes the main HSC reservoir at mid-gestation until HSCs start to colonize the spleen at E15 and the BM at E17 (Christensen et al., 2004) (Fig. 2).

The adult HSC niche

HSCs behave differently in the embryo (compared to adult) as they transit through several anatomical sites or niches, and are actively self-renewing (Bowie et al., 2006; Morrison et al., 1995). The embryonic microenvironment that composes the successive niches is still poorly described, but it certainly influences the equilibrium between HSC self-renewal and differentiation. In comparison, HSC niches in adult BM are well described (Levesque and Winkler, 2011). Two types of spatially close niches have been reported so far. In

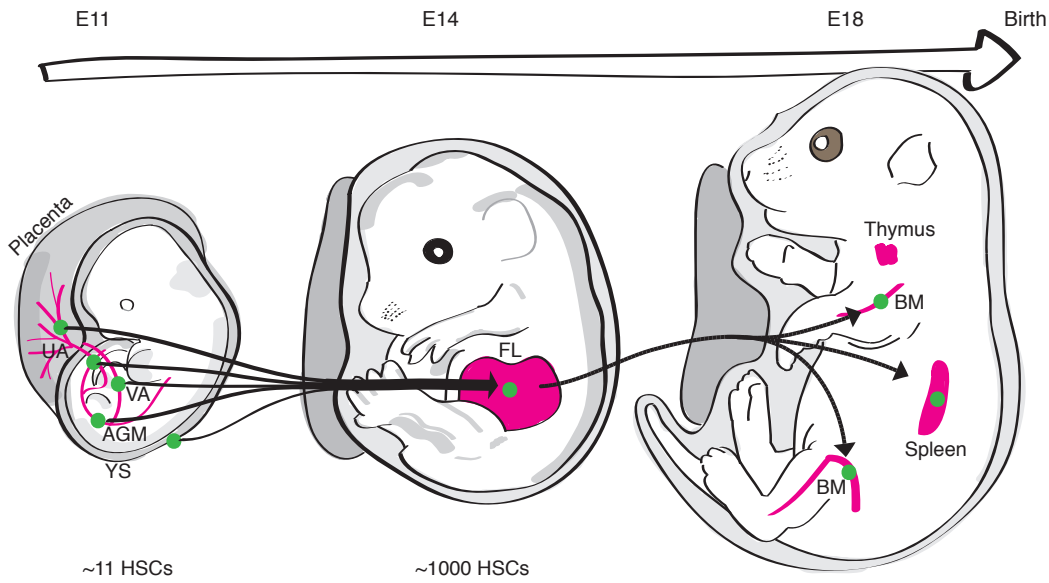

Figure 2
Location and migration of HSCs in the different successive embryonic niches from mid-gestation to birth. The first HSCs are detected at E10.5 in the AGM region and the umbilical and vitelline arteries. At E11, HSCs are also detected in the YS and placenta. Although the number of HSCs transiently amplifies in the placenta until E12, HSCs eventually migrate and massively expand in the FL, which becomes the main HSC reservoir at E14. Finally, HSCs start to migrate to the spleen at E15 and to the BM at E17. They will mainly reside in the BM during the rest of the organism life, while the FL looses its HSC potential. AGM: Aorta-Gonad-Mesonephros, YS: yolk sac, UA: umbilical artery, VA: vitelline artery, FL: Fetal Liver, BM: Bone Marrow, E: embryonic day post-coitus.

the endosteal niche, HSCs are in close contact with the endosteal bone surface where the main supportive cell type, the osteoblastic progenitor population, maintains HSCs in a quiescent/slow-cycling state (Calvi et al., 2003; Lo Celso et al., 2009; Raaijmakers et al., 2010; Zhang et al., 2003). In the second niche, HSCs are associated with the sinusoidal endothelium (Kiel et al., 2005), but it remains to be determined whether it represents a functional niche or only a transition site (Purton and Scadden, 2008). The use of *in vivo* and *ex vivo* time-lapse confocal microscopy imaging has nicely shown that transplanted HSCs preferentially localize close to the endosteal bone surface while committed progenitors localize further away (Lo Celso et al., 2009; Xie et al., 2009). Also, the most potent HSC niches are most likely hypoxic (Winkler et al., 2010a). The well-defined medullar microenvironment of the niches maintains most HSCs in an immature and quiescent/slow-cycling state, the quiescence status being the hallmark of their long-term HSC properties (Cheshier et al., 1999; Wilson et al., 2008). A small pool of HSCs will eventually self-renew only a few times during the lifetime (Wilson et al., 2008). However, perturbation of homeostasis promotes their self-renewal more rapidly (Wilson et al., 2008). Cells composing

the niche produce SDF-1α (CXCL12) and SCF (Stem Cell Factor) that are important for HSC maintenance. These factors are part of a non-exhaustive list of intrinsic and extrinsic factors essential for HSC fate regulation. It includes transcription factors (e.g. SCL, Runx1, Cbfβ, Lmo2, GATA2), cell cycle regulators (e.g. p27kip1, p21cip1/waf1, RB), hematopoietic cytokines (e.g. TPO, Flt3/Flk2 ligand, IL-3), developmental regulators (e.g. BMP- 4, Tie2/ Angiopoietin-1, Wnt/β-catenin, TGF-β/p21, VCAM-1, Hedgehog, Notch/ Jagged 1) (Zon, 2008), and interation molecules (e.g. Flamingo/frizzled 8, N-Caderin (Sugimura et al., 2012)). The cellular composition of the niche is nevertheless more complex and cannot be reduced to osteoblast and endothelial cells. For example, the nervous system is critical to regulate the attraction and dormancy of HSCs in the niche (Katayama et al., 2006; Yamazaki et al., 2011). So-called CXCL12-abundant reticular (CAR) cells, and macrophages help to retain HSCs in the niche (Sugiyama et al., 2006; Winkler et al., 2010b). In addition, some cells of the niche are able to self-renew. Some of these mesenchymal stem cells (which have adipogenic, osteogenic and chondrogenic potentials at the clonal level) express the intermediate filament protein nestin and were described as very important players in maintaining the function of the HSC niche (Mendez-Ferrer et al., 2010). Finally, adipocytes are negative HSC regulators in the BM (Naveiras et al., 2009).

The localization of HSCs at different time-points of development is now very well described. However, this raises the question of how HSCs transit through the different niches (during development or during normal adult physiology (Massberg et al., 2007)) and stay there for a couple of hours or days. As reviewed before, some adhesion molecules have been described to be important to maintain HSCs in the niches. Among all of these, integrins have an essential role in that mechanism.

The role of integrins in HSC migration and interaction with the niches

Integrins are transmembrane glycoproteins that participate in many cellular functions (e.g. survival, proliferation, differentiation, adhesion, migration, gene regulation, cytoskeletal arrangement). Functional integrins are formed by the association of two subunits called α and β. 18 α and 8 β subunits exist in the mouse, which associate to form 24 different integrins (as known so far). On the biochemical level, integrins work as bidirectional signaling molecules, described as inside-out and outside-in signaling between the intra- and extra-cellular spaces (Giancotti and Ruoslahti, 1999; Hynes, 2002; Shattil et al., 1998). Integrins can bind components of the Extra-Cellular Matrix (ECM) (e.g.

vitronectin, fibronectin, laminin, collagen), soluble extra-cellular molecules (e.g. osteopontin, von Willebrand factor) or cell surface membrane proteins (e.g. VCAM-1). Integrin binding to ECM compounds induces outside-in signaling through clustering of integrin heterodimers at focal adhesion sites. This will recruit other cell surface receptors and many proteins that will activate intracellular signaling pathways. Gene-deletion and function-blocking antibodies have helped to decipher the role of most integrins (Bouvard et al., 2001). In the hematopoietic system and especially in HSCs, the main function of integrins appears to be homing and migration (Bonig et al., 2006; Bonig et al., 2009; Grassinger et al., 2009; Lapidot et al., 2005). For example, fetal liver Lin^- $Sca\text{-}1^+$ $c\text{-}kit^+$ (LSK) cells incubated with α4 blocking antibodies were affected in their migration to the BM (Qian et al., 2007). In addition, conditional deletion of α4 in adults led to release of hematopoietic progenitors from the BM to the circulation (Scott et al., 2003), and to incomplete differentiation of progenitors of the different hematopoietic lineages (Arroyo et al., 1996, 1999). Also, β1 integrin is crucial for Hematopoietic Stem/Progenitor Cells (HSPCs) to colonize in the fetal liver and BM (Hirsch et al., 1996; Potocnik et al., 2000). However β1 is not required for the generation of HSPCs in the AGM and YS (Hirsch et al., 1996; Potocnik et al., 2000; Williams et al., 1991). β7 defect impairs lymphocyte migration to lymph nodes and to gut associated Peyer's patches (Kunkel et al., 1998; Wagner et al., 1996; Wagner et al., 1998). In addition to their function in HSPCs, integrins serve as important markers of HSCs (positively or negatively expressed). Adult HSCs for example express β3 (Umemoto et al., 2006), but not α2, which is expressed on short-term reconstituting HSCs (Wagers and Weissman, 2006). In human, α6 (CD49f) is expressed by HSCs but not by multipotent progenitors (Notta et al., 2011). During mouse embryonic development, the very first hematopoietic cells also express several integrin subunits. In fact, αIIb is one of the first markers indicative of hematopoietic commitment in mice (Corbel and Salaun, 2002; Ferkowicz et al., 2003; Mikkola et al., 2003; Mitjavila-Garcia et al., 2002) and avian embryos (Corbel et al., 2005), and is also expressed on human primitive myelo-lymphoid progenitors (Debili et al., 2001). Similarly, α4 is expressed by the first hematopoietic progenitors of the mouse embryo (Ogawa et al., 1999). However, the expression of integrins by the first HSCs is not yet clearly known, but it would certainly help for a better HSC enrichment. In addition, it is currently unknown whether integrins could play a role in the generation and/or maintenance of the first HSCs. These issues will be discussed in chapter 4 and 5.

The study of the various microenvironments and molecules regulating HSCs in the adult was very important to understand what controls their fate. Despite this knowledge, culturing HSCs *ex vivo* without losing their stem cell potential has been limited so far. Expanding transplantable HSCs is of great interest in a

clinical context where the number of HSCs available remains limited. Some of the missing clues might reside in the fetal steps where HSCs are generated and expended during the course of development, without stem cell potential loss. To that end, it is important to understand where HSCs are generated.

Intra- or extra-embryonic origin of hematopoietic stem cells: A long historical uncertainty

It has been impossible so far to ascertain the precise anatomical site(s) of HSC emergence in the mouse conceptus. Indeed, the blood is already circulating (starting at E8.25–8.5) (Ji et al., 2003) between extra- and intra-embryonic tissues at the time when the first HSCs are detected (E10.5) (Fig. 1). Thus, it cannot be ruled out that HSCs emerge in one site and rapidly colonize via the blood circulation another site. HSC ancestors might also be generated in one site and migrate to other anatomical sites where they will produce HSCs.

Lessons can be learned from experiments performed in the different mammalian and non-mammalian animal models available. In particular, the avian embryo is a very powerful model, which has been instructive since the beginning of research on developmental hematopoiesis. The in ovo development of avian embryos allows for easy access and manipulation, such as the injection of cells, the graft of tissues (prior to blood circulation) or the ex vivo development of embryos cultured in vitro (Stern, 2005). In the late 1960s, Moore and Owen hypothesized that all HSCs were of YS origin because the transplantation of 7-day YS cells into 14-day-old irradiated chicken embryos led to the colonization of lymphoid organs (Moore and Owen, 1967). The hypothesis of a YS HSC origin was soon challenged when hetero-specific chimeras, composed of quail embryos grafted on chick YS were generated, mainly before the start of circulation (Dieterlen-Lievre, 1975). Quail cells are easily recognizable from chicken cells by their dark nucleus, as well as by the use of species-specific antibodies. The analysis of chimeras revealed that all blood cells were of quail origin, thus demonstrating their intra-embryonic origin (ruling out their YS origin). Quail cells were indeed able to colonize the spleen and thymus rudiments, the bursa of Fabricius and BM (Dieterlen-Lievre, 1975). The generation of chick–chick homo-specific chimeras (allowing the growth of the animal until adulthood) definitively confirmed the intra-embryonic origin of adult blood, also called definitive hematopoiesis (Lassila et al., 1978). In the amphibian model, grafting strategies are also applicable due to the external development of the embryo. Blood cells in the Xenopus (frog) are found in two different compartments: the ventral blood island (VBI) and the dorsal lateral plate (DLP, mesodermal region containing the dorsal aorta). VBI is the mammalian YS equivalent and

DLP is the AGM equivalent. When VBI is grafted in a host Xenopus, it mostly contributes to the transient production of erythroid cells that last only during the embryonic stage. (Maeno et al., 1985; Turpen et al., 1981). In contrast, the graft of DLP leads to the durable production of both lymphoid and myeloid cells, proving the definitive hematopoietic potential of the DLP region (Maeno et al., 1985; Turpen et al., 1981). Noteworthy, about 20% of adult blood was VBI derived in these graft experiments.

The remarkable grafting experiments performed in avian and amphibian models mainly revealed an intra-embryonic origin of adult HSCs in both species. Such grafting strategies are not feasible so far in mammalian embryos due to their intra-uterine development. However, some trials have been made to determine the site of HSC origin. These experiments use tissues isolated before the onset of circulation to exclude any possible contamination by cells migrating from one site to another via the blood circulation. Pre-circulatory E8 YS cells injected into E8 host YS cavity could provide (1 month after transplantation) CFU-S progenitors able to form spleen colonies when the cells were transplanted into secondary recipients (Ueno and Weissman, 2010; Weissman et al., 1978). Unfortunately, the intra-embryonic counterpart was not tested in that study. In another approach, cultured pre-circulatory YS and P-Sp (E8) were tested for their ability to reconstitute adult irradiated immunodeficient mice ($Rag2^{-/-}\gamma c^{-/-}$ (Colucci et al., 1999)) (Cumano et al., 2001). The tissues were pre-cultured *in toto*, and dissociated before being further cultured on S17 stromal cell line. Because no cells isolated before E10.5 are able to reconstitute adult WT irradiated recipients (the classical test for HSCs), the authors used immunodeficient recipients, alymphoid and devoid of NK cell activity. This would allow easier engraftment of not fully potent HSCs. In this experiment, only the P-Sp region could provide long-term multilineage reconstitution. Cultured YS cells could only provide short-term myeloid reconstitution. Although this experiment suggests that HSCs could have an entirely intra-embryonic origin, one could conclude that the *ex vivo* cultured YS does not provide the appropriate environment for HSC precursors to mature into transplantable HSCs. Finally in another approach, Samokhvalov et al. used a genetic labeling approach to mark, by using a tamoxifen inducible promoter, Runx1 expressing cells during a restricted time period of early embryonic development (E7.5– E8.5) (Samokhvalov et al., 2007). Runx1 is an essential transcription factor for the formation of HSCs (Okuda et al., 1996; Sasaki et al., 1996; Wang et al., 1996), but is also expressed by early hematopoietic cells located in the YS blood islands (Samokhvalov et al., 2007). Assuming that tamoxifen induced labeling is restricted to the aforementioned period of time, they were able to trace the fate of YS Runx1 expressing cells. They found that all blood lineages were labeled in adults (9–12 months old), including the phenotypically defined HSC population (LSK) (Samokhvalov et al., 2007).

More recently, an opposite experiment has been performed by the same group. They restored Runx1 expression in the Runx1^{+} cells of *runx1*$^{-/-}$ embryos at different stages of development (with a Tamoxifen inducible Cre) (Tanaka et al., 2012). They found that HSC formation could only be rescued if Runx1 was re-expressed from E6.5 to E7.5. Here again, because Runx1 expressing cells are located in the YS at this stage, the data emphasize the importance of the YS in the formation of definitive HSCs. However, it is unknown from this study whether Runx1 was expressed in HSC ancestors or in other cell types critical for HSC formation.

Thus, it is worth mentioning that none of these aforementioned studies give a definitive answer concerning the potential origin of HSCs in the mouse conceptus. The issue is not constrained to the YS and the P-Sp since the chorion/allantois and the later placenta have been shown to generate *de novo* progenitors and thus have been hypothesized to also generate HSCs (Rhodes et al., 2008; Zeigler et al., 2006). To add to the complexity, it is possible, as shown in the Xenopus embryo (Turpen et al., 1997) and suggested in mouse (Matsuoka et al., 2001), that both YS and P-Sp have intrinsic HSC potential, but that the *in vivo* microenvironment would define the fate of HSC ancestor cells. Despite uncertainty on the anatomical origin of HSCs, much work has been performed to understand what cell type developmentally precedes HSCs.

Cellular origin of hematopoietic stem cells: The hemogenic endothelium.

The observation of both the temporal and spatial localizations of blood and endothelial cells in the YS blood islands has led to the concept of the hemangioblast, a common precursor for hematopoietic and endothelial cells (Sabin, 1920). The term "hemangioblast" was first proposed by Murray to describe the cells giving rise to endothelium and blood (in blood island) in opposition to "angioblast" who refers only to cells giving rise to the endothelium (Murray, 1932). Since then, genetic and functional evidence has supported this concept. For example, flk-1 deficient embryos lack blood and endothelium (Shalaby et al., 1995). Likewise, *flk-1*$^{-/-}$ Embryonic Stem Cells (ESCs) fail to contribute to blood and endothelial lineages in chimeras, suggesting the existence of Flk1^{+} hemangioblast cells (Shalaby et al., 1997). In chickens, mesodermal cells expressing the Flk1 homologue (VEGFR2) can differentiate clonally either into endothelial or hematopoietic lineages in the presence or absence of VEGF (Eichmann et al., 1997). Also, the blast colony-forming cells (BL-CFC), identified during mouse ESC differentiation, are able to generate cells of both endothelial and hematopoietic lineages (Choi et al., 1998). Such

bipotential precursors, most likely corresponding to the hemangioblast, can be detected in gastrulating mouse embryos (Huber et al., 2004). They arise in the primitive streak before migrating to the YS, where they will differentiate into hematopoietic, endothelial and vascular smooth muscle cells (Huber et al., 2004). In the zebrafish embryo, lineage tracing of single cells showed that hemangioblast cells could give rise to endothelium and hematopoiesis *in vivo* (Vogeli et al., 2006). The hemangioblast usually refers to the bipotential precursor at the origin of early YS hematopoiesis (Huber, 2010). However, a strikingly close connection between endothelial and hematopoietic cells can also be observed later on, in the main arteries (the dorsal aorta and the umbilical and vitelline arteries) (Dantschakoff, 1909; Dieterlen-Lievre et al., 2006; Yokomizo and Dzierzak, 2010). There, hematopoietic cells are often seen grouped together in clusters tightly attached to the endothelial layer of the vessels (Intra-Aortic Hematopoietic Clusters, IAHCs). This close association between endothelium and hematopoietic cells has led to the hypothesis in the early 20th century that specialized endothelial cells, termed hemogenic, would have the ability to give rise to hematopoietic cells (Dantschakoff, 1909; Jordan, 1917). The presence of IAHCs has then been described in many vertebrate species (reviewed in Dieterlen-Lievre et al., 2006). It was also shown by immunostaining on fixed embryo sections that IAHC cells express both hematopoietic and endothelial markers. This again emphasized the close developmental relationship between the two cell lineages (Garcia-Porrero et al., 1998). IAHCs, due to their morphologic

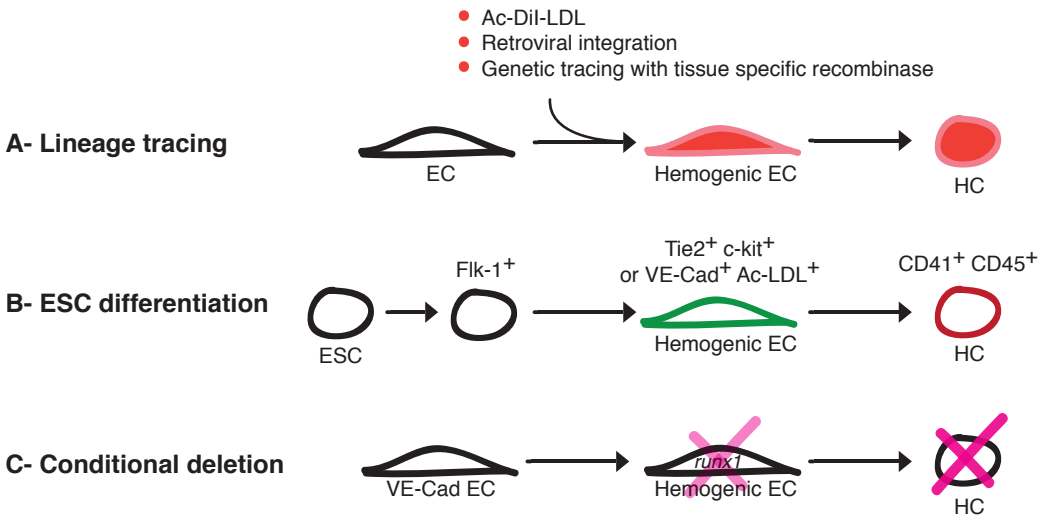

Figure 3
Experimental strategies to demonstrate (A and C) *in vivo* or (B) *in vitro* the endothelial origin of HSCs. EC: endothelial cell, HC: hematopoietic cell, ESC: embryonic stem cell.

and phenotypic characteristics, are presumed to contain HSPCs (Dieterlen-Lievre and Martin, 1981). Indeed, mice deficient for the transcription factor Runx1, that do not have any HSCs or progenitors, are also devoid of IAHCs (embryos die around E11.5) (Cai et al., 2000; North et al., 1999; Okuda et al., 1996; Wang et al., 1996). In addition, HSCs and IAHC cells co-express similar HSC markers (e.g. c-kit) and endothelial markers (e.g. CD31, VE-cadherin, CD34) at E11.5.

The hypothesized endothelial origin of IAHCs (and therefore of the putative HSCs) was first tested in the avian model. Pre-IAHC stage embryos were injected directly into the heart with Ac-DiI-LDL (endothelial cells specifically uptake this molecule), or a retroviral vector expressing LacZ, and were examined 24h later. Newly formed IAHCs were found to express the pan-hematopoietic marker CD45 while still retaining the Ac-DiI-LDL staining, or were expressing the newly integrated *LacZ* gene (Jaffredo et al., 2000; Jaffredo et al., 1998) (Fig.3 A). Such experiments therefore proved the endothelial origin of the newly formed hematopoietic cells. Such specialized endothelial cells capable of generating hematopoietic cells are referred to as hemogenic. The transition from endothelial cells to hematopoietic cells is now well known in the chicken embryo. The ventral endothelial cells become thicker, start to express CD45 and form IAHCs. The endothelial floor is progressively replaced by endothelial cells of somitic origin that are no longer hemogenic (Pouget et al., 2006). Such a process regulates the aortic hematopoietic production both in time and space. In mice, an alternative hypothesis has been proposed based on the observation of a cell population located in patches in the sub-aortic mesenchyme, which expresses hematopoietic markers like GATA3 or AA4.1 (Bertrand et al., 2005; Garcia-Porrero et al., 1998). According to this hypothesis, HSC precursors would migrate through the endothelium (without taking any characteristics of the endothelium) and bud into the lumen of the aorta to form IAHCs. Indeed, cells with HSC characteristics (revealed after re-aggregation with OP9 cells) are present outside of the aorta at E11.5 (Rybtsov et al., 2011).

Thus, various experimental approaches have been undertaken to determine the exact cellular origin of HSCs in different animal models. Constant cell labeling and time-lapse imaging performed during mouse ESC cultures and BL-CFC development have shown that the hemangioblast generates hematopoietic cells through the formation of a hemogenic endothelial intermediate population (Eilken et al., 2009; Lancrin et al., 2009) (Fig.3 B). Such cells are also present in gastrulating embryos. Another strategy was to perform lineage tracing of endothelial cells *in vivo*, by marking specifically these cells at a precise stage of development by using Cre-mediated recombination driven by the VE-Cadherin (mouse) (Oberlin et al., 2010; Zovein et al., 2008) or KDR promoter (zebrafish) (Bertrand et al., 2010a) (two genes expressed by endothelial cells)

(Fig. 3A). In these conditions, a portion of adult hematopoietic cells from all hematopoietic lineages were labeled indicating that their ancestors had undergone an endothelial step at an earlier stage during mouse and zebrafish embryonic development. Noteworthy, VE-Cadherin in the mouse and KDR in the zebrafish are also expressed by IAHC cells. Furthermore, conditional deletion of runx1 in the endothelial compartment completely impaired HSC as well as IAHC formation (Chen et al., 2009) (Fig. 3C). As a whole, these experiments give further and strong support to the endothelial origin of adult HSCs.

Yet, the locations of the specialized hemogenic endothelial cells (which are so far undistinguishable from non-hemogenic endothelial cells) as well as insight into the mechanism leading to hematopoietic cell commitment remain unclear. These fundamental questions are treated in the chapter 2 and 3. It should be noted that a consensus definition for hemogenic endothelium and hemangioblast is lacking, despite the two referring to the close association between blood and endothelium. For instance, the hemangioblast is defined functionally by its ability to differentiate clonally into both hematopoietic and endothelial lineages. However it is not clear whether a hemogenic endothelial cell is also able to do so. If this were true, a hemogenic endothelial cell would then be a hemangioblast with the morphology and phenotype of an endothelial cell (that would be integrated into the vessel endothelial layer). If not, such hemogenic endothelial cells would only give rise to blood cells and not to endothelial cells. Thus, more work needs to be carried out in order to clarify this issue.

The IAHCs ambiguity

The presence of numerous IAHCs in the aorta raises many questions based on several observations. (1) Although IAHCs are generally believed to be HSCs, there is an obvious incongruity between the low number of HSCs (around 2 per aorta and 11 in the total conceptus at E11.5) (Gekas et al., 2005; Kumaravelu et al., 2002; Robin et al., 2006) and the number of IAHC cells (between 350 and 600 c-kit$^+$ IAHC cells at E11.5) (Yokomizo and Dzierzak, 2010). Thus, most IAHC cells are not genuine HSCs (Fig. 4). (2) Another discrepancy concerns the temporal delay between the appearance of IAHCs (> E9.5) and HSCs (> E10.5) (Muller et al., 1994; Yokomizo and Dzierzak, 2010) (Fig. 4). (3) HSCs are restricted to the ventral part of the aorta (Taoudi and Medvinsky, 2007), whereas IAHCs are present all around the aorta of the mouse embryo (Yokomizo and Dzierzak, 2010). It is important to note that all other species tested have IAHCs present strictly in the ventral part of the aorta. In addition,

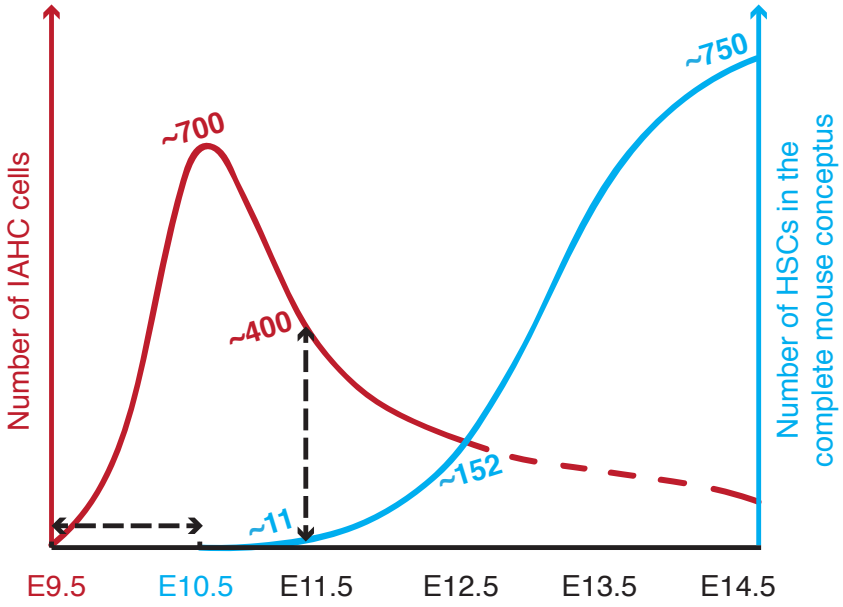

Figure 4
Graph comparing the number of Intra-Aortic Hematopoietic Cells (IAHCs, in red), and the number of HSCs in the complete mouse conceptus during development (in blue). Numbers shown on the graph are averages based on (Gekas et al., 2005; Yokomizo et al., 2011). Dashed black arrows highlight the differences in the numbers and time points of detection between IAHCs and HSCs. E: embryonic day post-coitus.

(4) the total number of HSCs present in the entire embryo increases from 11 to 152 HSCs in 24 h (from E11.5 to E12.5) (Gekas et al., 2005) (Fig. 4). Such an amplification would imply ~4 symmetrical divisions (one division every 6 h), which remain to be observed.

All the discrepancies concerning HSCs and IAHCs have led to the idea that an intermediate cell state might exist between the hemogenic endothelium and the HSC state. These cells are referred to as pre-HSCs, HSC precursors or pre-definitive HSCs (Medvinsky et al., 2011). No cells isolated from early embryonic stages (< E10.5) are able to reconstitute a wild-type adult irradiated recipient, the classical assay to identify HSCs. The first evidence of pre-HSCs came from experiments showing that YS cells or circulating blood cells from E9 mouse embryos could long-term reconstitute different W (c-kit) mutants when injected *in utero* into E11–E15 fetuses (Toles et al., 1989). Some of the pregnant dams even showed long-term chimerism. These cells have not yet been shown to reconstitute an adult irradiated recipient and thus, by definition, are not classically defined as HSCs. Nevertheless, they were capable of self-renewal (multilineage reconstitution was unfortunately not tested in these experiments) (Toles et al., 1989). It was also shown that E9 YS and P-Sp cells can reconstitute (long-term and multilineage) busulfan treated newborn recipients or unconditioned W^{41}/W^{41} neonatal mice (Peeters et al., 2005; Yoder

and Hiatt, 1997; Yoder et al., 1997a; Yoder et al., 1997b) (Fig. 1). The donor cells from the primary transplanted recipient could also reconstitute secondary adult recipients (Yoder and Hiatt, 1997). Thus, cells with HSC characteristics (pre-HSCs) exist before genuine adult-type HSCs. It has been suggested that pre-HSCs are unable to engraft an adult recipient because lack the ability to locate properly in an adult microenvironment (Yoder et al., 1997b). For example, they might not express the required homing molecules or chemokine/growth factor receptors. In addition, MHC class I molecules are hardly expressed by embryonic cells isolated before E10.5, thus becoming potential targets for the host adult NK cells (Cumano et al., 2001; Jaffe et al., 1990;Kieusseian et al., 2012). Therefore neonates, in which NK activity is absent before 3 weeks of age (Dussault and Miller, 1995), as well as adult *rag2*$^{-/-}\gamma c^{-/-}$ recipients, also devoid of NK activity (Colucci et al., 1999) are more permissive for the engraftment of embryonic cells (pre-HSCs).

An attempt was made to establish the link between pre-HSCs and HSCs. *Ex vivo* culture of dissociated/reaggregated E11.5 AGMs have been used as a tool to study the dynamics of HSC production (Taoudi et al., 2008). After 96h of culture, a 150-fold HSC expansion was observed in the reaggregates. Because this happened mostly in the last 24 h of culture, and HSCs were mainly found in the slow-cycling population, such cell expansion would be better explained by the maturation of pre-HSCs into HSCs, rather than cell division of a small pool of HSCs. Pre-HSCs appear to be restricted to the VE-Cadherin^{+} CD45^{-} subpopulation at E10.5, which mature into a VE-Cadherin^{+} CD45^{+} subpopulation at E11.5 (Rybtsov et al., 2011; Taoudi et al., 2008). Given that IAHCs also express VE-Cadherin and differentially express CD45 (Mizuochi et al., 2012; Yokomizo and Dzierzak, 2010), it seems plausible that IAHCs contain pre-HSCs. However, it must be remembered that the culture of the AGM region as explants performed at early E10 do not provide any HSCs capable of adult reconstitution (but do after E10.5) (Medvinsky and Dzierzak, 1996), although the aorta contains many IAHCs (Yokomizo and Dzierzak, 2010) and cells capable of newborn reconstitution during these early stages (Yoder et al., 1997a; Yoder et al., 1997b). Thus, new approaches are required in order to determine the intermediate steps needed for hemogenic endothelial cells to generate fully potent HSCs. This issue will be treated in the chapter 6 of this thesis.

The environment influences HSC formation

An interesting remaining question is whether hemogenic endothelial cells are already committed to producing blood or whether any endothelial cell is capable

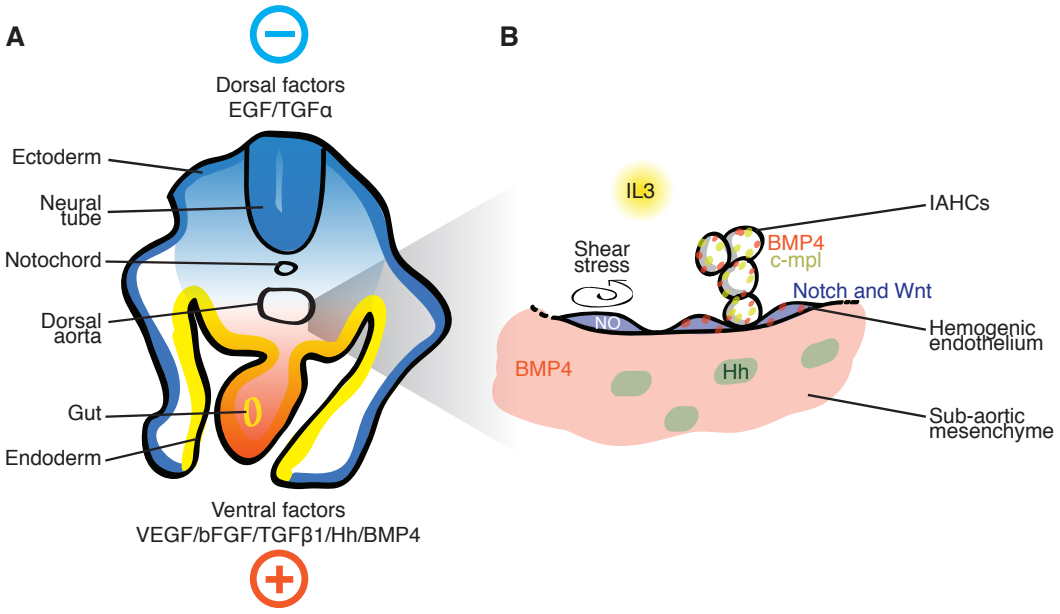

Figure 5
Environmental factors driving the generation and maintenance of the first HSCs in the aorta of the vertebrate embryo. (A) Embryo transversal section, and (B) enlargement of the aortic floor region. The factors presented here were determined for the zebrafish, avian and mouse embryo. All molecules are secreted factors, at the exception of c-mpl, the receptor for TPO. NO: Nitric oxide, Hh: Hedgehog.

of doing so depending on the influence of a singular environment. It is of interest to note that hemogenic endothelial cells found in different animal models are ventrally polarized. Strikingly, in the mouse IAHCs are present in the roof part of the aorta, albeit in fewer number, which suggest that hemogenic endothelial cells are not as strictly polarized as in other species. However, transplantable HSCs reside in the sub-dissected ventral part of the aorta while both dorsal and ventral parts contain hematopoietic progenitors (Taoudi and Medvinsky, 2007). Although there is a clear polarized location of HSCs in the aorta, the mechanisms behind it are unclear, but would give profound insight into how HSCs are generated. In the avian model, the embryonic aorta is formed by endothelial cells of mixed origins. The roof and sides of the aorta are formed by endothelial precursors originating from somitic mesoderm (Pardanaud et al., 1996). On the other hand, the floor of the aorta, capable of hematopoietic production, is formed by precursors migrating from the splanchnopleural mesoderm (Pardanaud et al., 1996). Since no clonal experiments were done, it is difficult to conclude on the precise nature of these precursors. They could be hemangioblasts (that would form the mature endothelium and hemogenic endothelium) or already be committed to hemogenic endothelial cell precursors (that would only integrate with the ventral aortic endothelium to generate hematopoietic cells).

Following the establishment of the aortic endothelium, the importance of environmental cues in the fate of specialized endothelial cells was highlighted. Quail somatopleural mesoderm placed in contact with endoderm tissues could thereafter integrate into the floor of the dorsal aorta (although initially lacking such potential) and form IAHCs. On the other hand, splanchnopleural mesoderm placed in contact with ectoderm tissues had a lower potential to integrate into the floor of the aorta (Pardanaud and Dieterlen-Lievre, 1999). These experiments suggest that the different types of mesoderm contain cells with hemogenic endothelial potential, but that only the splanchnopleural mesoderm instructs these cells to ultimately become hemogenic. In the mouse model, the aorta dissected along with ventral endoderm tissues (including the gut) provided a greater repopulation in irradiated adult recipients when compared to the aorta dissected along with dorsal ectoderm tissues (including the neural tube) (Peeters et al., 2009). Such results suggest that polarized factors determine hematopoietic fate. In this case, the next question is to determine which factors are implicated. In chicken embryos, growth factors such as VEGF, bFGF or TGFβ1 led to similar effects on quail somatopleural mesoderm, as with exposure to endoderm tissues (Pardanaud and Dieterlen-Lievre, 1999) (Fig. 5). On the other hand, growth factors like EGF and TGFα could mimic the effect of contact between splanchnopleural mesoderm and ectoderm (Pardanaud and Dieterlen-Lievre, 1999) (Fig. 5). In mice, the culture of AGM as explant in presence of hedgehog proteins during 3 days enhances the hematopoietic activity in the AGM (similarly to the explant culture of AGM plus gut) (Peeters et al., 2009). However, the reverse situation was observed when AGM dissected with endoderm (gut) tissue was incubated with blocking antibody targeting hedgehogs (similar to the explant culture of AGM plus dorsal tissue), at least in the early stage of HSC emergence (E10.5) (Peeters et al., 2009). Likewise, in zebrafish embryos, hedgehog seems to affect the stage before HSC emergence, when the dorsal aorta is forming, which eventually affects definitive hematopoietic specification (Gering and Patient, 2005; Wilkinson et al., 2009). Noteworthy, in the mouse, deletion of sonic hedgehog, desert hedgehog or indian hedgehog do not lead to full embryonic lethality, since some embryos develop until birth (Bitgood et al., 1996; Byrd et al., 2002; Chiang et al., 1996). On the other hand, the deletion of smoothened (a component of the hedgehog signalling pathway) leads to early embryonic lethality (<E9.5) (Byrd et al., 2002). So it remains to be determined whether Hedgehog signalling is critical in the mouse embryo for the development of HSCs. Bone Morphogenetic Protein (BMP) 4 is another inducer of the hematopoietic fate. Bone Morphogenetic Protein (BMP) 4 is another inducer of the hematopoietic fate. Again in zebrafish, it was shown that BMP4 is required for HSC emergence, while not affecting the arterial specification, suggesting that BMP4 has a later effect on HSC specification in comparison to Hedgehog. In mice, a mild increase in HSC activity was observed

after the addition of BMP4 to AGM explant cultures whereas the addition of Gremlin, a BMP antagonist, greatly decreased it. Notably, BMP4 expression was predominant in the ventral part of the aorta in different cell populations, including the surrounding mesenchyme and cells of the IAHCs (Durand et al., 2007). VEGF is an important factor for blood vessel formation, including the dorsal aorta, which is abnormally developed if a single VEGF allele is missing (Carmeliet et al., 1996; Ferrara et al., 1996). In the xenopus embryo, Tel1-driven VEGFA expression specifies the HSC program at the hemangioblast stage (Ciau-Uitz et al., 2010). The absence of Tel1-VEGFA signalling led to dorsal aorta formation but no definitive hematopoiesis was observed. In contrast in the chicken embryo, VEGF could specify single VEGFR2^{+} cells (also called KDR or Flk-1) to the endothelial lineage, whereas the absence of VEGF led to hematopoietic production (Eichmann et al., 1997). Correspondingly, the BMP antagonist Gremlin can also act as a VEGFR2 agonist, thus probably reinforcing the inhibition of the HSC program in the chicken (Mitola et al., 2010; Stabile et al., 2007). IL-3, a well-known adult hematopoietic interleukin, is also a potent survival and amplification factor of mouse embryonic HSCs (Robin and Durand, 2010; Robin et al., 2006). It seems to be expressed by cells present in the circulation and could thus be a systemic factor. Another essential player for definitive hematopoiesis formation is Notch. However, it seems to be required mainly when HSCs emerge from the endothelium, either in zebrafish (Bertrand et al., 2010b; Gering and Patient, 2005; Lee et al., 2009) or mice (Kumano et al., 2003; Robert-Moreno et al., 2005; Robert-Moreno et al., 2008). Furthermore, the notch ligands regulator mind bomb-1 was shown to be crucial for intra-embryonic hematopoietic progenitor formation, mainly when expressed in the non-endothelial compartment. This suggests a paracrine action of the notch ligands on the endothelial cells (Yoon et al., 2008). c-Mpl, the receptor for thrombopoeitin has been shown to be expressed by IAHC in mice, and its absence led to diminished HSC activity in E11 AGMs (Petit-Cocault et al., 2007). Also, the Wnt/β-Catenin pathway was reported to be crucial for the emergence of HSCs (Ruiz-Herguido et al., 2012). Indeed, the deletion of β-Catenin in the embryonic endothelial compartment impaired the formation of HSCs, but not if deleted in the vav1 compartment (expressed by HSCs only later on during development from E12.5). Finally, blood flow induced sheer stress and the subsequent activation of the nitric oxide (NO) pathway have been shown to stimulate the formation of hematopoietic cells in the aorta of zebrafish and mouse embryos (Adamo et al., 2009; North et al., 2009). Although it is clear that Hedgehogs, BMP4, IL-3, Notch, TPO, Wnt and NO pathways act to induce definitive hematopoietic formation, it remains to be shown which cell types produce and/or respond to these signals: mesodermic precursor, hemogenic endothelial cells and/or IAHC cells (Fig. 5).

Aim of this thesis

The aim of this thesis is to understand the very early steps of HSCs formation. The question is nevertheless very wide and we thus attempted to comprehend specific but central issues in the field. Chapter 2 and 3 of this thesis will focus on how endothelial cells are able to form hematopoietic stem/progenitor cells in the aorta of the mouse embryo. To that end, we developed a technique to directly visualize the mouse embryonic aorta in a near *in vivo* context. This method will be extensively described in chapter 2. In chapter 3, I will describe how this technique was used to image the aortic endothelium, and to visualize in time-lapse the transition from endothelial cells to hematopoietic stem/progenitor cells. Chapter 4 and 5 will describe the expression pattern of the integrins αIIbβ3 and αvβ3 on HSCs during development, and also importantly the role of αIIb in the maintenance of the first HSCs in the AGM. Finally in chapter 6, I will develop a hypothesis on how the endothelium generates HSCs, not directly, but through multiple steps where pre-HSCs located in the IAHCs progressively mature into HSCs.

References

Adamo, L., Naveiras, O., Wenzel, P.L., McKinney-Freeman, S., Mack, P.J., Gracia-Sancho, J., Suchy-Dicey, A., Yoshimoto, M., Lensch, M.W., Yoder, M.C., et al. (2009). Biomechanical forces promote embryonic haematopoiesis. Nature 459, 1131-1135.

Alvarez-Silva, M., Belo-Diabangouaya, P., Salaun, J., and Dieterlen-Lievre, F. (2003). Mouse placenta is a major hematopoietic organ. Development 130, 5437-5444.

Arroyo, A.G., Yang, J.T., Rayburn, H., and Hynes, R.O. (1996). Differential requirements for alpha4 integrins during fetal and adult hematopoiesis. Cell 85, 997-1008.

Arroyo, A.G., Yang, J.T., Rayburn, H., and Hynes, R.O. (1999). Alpha4 integrins regulate the proliferation/differentiation balance of multilineage hematopoietic progenitors in vivo. Immunity 11, 555-566.

Becker, A.J., Mc, C.E., and Till, J.E. (1963). Cytological demonstration of the clonal nature of spleen colonies derived from transplanted mouse marrow cells. Nature 197, 452-454.

Bertrand, J.Y., Chi, N.C., Santoso, B., Teng, S., Stainier, D.Y., and Traver, D. (2010a). Haematopoietic stem cells derive directly from aortic endothelium during development. Nature 464, 108-111.

Bertrand, J.Y., Cisson, J.L., Stachura, D.L., and Traver, D. (2010b). Notch signaling distinguishes 2 waves of definitive hematopoiesis in the zebrafish embryo. Blood 115, 2777-2783.

Bertrand, J.Y., Giroux, S., Golub, R., Klaine, M., Jalil, A., Boucontet, L., Godin, I., and Cumano, A. (2005). Characterization of purified intraembryonic hematopoietic stem cells as a tool to define their site of origin. Proc Natl Acad Sci U S A 102, 134-139.

Bitgood, M.J., Shen, L., and McMahon, A.P. (1996). Sertoli cell signaling by Desert hedgehog regulates the male germline. Curr Biol 6, 298-304.

Bonig, H., Priestley, G.V., and Papayannopoulou, T. (2006). Hierarchy of molecular-pathway usage in bone marrow homing and its shift by cytokines. Blood 107, 79-86.

Bonig, H., Watts, K.L., Chang, K.H., Kiem, H.P., and Papayannopoulou, T. (2009). Concurrent blockade of alpha4-integrin and CXCR4 in hematopoietic stem/progenitor cell mobilization. Stem Cells 27, 836-837.

Bouvard, D., Brakebusch, C., Gustafsson, E., Aszodi, A., Bengtsson, T., Berna, A., and Fassler, R. (2001). Functional consequences of integrin gene mutations in mice. Circ Res 89, 211-223.

Bowie, M.B., McKnight, K.D., Kent, D.G., McCaffrey, L., Hoodless, P.A., and Eaves, C.J. (2006). Hematopoietic stem cells proliferate until after birth and show a reversible phase-specific engraftment defect. J Clin Invest 116, 2808-2816.

Byrd, N., Becker, S., Maye, P., Narasimhaiah, R., St-Jacques, B., Zhang, X., McMahon, J., McMahon, A., and

Grabel, L. (2002). Hedgehog is required for murine yolk sac angiogenesis. Development 129, 361-372.

Cai, Z., de Bruijn, M., Ma, X., Dortland, B., Luteijn, T., Downing, R.J., and Dzierzak, E. (2000). Haploinsufficiency of AML1 affects the temporal and spatial generation of hematopoietic stem cells in the mouse embryo. Immunity 13, 423-431.

Calvi, L.M., Adams, G.B., Weibrecht, K.W., Weber, J.M., Olson, D.P., Knight, M.C., Martin, R.P., Schipani, E., Divieti, P., Bringhurst, F.R., et al. (2003). Osteoblastic cells regulate the haematopoietic stem cell niche. Nature 425, 841-846.

Carmeliet, P., Ferreira, V., Breier, G., Pollefeyt, S., Kieckens, L., Gertsenstein, M., Fahrig, M., Vandenhoeck, A., Harpal, K., Eberhardt, C., et al. (1996). Abnormal blood vessel development and lethality in embryos lacking a single VEGF allele. Nature 380, 435-439.

Chen, M.J., Yokomizo, T., Zeigler, B.M., Dzierzak, E., and Speck, N.A. (2009). Runx1 is required for the endothelial to haematopoietic cell transition but not thereafter. Nature 457, 887-891.

Cheshier, S.H., Morrison, S.J., Liao, X., and Weissman, I.L. (1999). In vivo proliferation and cell cycle kinetics of long-term self-renewing hematopoietic stem cells. Proc Natl Acad Sci U S A 96, 3120-3125.

Chiang, C., Litingtung, Y., Lee, E., Young, K.E., Corden, J.L., Westphal, H., and Beachy, P.A. (1996). Cyclopia and defective axial patterning in mice lacking Sonic hedgehog gene function. Nature 383, 407-413.

Choi, K., Kennedy, M., Kazarov, A., Papadimitriou, J.C., and Keller, G. (1998). A common precursor for hematopoietic and endothelial cells. Development 125, 725-732.

Christensen, J.L., Wright, D.E., Wagers, A.J., and Weissman, I.L. (2004). Circulation and chemotaxis of fetal hematopoietic stem cells. PLoS Biol 2, E75.

Ciau-Uitz, A., Pinheiro, P., Gupta, R., Enver, T., and Patient, R. (2010). Tel1/ETV6 specifies blood stem cells through the agency of VEGF signaling. Dev Cell 18, 569-578.

Colucci, F., Soudais, C., Rosmaraki, E., Vanes, L., Tybulewicz, V.L., and Di Santo, J.P. (1999). Dissecting NK cell development using a novel alymphoid mouse model: investigating the role of the c-abl proto-oncogene in murine NK cell differentiation. J Immunol 162, 2761-2765.

Corbel, C., and Salaun, J. (2002). AlphaIIb integrin expression during development of the murine hemopoietic system. Dev Biol 243, 301-311.

Corbel, C., Salaun, J., Belo-Diabangouaya, P., and Dieterlen-Lievre, F. (2007). Hematopoietic potential of the pre-fusion allantois. Dev Biol 301, 478-488.

Corbel, C., Vaigot, P., and Salaun, J. (2005). (alpha)IIb Integrin, a novel marker for hemopoietic progenitor cells. Int J Dev Biol 49, 279-284.

Cumano, A., Dieterlen-Lievre, F., and Godin, I. (1996). Lymphoid potential, probed before circulation in mouse, is restricted to caudal intraembryonic splanchnopleura. Cell 86, 907-916.

Cumano, A., Ferraz, J.C., Klaine, M., Di Santo, J.P., and Godin, I. (2001). Intraembryonic, but not yolk sac hematopoietic precursors, isolated before circulation, provide long-term multilineage reconstitution. Immunity 15, 477-485.

Dantschakoff, V. (1909). Untersuchungen uber die Entwickelung von Blut und Bindegewebe bei Vogeln. Das lockere Bindegewebe des Huhnchens in Fetalen Leben. Arch f mikr Anat 73, 117-181.

de Bruijn, M.F., Speck, N.A., Peeters, M.C., and Dzierzak, E. (2000). Definitive hematopoietic stem cells first develop within the major arterial regions of the mouse embryo. Embo J 19, 2465-2474.

Debili, N., Robin, C., Schiavon, V., Letestu, R., Pflumio, F., Mitjavila-Garcia, M.T., Coulombel, L., and Vainchenker, W. (2001). Different expression of CD41 on human lymphoid and myeloid progenitors from adults and neonates. Blood 97, 2023-2030.

Dieterlen-Lievre, F. (1975). On the origin of haemopoietic stem cells in the avian embryo: an experimental approach. J Embryol Exp Morphol 33, 607-619.

Dieterlen-Lievre, F., and Martin, C. (1981). Diffuse intraembryonic hemopoiesis in normal and chimeric avian development. Dev Biol 88, 180-191.

Dieterlen-Lievre, F., Pouget, C., Bollerot, K., and Jaffredo, T. (2006). Are intra-aortic hemopoietic cells derived from endothelial cells during ontogeny? Trends Cardiovasc Med 16, 128-139.

Durand, C., Robin, C., Bollerot, K., Baron, M.H., Ottersbach, K., and Dzierzak, E. (2007). Embryonic stromal clones reveal developmental regulators of definitive hematopoietic stem cells. Proc Natl Acad Sci U S A 104, 20838-20843.

Dussault, I., and Miller, S.C. (1995). Suppression of natural killer cell activity in infant mice occurs after target cell binding. Natural immunity 14, 35-43.

Eichmann, A., Corbel, C., Nataf, V., Vaigot, P., Breant, C., and Le Douarin, N.M. (1997). Ligand-dependent development of the endothelial and hemopoietic lineages from embryonic mesodermal cells expressing vascular endothelial growth factor receptor 2. Proc Natl Acad Sci U S A 94, 5141-5146.

Eilken, H.M., Nishikawa, S., and Schroeder, T. (2009). Continuous single-cell imaging of blood generation from haemogenic endothelium. Nature 457, 896-900.

Ferkowicz, M.J., Starr, M., Xie, X., Li, W., Johnson, S.A., Shelley, W.C., Morrison, P.R., and Yoder, M.C. (2003). CD41 expression defines the onset of primitive and definitive hematopoiesis in the murine embryo. Development 130, 4393-4403.

Ferkowicz, M.J., and Yoder, M.C. (2005). Blood island formation: longstanding observations and modern interpretations. Exp Hematol 33, 1041-1047.

Ferrara, N., Carver-Moore, K., Chen, H., Dowd, M., Lu, L., O'Shea, K.S., Powell-Braxton, L., Hillan, K.J., and Moore, M.W. (1996). Heterozygous embryonic lethality induced by targeted inactivation of the VEGF gene. Nature 380, 439-442.

Furuta, C., Ema, H., Takayanagi, S., Ogaeri, T., Okamura, D., Matsui, Y., and Nakauchi, H. (2006). Discordant developmental waves of angioblasts and hemangioblasts in the early gastrulating mouse embryo. Development 133, 2771-2779.

Garcia-Porrero, J.A., Manaia, A., Jimeno, J., Lasky, L.L., Dieterlen-Lievre, F., and Godin, I.E. (1998). Antigenic profiles of endothelial and hemopoietic lineages in murine intraembryonic hemogenic sites. Developmental and comparative immunology 22, 303-319.

Gekas, C., Dieterlen-Lievre, F., Orkin, S.H., and Mikkola, H.K. (2005). The placenta is a niche for hematopoietic stem cells. Dev Cell 8, 365-375.

Gering, M., and Patient, R. (2005). Hedgehog signaling is required for adult blood stem cell formation in zebrafish embryos. Dev Cell 8, 389-400.

Giancotti, F.G., and Ruoslahti, E. (1999). Integrin signaling. Science 285, 1028-1032.

Godin, I., Dieterlen-Lievre, F., and Cumano, A. (1995). Emergence of multipotent hemopoietic cells in the yolk sac and paraaortic splanchnopleura in mouse embryos, beginning at 8.5 days postcoitus. Proc Natl Acad Sci U S A 92, 773-777.

Grassinger, J., Haylock, D.N., Storan, M.J., Haines, G.O., Williams, B., Whitty, G.A., Vinson, A.R., Be, C.L., Li, S., Sorensen, E.S., et al. (2009). Thrombin-cleaved osteopontin regulates hemopoietic stem and progenitor cell functions through interactions with alpha9beta1 and alpha4beta1 integrins. Blood 114, 49-59.

Haar, J.L., and Ackerman, G.A. (1971). A phase and electron microscopic study of vasculogenesis and erythropoiesis in the yolk sac of the mouse. Anat Rec 170, 199-223.

Hirsch, E., Iglesias, A., Potocnik, A.J., Hartmann, U., and Fassler, R. (1996). Impaired migration but not differentiation of haematopoietic stem cells in the absence of beta1 integrins. Nature 380, 171-175.

Huber, T.L. (2010). Dissecting hematopoietic differentiation using the embryonic stem cell differentiation model. Int J Dev Biol 54, 991-1002.

Huber, T.L., Kouskoff, V., Fehling, H.J., Palis, J., and Keller, G. (2004). Haemangioblast commitment is initiated in the primitive streak of the mouse embryo. Nature 432, 625-630.

Hynes, R.O. (2002). Integrins: bidirectional, allosteric signaling machines. Cell 110, 673-687.

Jaffe, L., Jeannotte, L., Bikoff, E.K., and Robertson, E.J. (1990). Analysis of beta 2-microglobulin gene expression in the developing mouse embryo and placenta. J Immunol 145, 3474-3482.

Jaffredo, T., Gautier, R., Brajeul, V., and Dieterlen-Lievre, F. (2000). Tracing the progeny of the aortic hemangioblast in the avian embryo. Dev Biol 224, 204-214.

Jaffredo, T., Gautier, R., Eichmann, A., and Dieterlen-Lievre, F. (1998). Intraaortic hemopoietic cells are derived from endothelial cells during ontogeny. Development 125, 4575-4583.

Ji, R.P., Phoon, C.K., Aristizabal, O., McGrath, K.E., Palis, J., and Turnbull, D.H. (2003). Onset of cardiac function during early mouse embryogenesis coincides with entry of primitive erythroblasts into the embryo proper. Circ Res 92, 133-135.

Jordan, H.E. (1917). Aortic Cell Clusters in Vertebrate Embryos. Proc Natl Acad Sci U S A 3, 149-156.

Katayama, Y., Battista, M., Kao, W.M., Hidalgo, A., Peired, A.J., Thomas, S.A., and Frenette, P.S. (2006). Signals from the sympathetic nervous system regulate hematopoietic stem cell egress from bone marrow. Cell 124, 407-421.

Kiel, M.J., Yilmaz, O.H., Iwashita, T., Terhorst, C., and Morrison, S.J. (2005). SLAM family receptors distinguish hematopoietic stem and progenitor cells and reveal endothelial niches for stem cells. Cell 121, 1109-1121.

Kieusseian, A., Brunet de la Grange, P., Burlen-Defranoux, O., Godin, I., and Cumano, A. (2012). Immature hematopoietic stem cells undergo maturation in the fetal liver. Development.

Kim, I., He, S., Yilmaz, O.H., Kiel, M.J., and Morrison, S.J. (2006). Enhanced purification of fetal liver hematopoietic stem cells using SLAM family receptors. Blood 108, 737-744.

Kumano, K., Chiba, S., Kunisato, A., Sata, M., Saito, T., Nakagami-Yamaguchi, E., Yamaguchi, T., Masuda, S., Shimizu, K., Takahashi, T., et al. (2003). Notch1 but not Notch2 is essential for generating hematopoietic stem cells from endothelial cells. Immunity 18, 699-711.

Kumaravelu, P., Hook, L., Morrison, A.M., Ure, J., Zhao, S., Zuyev, S., Ansell, J., and Medvinsky, A. (2002). Quantitative developmental anatomy of definitive haematopoietic stem cells/long-term repopulating units (HSC/RUs): role of the aorta-gonad- mesonephros (AGM) region and the yolk sac in colonisation of the mouse embryonic liver. Development 129, 4891-4899.

Kunkel, E.J., Ramos, C.L., Steeber, D.A., Muller, W., Wagner, N., Tedder, T.F., and Ley, K. (1998). The roles of L-selectin, beta 7 integrins, and P-selectin in leukocyte rolling and adhesion in high endothelial venules of Peyer's patches. J Immunol 161, 2449-2456.

Lancrin, C., Sroczynska, P., Stephenson, C., Allen, T., Kouskoff, V., and Lacaud, G. (2009). The haemangioblast generates haematopoietic cells through a haemogenic endothelium stage. Nature 457, 892-895.

Lapidot, T., Dar, A., and Kollet, O. (2005). How do stem cells find their way home? Blood 106, 1901-1910.

Lassila, O., Eskola, J., Toivanen, P., Martin, C., and Dieterlen-Lievre, F. (1978). The origin of lymphoid stem cells

studied in chick yold sac-embryo chimaeras. Nature 272, 353-354.

Lee, C.Y., Vogeli, K.M., Kim, S.H., Chong, S.W., Jiang, Y.J., Stainier, D.Y., and Jin, S.W. (2009). Notch signaling functions as a cell-fate switch between the endothelial and hematopoietic lineages. Curr Biol 19, 1616-1622.

Levesque, J.P., and Winkler, I.G. (2011). Hierarchy of immature hematopoietic cells related to blood flow and niche. Curr Opin Hematol 18, 220-225.

Lo Celso, C., Fleming, H.E., Wu, J.W., Zhao, C.X., Miake-Lye, S., Fujisaki, J., Cote, D., Rowe, D.W., Lin, C.P., and Scadden, D.T. (2009). Live-animal tracking of individual haematopoietic stem/progenitor cells in their niche. Nature 457, 92-96.

Maeno, M., Tochinai, S., and Katagiri, C. (1985). Differential participation of ventral and dorsolateral mesoderms in the hemopoiesis of Xenopus, as revealed in diploid-triploid or interspecific chimeras. Dev Biol 110, 503-508.

Massberg, S., Schaerli, P., Knezevic-Maramica, I., Kollnberger, M., Tubo, N., Moseman, E.A., Huff, I.V., Junt, T., Wagers, A.J., Mazo, I.B., et al. (2007). Immunosurveillance by hematopoietic progenitor cells trafficking through blood, lymph, and peripheral tissues. Cell 131, 994-1008.

Mathe, G., Amiel, J.L., Schwarzenberg, L., Cattan, A., and Schneider, M. (1963). Haematopoietic Chimera in Man after Allogenic (Homologous) Bone-Marrow Transplantation. (Control of the Secondary Syndrome. Specific Tolerance Due to the Chimerism). Br Med J 2, 1633-1635.

Mathe, G., Jammet, H., Pendic, B., Schwarzenberg, L., Duplan, J.F., Maupin, B., Latarjet, R., Larrieu, M.J., Kalic, D., and Djukic, Z. (1959). [Transfusions and grafts of homologous bone marrow in humans after accidental high dosage irradiation] Transfusions et greffes de moelle osseuse homologue chez des humains irradies a haute dose accidentellement. Rev Fr Etud Clin Biol 4, 226-238.

Matsuoka, S., Tsuji, K., Hisakawa, H., Xu, M., Ebihara, Y., Ishii, T., Sugiyama, D., Manabe, A., Tanaka, R., Ikeda, Y., et al. (2001). Generation of definitive hematopoietic stem cells from murine early yolk sac and paraaortic splanchnopleures by aorta-gonad-mesonephros region-derived stromal cells. Blood 98, 6-12.

Maximow, A.A. (1909). Untersuchungen uber blut und bindegewebe 1. Die fruhesten entwicklungsstadien der blut- und binde- gewebszellan bein saugetierembryo, bis zum anfang der blutbilding unden leber. Arch Mikroskop Anat 73, 444-561.

Mazzarello, P. (1999). A unifying concept: the history of cell theory. Nat Cell Biol 1, E13-15.

McGrath, K.E., Frame, J.M., Fromm, G.J., Koniski, A.D., Kingsley, P.D., Little, J., Bulger, M., and Palis, J. (2011). A transient definitive erythroid lineage with unique regulation of the beta-globin locus in the mammalian embryo. Blood 117, 4600-4608.

McKinney-Freeman, S.L., Naveiras, O., Yates, F., Loewer, S., Philitas, M., Curran, M., Park, P.J., and Daley, G.Q. (2009). Surface antigen phenotypes of hematopoietic stem cells from embryos and murine embryonic stem cells. Blood 114, 268-278.

Medvinsky, A., and Dzierzak, E. (1996). Definitive hematopoiesis is autonomously initiated by the AGM region. Cell 86, 897-906.

Medvinsky, A., Rybtsov, S., and Taoudi, S. (2011). Embryonic origin of the adult hematopoietic system: advances and questions. Development 138, 1017-1031.

Medvinsky, A.L., Samoylina, N.L., Muller, A.M., and Dzierzak, E.A. (1993). An early pre-liver intraembryonic source of CFU-S in the developing mouse. Nature 364, 64-67.

Mendez-Ferrer, S., Michurina, T.V., Ferraro, F., Mazloom, A.R., Macarthur, B.D., Lira, S.A., Scadden, D.T., Ma'ayan, A., Enikolopov, G.N., and Frenette, P.S. (2010). Mesenchymal and haematopoietic stem cells form a unique bone marrow niche. Nature 466, 829-834.

Mikkola, H.K., Fujiwara, Y., Schlaeger, T.M., Traver, D., and Orkin, S.H. (2003). Expression of CD41 marks the initiation of definitive hematopoiesis in the mouse embryo. Blood 101, 508-516.

Mitjavila-Garcia, M.T., Cailleret, M., Godin, I., Nogueira, M.M., Cohen-Solal, K., Schiavon, V., Lecluse, Y., Le Pesteur, F., Lagrue, A.H., and Vainchenker, W. (2002). Expression of CD41 on hematopoietic progenitors derived from embryonic hematopoietic cells. Development 129, 2003-2013.

Mitola, S., Ravelli, C., Moroni, E., Salvi, V., Leali, D., Ballmer-Hofer, K., Zammataro, L., and Presta, M. (2010). Gremlin is a novel agonist of the major proangiogenic receptor VEGFR2. Blood 116, 3677-3680.

Mizuochi, C., Fraser, S.T., Biasch, K., Horio, Y., Kikushige, Y., Tani, K., Akashi, K., Tavian, M., and Sugiyama, D. (2012). Intra-aortic clusters undergo endothelial to hematopoietic phenotypic transition during early embryogenesis. PloS one 7, e35763.

Moore, M.A., and Metcalf, D. (1970). Ontogeny of the haemopoietic system: yolk sac origin of in vivo and in vitro colony forming cells in the developing mouse embryo. Br J Haematol 18, 279-296.

Moore, M.A., and Owen, J.J. (1967). Chromosome marker studies in the irradiated chick embryo. Nature 215, 1081-1082.

Morrison, S.J., Hemmati, H.D., Wandycz, A.M., and Weissman, I.L. (1995). The purification and characterization of fetal liver hematopoietic stem cells. Proc Natl Acad Sci U S A 92, 10302-10306.

Muller, A.M., Medvinsky, A., Strouboulis, J., Grosveld, F., and Dzierzak, E. (1994). Development of hematopoietic stem cell activity in the mouse embryo. Immunity 1, 291-301.

Muller-Sieburg, C.E., Whitlock, C.A., and Weissman, I.L. (1986). Isolation of two early B lymphocyte progenitors

from mouse marrow: a committed pre-pre-B cell and a clonogenic Thy-1-lo hematopoietic stem cell. Cell 44, 653-662.

Murray, P.D.F. (1932). The Development in vitro of the Blood of the Early Chick Embryo. Proceedings of the Royal Society of London 111, 497-521.

Naveiras, O., Nardi, V., Wenzel, P.L., Hauschka, P.V., Fahey, F., and Daley, G.Q. (2009). Bone-marrow adipocytes as negative regulators of the haematopoietic microenvironment. Nature 460, 259-263.

North, T., Gu, T.L., Stacy, T., Wang, Q., Howard, L., Binder, M., Marin-Padilla, M., and Speck, N.A. (1999). Cbfa2 is required for the formation of intra-aortic hematopoietic clusters. Development 126, 2563-2575.

North, T.E., Goessling, W., Peeters, M., Li, P., Ceol, C., Lord, A.M., Weber, G.J., Harris, J., Cutting, C.C., Huang, P., et al. (2009). Hematopoietic stem cell development is dependent on blood flow. Cell 137, 736-748.

Notta, F., Doulatov, S., Laurenti, E., Poeppl, A., Jurisica, I., and Dick, J.E. (2011). Isolation of single human hematopoietic stem cells capable of long-term multilineage engraftment. Science 333, 218-221.

Oberlin, E., El Hafny, B., Petit-Cocault, L., and Souyri, M. (2010). Definitive human and mouse hematopoiesis originates from the embryonic endothelium: a new class of HSCs based on VE-cadherin expression. Int J Dev Biol 54, 1165-1173.

Ogawa, M., Kizumoto, M., Nishikawa, S., Fujimoto, T., Kodama, H., and Nishikawa, S.I. (1999). Expression of alpha4-integrin defines the earliest precursor of hematopoietic cell lineage diverged from endothelial cells. Blood 93, 1168-1177.

Okuda, T., van Deursen, J., Hiebert, S.W., Grosveld, G., and Downing, J.R. (1996). AML1, the target of multiple chromosomal translocations in human leukemia, is essential for normal fetal liver hematopoiesis. Cell 84, 321-330.

Osawa, M., Hanada, K., Hamada, H., and Nakauchi, H. (1996). Long-term lymphohematopoietic reconstitution by a single CD34-low/negative hematopoietic stem cell. Science 273, 242-245.

Ottersbach, K., and Dzierzak, E. (2005). The murine placenta contains hematopoietic stem cells within the vascular labyrinth region. Dev Cell 8, 377-387.

Palis, J., Robertson, S., Kennedy, M., Wall, C., and Keller, G. (1999). Development of erythroid and myeloid progenitors in the yolk sac and embryo proper of the mouse. Development 126, 5073-5084.

Pardanaud, L., and Dieterlen-Lievre, F. (1999). Manipulation of the angiopoietic/hemangiopoietic commitment in the avian embryo. Development 126, 617-627.

Pardanaud, L., Luton, D., Prigent, M., Bourcheix, L.M., Catala, M., and Dieterlen-Lievre, F. (1996). Two distinct endothelial lineages in ontogeny, one of them related to hemopoiesis. Development 122, 1363-1371.

Peeters, M., Ling, K.W., Oziemlak, A., Robin, C., and Dzierzak, E. (2005). Multipotential hematopoietic progenitor cells from embryos developed in vitro engraft unconditioned W41/W41 neonatal miceB. Haematologica 90, 734-739.

Peeters, M., Ottersbach, K., Bollerot, K., Orelio, C., de Bruijn, M., Wijgerde, M., and Dzierzak, E. (2009). Ventral embryonic tissues and Hedgehog proteins induce early AGM hematopoietic stem cell development. Development 136, 2613-2621.

Petit-Cocault, L., Volle-Challier, C., Fleury, M., Peault, B., and Souyri, M. (2007). Dual role of Mpl receptor during the establishment of definitive hematopoiesis. Development 134, 3031-3040.

Potocnik, A.J., Brakebusch, C., and Fassler, R. (2000). Fetal and adult hematopoietic stem cells require beta1 integrin function for colonizing fetal liver, spleen, and bone marrow. Immunity 12, 653-663.

Pouget, C., Gautier, R., Teillet, M.A., and Jaffredo, T. (2006). Somite-derived cells replace ventral aortic hemangioblasts and provide aortic smooth muscle cells of the trunk. Development 133, 1013-1022.

Purton, L.E., and Scadden, D.T. (2007). Limiting factors in murine hematopoietic stem cell assays. Cell Stem Cell 1, 263-270.

Purton, L.E., and Scadden, D.T. (2008). The hematopoietic stem cell niche. StemBook [Internet] Cambridge (MA): Harvard Stem Cell Institute; 2008.

Qian, H., Georges-Labouesse, E., Nystrom, A., Domogatskaya, A., Tryggvason, K., Jacobsen, S.E., and Ekblom, M. (2007). Distinct roles of integrins alpha6 and alpha4 in homing of fetal liver hematopoietic stem and progenitor cells. Blood 110, 2399-2407.

Raaijmakers, M.H., Mukherjee, S., Guo, S., Zhang, S., Kobayashi, T., Schoonmaker, J.A., Ebert, B.L., Al-Shahrour, F., Hasserjian, R.P., Scadden, E.O., et al. (2010). Bone progenitor dysfunction induces myelodysplasia and secondary leukaemia. Nature 464, 852-857.

Ramalho-Santos, M., and Willenbring, H. (2007). On the origin of the term "stem cell". Cell Stem Cell 1, 35-38.

Rhodes, K.E., Gekas, C., Wang, Y., Lux, C.T., Francis, C.S., Chan, D.N., Conway, S., Orkin, S.H., Yoder, M.C., and Mikkola, H.K. (2008). The emergence of hematopoietic stem cells is initiated in the placental vasculature in the absence of circulation. Cell Stem Cell 2, 252-263.

Robert-Moreno, A., Espinosa, L., de la Pompa, J.L., and Bigas, A. (2005). RBPjkappa-dependent Notch function regulates Gata2 and is essential for the formation of intra-embryonic hematopoietic cells. Development 132, 1117-1126.

Robert-Moreno, A., Guiu, J., Ruiz-Herguido, C., Lopez, M.E., Ingles-Esteve, J., Riera, L., Tipping, A., Enver, T., Dzierzak, E., Gridley, T., et al. (2008). Impaired embryonic haematopoiesis yet normal arterial development in the absence of the Notch ligand Jagged1. EMBO J 27, 1886-1895.

Robin, C., and Durand, C. (2010). The roles of BMP and IL-3 signaling pathways in the control of hematopoietic stem cells in the mouse embryo. Int J Dev Biol 54, 1189-1200.

Robin, C., Ottersbach, K., Boisset, J.C., Oziemlak, A., and Dzierzak, E. (2011). CD41 is developmentally regulated and differentially expressed on mouse hematopoietic stem cells. Blood 117, 5088-5091.

Robin, C., Ottersbach, K., Durand, C., Peeters, M., Vanes, L., Tybulewicz, V., and Dzierzak, E. (2006). An unexpected role for IL-3 in the embryonic development of hematopoietic stem cells. Dev Cell 11, 171-180.

Ruiz-Herguido, C., Guiu, J., D'Altri, T., Ingles-Esteve, J., Dzierzak, E., Espinosa, L., and Bigas, A. (2012). Hematopoietic stem cell development requires transient Wnt/beta-catenin activity. J Exp Med 209, 1457-1468.

Rybtsov, S., Sobiesiak, M., Taoudi, S., Souilhol, C., Senserrich, J., Liakhovitskaia, A., Ivanovs, A., Frampton, J., Zhao, S., and Medvinsky, A. (2011). Hierarchical organization and early hematopoietic specification of the developing HSC lineage in the AGM region. J Exp Med 208, 1305-1315.

Sabin, F.R. (1920). Studies on the origin of blood vessels and of red corpuscles as seen in the living blastoderm of the chick during the second day of incubation. Contributions to Embryology 9, 213-262.

Samokhvalov, I.M., Samokhvalova, N.I., and Nishikawa, S. (2007). Cell tracing shows the contribution of the yolk sac to adult haematopoiesis. Nature 446, 1056-1061.

Sanchez, M.J., Holmes, A., Miles, C., and Dzierzak, E. (1996). Characterization of the first definitive hematopoietic stem cells in the AGM and liver of the mouse embryo. Immunity 5, 513-525.

Sasaki, K., Yagi, H., Bronson, R.T., Tominaga, K., Matsunashi, T., Deguchi, K., Tani, Y., Kishimoto, T., and Komori, T. (1996). Absence of fetal liver hematopoiesis in mice deficient in transcriptional coactivator core binding factor beta. Proc Natl Acad Sci U S A 93, 12359-12363.

Scott, L.M., Priestley, G.V., and Papayannopoulou, T. (2003). Deletion of alpha4 integrins from adult hematopoietic cells reveals roles in homeostasis, regeneration, and homing. Molecular and cellular biology 23, 9349-9360.

Shalaby, F., Ho, J., Stanford, W.L., Fischer, K.D., Schuh, A.C., Schwartz, L., Bernstein, A., and Rossant, J. (1997). A requirement for Flk1 in primitive and definitive hematopoiesis and vasculogenesis. Cell 89, 981-990.

Shalaby, F., Rossant, J., Yamaguchi, T.P., Gertsenstein, M., Wu, X.F., Breitman, M.L., and Schuh, A.C. (1995). Failure of blood-island formation and vasculogenesis in Flk-1-deficient mice. Nature 376, 62-66.

Shattil, S.J., Kashiwagi, H., and Pampori, N. (1998). Integrin signaling: the platelet paradigm. Blood 91, 2645-2657.

Siminovitch, L., McCulloch, E.A., and Till, J.E. (1963). The Distribution of Colony-Forming Cells among Spleen Colonies. J Cell Physiol 62, 327-336.

Stabile, H., Mitola, S., Moroni, E., Belleri, M., Nicoli, S., Coltrini, D., Peri, F., Pessi, A., Orsatti, L., Talamo, F., et al. (2007). Bone morphogenic protein antagonist Drm/gremlin is a novel proangiogenic factor. Blood 109, 1834-1840.

Stern, C.D. (2005). The chick; a great model system becomes even greater. Dev Cell 8, 9-17.

Sugimura, R., He, X.C., Venkatraman, A., Arai, F., Box, A., Semerad, C., Haug, J.S., Peng, L., Zhong, X.B., Suda, T., et al. (2012). Noncanonical wnt signaling maintains hematopoietic stem cells in the niche. Cell 150, 351-365.

Sugiyama, T., Kohara, H., Noda, M., and Nagasawa, T. (2006). Maintenance of the hematopoietic stem cell pool by CXCL12-CXCR4 chemokine signaling in bone marrow stromal cell niches. Immunity 25, 977-988.

Tanaka, Y., Hayashi, M., Kubota, Y., Nagai, H., Sheng, G., Nishikawa, S., and Samokhvalov, I.M. (2012). Early ontogenic origin of the hematopoietic stem cell lineage. Proc Natl Acad Sci U S A 109, 4515-4520.

Taoudi, S., Gonneau, C., Moore, K., Sheridan, J.M., Blackburn, C.C., Taylor, E., and Medvinsky, A. (2008). Extensive hematopoietic stem cell generation in the AGM region via maturation of VE-cadherin+CD45+ predefinitive HSCs. Cell Stem Cell 3, 99-108.

Taoudi, S., and Medvinsky, A. (2007). Functional identification of the hematopoietic stem cell niche in the ventral domain of the embryonic dorsal aorta. Proc Natl Acad Sci U S A 104, 9399-9403.

Taoudi, S., Morrison, A.M., Inoue, H., Gribi, R., Ure, J., and Medvinsky, A. (2005). Progressive divergence of definitive haematopoietic stem cells from the endothelial compartment does not depend on contact with the foetal liver. Development 132, 4179-4191.

Thomas, E.D., Lochte, H.L., Jr., Lu, W.C., and Ferrebee, J.W. (1957). Intravenous infusion of bone marrow in patients receiving radiation and chemotherapy. N Engl J Med 257, 491-496.

Till, J.E., and Ea, M. (1961). A direct measurement of the radiation sensitivity of normal mouse bone marrow cells. Radiat Res 14, 213-222.

Toles, J.F., Chui, D.H., Belbeck, L.W., Starr, E., and Barker, J.E. (1989). Hemopoietic stem cells in murine embryonic yolk sac and peripheral blood. Proc Natl Acad Sci U S A 86, 7456-7459.

Turpen, J.B., Kelley, C.M., Mead, P.E., and Zon, L.I. (1997). Bipotential primitive-definitive hematopoietic progenitors in the vertebrate embryo. Immunity 7, 325-334.

Turpen, J.B., Knudson, C.M., and Hoefen, P.S. (1981). The early ontogeny of hematopoietic cells studied by grafting cytogenetically labeled tissue anlagen: localization of a prospective stem cell compartment. Dev Biol 85, 99-112.

Ueno, H., and Weissman, I.L. (2010). The origin and

fate of yolk sac hematopoiesis: application of chimera analyses to developmental studies. Int J Dev Biol 54, 1019-1031.

Umemoto, T., Yamato, M., Shiratsuchi, Y., Terasawa, M., Yang, J., Nishida, K., Kobayashi, Y., and Okano, T. (2006). Expression of Integrin beta3 is correlated to the properties of quiescent hemopoietic stem cells possessing the side population phenotype. J Immunol 177, 7733-7739.

Vogeli, K.M., Jin, S.W., Martin, G.R., and Stainier, D.Y. (2006). A common progenitor for haematopoietic and endothelial lineages in the zebrafish gastrula. Nature 443, 337-339.

Wagers, A.J., and Weissman, I.L. (2006). Differential expression of alpha2 integrin separates long-term and short-term reconstituting Lin-/loThy1.1(lo)c-kit+ Sca-1+ hematopoietic stem cells. Stem Cells 24, 1087-1094.

Wagner, N., Lohler, J., Kunkel, E.J., Ley, K., Leung, E., Krissansen, G., Rajewsky, K., and Muller, W. (1996). Critical role for beta7 integrins in formation of the gut-associated lymphoid tissue. Nature 382, 366-370.

Wagner, N., Lohler, J., Tedder, T.F., Rajewsky, K., Muller, W., and Steeber, D.A. (1998). L-selectin and beta7 integrin synergistically mediate lymphocyte migration to mesenteric lymph nodes. European journal of immunology 28, 3832-3839.

Wang, Q., Stacy, T., Binder, M., Marin-Padilla, M., Sharpe, A.H., and Speck, N.A. (1996). Disruption of the Cbfa2 gene causes necrosis and hemorrhaging in the central nervous system and blocks definitive hematopoiesis. Proc Natl Acad Sci U S A 93, 3444-3449.

Weissman, I.L., Papaioannou, V., and Gardner, R. (1978). Fetal hematopoietic origins of the adult hematolymphoid system. Differentiation of normal and neoplastic hematopoietic cells, 33-47.

Wilkinson, R.N., Pouget, C., Gering, M., Russell, A.J., Davies, S.G., Kimelman, D., and Patient, R. (2009). Hedgehog and Bmp polarize hematopoietic stem cell emergence in the zebrafish dorsal aorta. Dev Cell 16, 909-916.

Williams, D.A., Rios, M., Stephens, C., and Patel, V.P. (1991). Fibronectin and VLA-4 in haematopoietic stem cell-microenvironment interactions. Nature 352, 438-441.

Wilson, A., Laurenti, E., Oser, G., van der Wath, R.C., Blanco-Bose, W., Jaworski, M., Offner, S., Dunant, C.F., Eshkind, L., Bockamp, E., et al. (2008). Hematopoietic stem cells reversibly switch from dormancy to self-renewal during homeostasis and repair. Cell 135, 1118-1129.

Winkler, I.G., Barbier, V., Wadley, R., Zannettino, A.C., Williams, S., and Levesque, J.P. (2010a). Positioning of bone marrow hematopoietic and stromal cells relative to blood flow in vivo: serially reconstituting hematopoietic stem cells reside in distinct nonperfused niches. Blood 116, 375-385.

Winkler, I.G., Sims, N.A., Pettit, A.R., Barbier, V., Nowlan, B., Helwani, F., Poulton, I.J., van Rooijen, N., Alexander, K.A., Raggatt, L.J., et al. (2010b). Bone marrow macrophages maintain hematopoietic stem cell (HSC) niches and their depletion mobilizes HSCs. Blood 116, 4815-4828.

Xie, Y., Yin, T., Wiegraebe, W., He, X.C., Miller, D., Stark, D., Perko, K., Alexander, R., Schwartz, J., Grindley, J.C., et al. (2009). Detection of functional haematopoietic stem cell niche using real-time imaging. Nature 457, 97-101.

Xu, M.J., Matsuoka, S., Yang, F.C., Ebihara, Y., Manabe, A., Tanaka, R., Eguchi, M., Asano, S., Nakahata, T., and Tsuji, K. (2001). Evidence for the presence of murine primitive megakaryocytopoiesis in the early yolk sac. Blood 97, 2016-2022.

Yamazaki, S., Ema, H., Karlsson, G., Yamaguchi, T., Miyoshi, H., Shioda, S., Taketo, M.M., Karlsson, S., Iwama, A., and Nakauchi, H. (2011). Nonmyelinating Schwann cells maintain hematopoietic stem cell hibernation in the bone marrow niche. Cell 147, 1146-1158.

Yoder, M.C., and Hiatt, K. (1997). Engraftment of embryonic hematopoietic cells in conditioned newborn recipients. Blood 89, 2176-2183.

Yoder, M.C., Hiatt, K., Dutt, P., Mukherjee, P., Bodine, D.M., and Orlic, D. (1997a). Characterization of definitive lymphohematopoietic stem cells in the day 9 murine yolk sac. Immunity 7, 335-344.

Yoder, M.C., Hiatt, K., and Mukherjee, P. (1997b). In vivo repopulating hematopoietic stem cells are present in the murine yolk sac at day 9.0 postcoitus. Proc Natl Acad Sci U S A 94, 6776-6780.

Yokomizo, T., and Dzierzak, E. (2010). Three-dimensional cartography of hematopoietic clusters in the vasculature of whole mouse embryos. Development 137, 3651-3661.

Yokomizo, T., Ng, C.E., Osato, M., and Dzierzak, E. (2011). Three-dimensional imaging of whole midgestation murine embryos shows an intravascular localization for all hematopoietic clusters. Blood 117, 6132-6134.

Zeigler, B.M., Sugiyama, D., Chen, M., Guo, Y., Downs, K.M., and Speck, N.A. (2006). The allantois and chorion, when isolated before circulation or chorio-allantoic fusion, have hematopoietic potential. Development 133, 4183-4192.

Zhang, J., Niu, C., Ye, L., Huang, H., He, X., Tong, W.G., Ross, J., Haug, J., Johnson, T., Feng, J.Q., et al. (2003). Identification of the haematopoietic stem cell niche and control of the niche size. Nature 425, 836-841.

Zon, L.I. (2008). Intrinsic and extrinsic control of haematopoietic stem-cell self-renewal. Nature 453, 306-313.

Zovein, A.C., Hofmann, J.J., Lynch, M., French, W.J., Turlo, K.A., Yang, Y., Becker, M.S., Zanetta, L., Dejana, E., Gasson, J.C., et al. (2008). Fate tracing reveals the endothelial origin of hematopoietic stem cells. Cell Stem Cell 3, 625-636.


Personna
SUPER
SUPER
SUPER


Personna
SUPER
MADE IN U.S.A.
PERSONNA

Chapter 2 – *Ex vivo* time-lapse confocal imaging of the mouse embryo aorta

This chapter was published in Nature Protocols (2011) 6, 1792–805

Chapter 3 – *In vivo* imaging of haematopoietic cells emerging from the mouse aortic endothelium

This chapter was published in Nature (2010) 6, 1792–805

Chapter 4 – CD41 is developmentally regulated and differentially expressed on mouse hematopoietic stem cells

This chapter was published in Blood (2011) 117, 5088–91

Brief report

CD41 is developmentally regulated and differentially expressed on mouse hematopoietic stem cells

*Catherine Robin,[1] *Katrin Ottersbach,[1] Jean-Charles Boisset,[1] Aneta Oziemlak,[1] and Elaine Dzierzak[1]

[1]Department of Cell Biology, Erasmus Medical Center, Erasmus MC Stem Cell Institute, Rotterdam, The Netherlands

CD41 expression is associated with the earliest stages of mouse hematopoiesis. It is notably expressed on some cells of the intra-aortic hematopoietic clusters, an area where the first adult-repopulating hematopoietic stem cells (HSCs) are generated. Although it is generally accepted that CD41 expression marks the onset of primitive/definitive hematopoiesis, there are few published data concerning its expression on HSCs. It is as yet uncertain whether HSCs express CD41 throughout development, and if so, to what level. We performed a complete in vivo transplantation analysis with yolk sac, aorta, placenta, and fetal liver cells, sorted based on CD41 expression level. Our data show that the earliest emerging HSCs in the aorta express CD41 in a time-dependent manner. In contrast, placenta and liver HSCs are CD41$^-$. Thus, differential and temporal expression of CD41 by HSCs in the distinct hematopoietic territories suggests a developmental/dynamic regulation of this marker throughout development. (*Blood*. 2011;117(19):5088-5091)

Introduction

CD41 (or integrin αIIb) is a marker of the megakaryocytic lineage and also of other clonogenic progenitors.[1-5] CD41 marks the onset of murine primitive and definitive hematopoiesis.[5-9] At embryonic day 7 (E7), yolk sac (YS) primitive erythroid progenitors express low levels of CD41.[7] By E8.25/E9.5, most YS definitive hematopoietic progenitors express CD41 to high levels,[7] and definitive hematopoietic progenitors in the intraembryonic para-aortic splanchnopleura or aorta-gonad-mesonephros (AGM) region also express CD41.[5,7-9] These embryonic CD41$^+$ hematopoietic cells possess no endothelial potential.[10,11] Immunostainings show CD41$^+$ hematopoietic cells within YS blood islands,[7,8,12] intra-aortic clusters,[12-14] and attached to vessel walls of the placenta labyrinth.[15,16] Real-time vital imaging demonstrates that rare phenotypically defined hematopoietic stem cells (HSCs) become CD41$^+$ as soon as they emerge from the aortic endothelium.[13] Based on these findings, CD41 has been suggested as a marker expressed by nascent HSCs, denoting the onset of hematopoietic fate. However, it is still unclear whether HSCs express CD41 throughout development.

HSCs (as defined by the ability to long-term, high-level, multilineage repopulate the hematopoietic system of irradiated adult mouse recipients) start to be detected at E10.5 in the aorta and vitelline/umbilical arteries[17-20] and emerge from hemogenic endothelium.[13,21,22] HSCs are also in the YS, placenta, and fetal liver (FL) beginning at E11.5.[23] Only few transplantation data are available for CD41-sorted AGM cells.[24,25] When sorted in the context of other markers (CD48, CD150, CD45, and endomucin), HSCs were in both CD41$^+$ and CD41$^-$ fractions. To clarify whether CD41 is a HSC marker during development, we performed a comprehensive analysis of CD41 expression (negative, intermediate, high) on HSCs (during and subsequent to the developmental time in which they are generated) in the various HSC-containing tissues. We show that all E11 AGM HSCs express CD41 to intermediate levels and that expression is time and hematopoietic territory dependent.

Methods

Embryos and cell preparations

Timed matings were set up between males of transgenic mouse line *Ln72*[26] or *Ly6A GFP*[17] and wild-type (C57BL/10 × CBA)F1 females; or C57BL6 Ly5.1 males and females. Vaginal plug day is E0. Recipients were (C57BL/10 × CBA)F1 or C57BL6 Ly5.2 (8-10 weeks old). Animals were housed according to institutional guidelines, and procedures were performed in compliance with Standards for Care and Use of Laboratory Animals with approval from the Erasmus MC ethical review board.

E11/E12 AGM and YS, and E12 placenta and E14 FL were dissected and collagenase dissociated (0.125% weight/volume, type 1, Sigma-Aldrich Chemie) or crushed (FL). Cells were washed, counted, and suspended in phosphate-buffered saline (PBS), 10% fetal calf serum, and penicillin/streptomycin. Cells were stained with antibodies (supplemental Table 1, available on the *Blood* Web site; see the Supplemental Materials link at the top of the online article) for 30 minutes on ice in PBS/fetal calf serum/penicillin/streptomycin, washed and stained with Hoechst 33258, before analysis or sorting on FACScan or ArialII (BD Biosciences).

Hematopoietic assays

In vitro clonogenic analysis was performed on dilutions of sorted cells plated in methylcellulose (M3434; StemCell Technologies). Hematopoietic colonies were counted at day 12.

For in vivo HSC analysis, sorted cells (various cell doses) were intravenously coinjected with 2×10^5 wild-type spleen cells into irradiated (9 Gy split-dose, ^{137}Cs-source) recipients. After 4 months, donor chimerism (*Ln72* or *Ly6A GFP*) was analyzed by semiquantitative polymerase chain

Submitted January 11, 2011; accepted February 21, 2011. Prepublished online as *Blood* First Edition paper, March 17, 2011; DOI 10.1182/blood-2011-01-329516.

*C.R. and K.O. contributed equally to this study.

The online version of this article contains a data supplement.

The publication costs of this article were defrayed in part by page charge payment. Therefore, and solely to indicate this fact, this article is hereby marked "advertisement" in accordance with 18 USC section 1734.

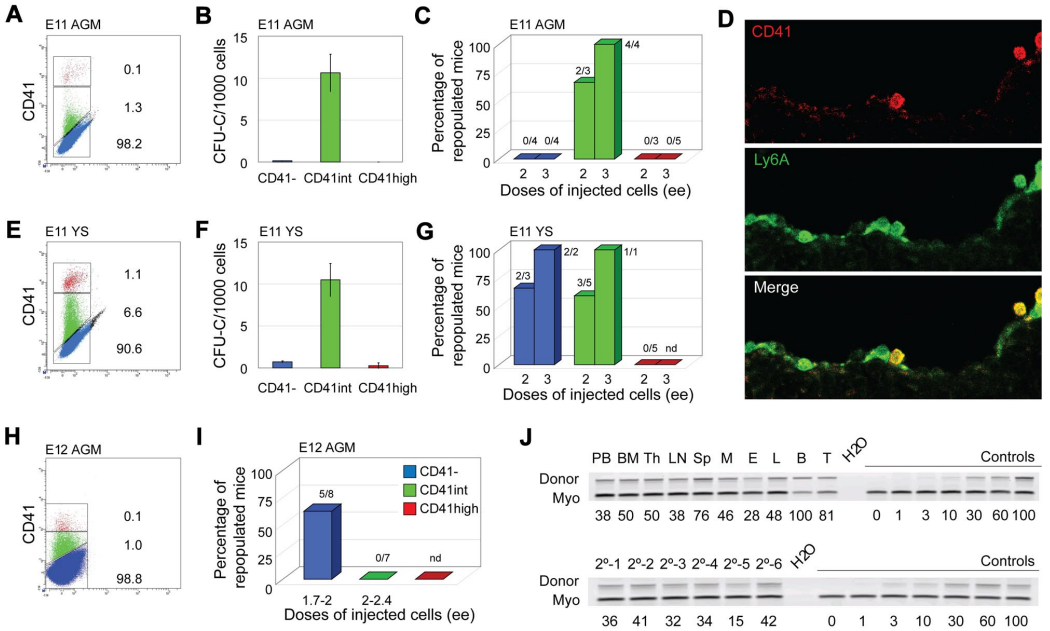

Figure 1. Phenotypic and functional analyses of CD41-sorted cell fractions of E11 and E12 embryonic tissues. (A-D,J) E11 AGM, (H,I) E12 AGM, and (E-G) E11 YS. (A,E,H) Flow cytometric analysis of E11 AGM, E11 YS, and E12 AGM, respectively. Representative sorting gates (red represents CD41^{high}; green, CD41^{int}; and blue, CD41^{-}). The percentage of cells in each fraction is indicated. (B,F) In vitro colony-forming unit in culture (CFU-C) analyses show the number of total hematopoietic progenitors per 1000 cells in each CD41-sorted fraction of E11 AGM and E11 YS cells. Each sample was analyzed in triplicate for each dilution. n = 4 for E11 AGM, and n = 2 for E11 YS. (C,G,I) In vivo hematopoietic repopulation analysis of CD41-sorted fractions of E11 AGM, E11 YS, and E12 AGM 4 months after transplantation. Percentage of repopulated mice showing greater than 10% donor chimerism in peripheral blood is shown. Numbers above columns indicate the number of mice repopulated/number of mice transplanted. Dose of injected cells is indicated as embryo equivalents (ee). n = 3 for E11 AGM, n = 4 for E11 YS, and n = 2 for E12 AGM. nd indicates not done. (D) CD41 immunostaining of E11 Ly6A GFP embryo section showing the ventral wall of the aorta. (Top panel) Red fluorescent CD41 expression in hematopoietic cells. (Middle panel) Green fluorescent Ly6A GFP expression in hematopoietic cells and some endothelial cells. (Bottom panel) Merged fluorescence. Yellow represents overlap of CD41 and Ly6A GFP expression in hematopoietic cells closely associated with the aortic endothelium. Image acquisition was from LSM510NLO/FCS confocal microscope (Carl Zeiss BV) with 40×/1.3 NA water objective and Vectashield medium (Vector Laboratories). LSM image software was used (Carl Zeiss BV). (J) Representative semiquantitative PCR analysis of hematopoietic tissue DNA from (upper panel) a primary recipient injected with 3 ee of E11 AGM CD41^{int} cells and (lower panel) peripheral blood DNA from 6 secondary recipients injected with BM cells from the primary recipient 4 months after transplantation. Donor indicates the human β-globin PCR fragment, and Myo indicates the myogenin DNA normalization control PCR fragment. DNA dilution controls (0%-100%) were used to quantitate percentages of donor chimerism that are indicated below each lane. PB indicates peripheral blood; Th, thymus; LN, lymph node; Sp, spleen; M, myeloid (sorted cells from BM); E, erythroid (sorted from BM); L, lymphoid (sorted from BM); B, B lymphoid (sorted from spleen); and T, T lymphoid (sorted from spleen).

reaction (PCR). Signal quantitation was by DNA normalization (*myogenin*) and *Ln72* or *Ly6A GFP* control DNA dilutions. For multilineage repopulation analysis, T, B, erythroid, and myeloid cells were sorted from recipient bone marrow (BM) and spleens after antibody staining (supplemental Table 1). Primary recipient BM (2×10^6) cells were injected into secondary irradiated recipients to assess self-renewal capacity. For the Ly5.2 recipients injected with Ly5.1 cells, percentage chimerism was determined by flow cytometry on blood after erythrocyte lysis (Beckman Coulter) and antibody and 7-amino-actinomycin D staining (supplemental Table 1).

Immunostaining

E11 *Ly6A GFP* embryos were fixed (2% paraformaldehyde/PBS, 4°C, 1-2 hours), cryoprotected (30% sucrose/PBS, 4°C overnight), Tissue Tek embedded, frozen (dry ice), and cryosectioned. Immunohistochemical staining was as described[17] with anti-CD41 purified, anti–rat IgG1 biotin, and streptavidin-Cy5 (supplemental Table 1) and detected by laser scanning microscopy.

Results and discussion

Flow cytometric analysis of CD41 expression was performed on cells from E11 and E12 AGM and YS, E12 placenta, and E14 FL. Time points correspond to organ-specific peaks of HSC activity. In all tissues, AGM (Figure 1A,H), YS (Figure 1E), placenta (Figure 2A), and FL (Figure 2E), 3 distinct cell populations were observed: CD41^{-}, CD41$^{intermediate\ (int)}$ and CD41^{high}, in agreement with YS and AGM data.[7] The highest percentage of CD41$^{int\ +\ high}$ cells is found in placenta, compared with AGM, YS, and FL. This is consistent with the high number of hematopoietic progenitors and HSCs in E12 placenta compared with the other tissues as previously described[15,27,28] and the high proportion of megakaryocytic lineage (CD41^{high}) cells as determined by coexpression of Gp1bβ (not shown). In all tissues, the frequency of CD41^{int} cells is greater than that of CD41^{high} cells.

To test which CD41 fractions contain hematopoietic progenitors, sorted cells were plated in methylcellulose and colonies counted. Hematopoietic progenitors were found almost exclusively in the CD41^{int} fraction of E11 AGM and YS cells (Figure 1B,F). Although the majority of E12 placenta and E14 FL hematopoietic progenitors were present in the CD41^{int} fractions, some were also CD41^{-} (Figure 2B,F). Together, these data suggest that CD41 expression on hematopoietic progenitors is developmentally regulated and/or dependent on the specific tissue microenvironment.

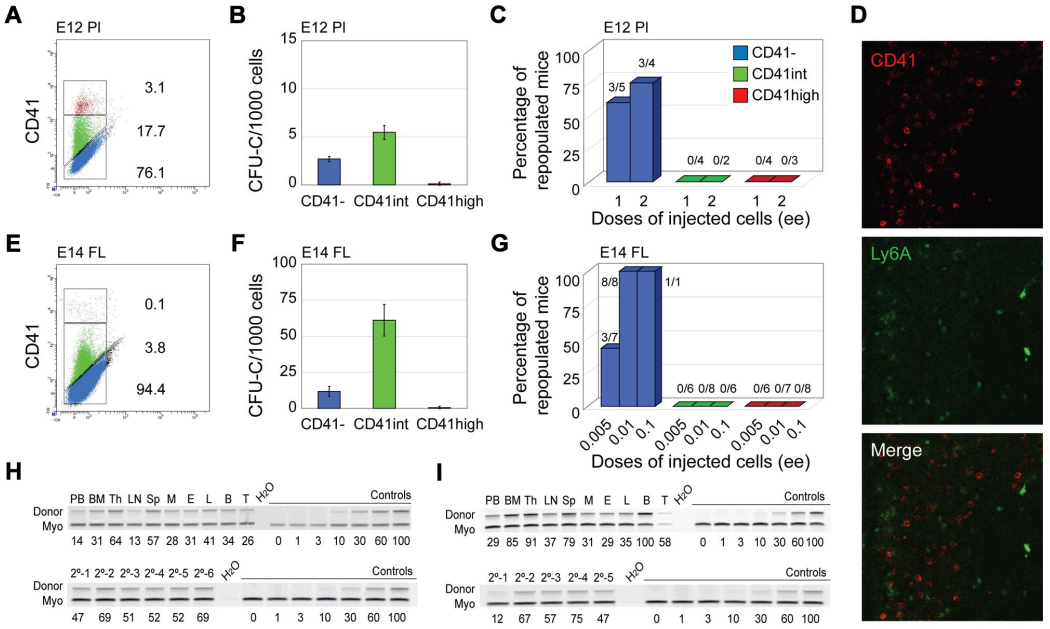

Figure 2. Phenotypic and functional analyses of CD41-sorted cell fractions of embryonic HSC reservoirs. E12 placenta (A-C,H) and E11/E14 liver (D-G,I). (A,E) Flow cytometric analysis of E12 placenta and E14 fetal liver (FL) showing representative sorting gates (red represents CD41^{high}; green, CD41^{int}; and blue, CD41^{-}) and percentages of cells in each fraction. (B,F) In vitro colony-forming unit in culture (CFU-C) analyses showing the total number of hematopoietic progenitors per 1000 cells in each CD41-sorted fraction of E12 placenta and E14 FL cells. Each sample was analyzed in triplicate for each dilution. n = 2 for E12 placenta, and n = 3 for E14 FL. (C,G) In vivo hematopoietic repopulation analysis of CD41-sorted fractions of E12 placenta and E14 FL 4 months after transplantation. Percentage of repopulated mice showing greater than 10% donor chimerism in peripheral blood is shown. Numbers above columns indicate the number of mice repopulated/number of mice transplanted. Dose of injected cells is indicated as embryo equivalents (ee). n = 5 for E12 placenta, and n = 3 for E14 FL. (D) CD41 immunostaining of E11 Ly6A GFP embryo section showing the liver. (Top panel) Red fluorescent CD41 expression in hematopoietic cells. (Middle panel) Green fluorescent Ly6A GFP expression in hematopoietic cells. (Bottom panel) Merged fluorescence. The lack of yellow fluorescence indicates no coexpression of CD41 and Ly6A in liver hematopoietic cells. Image acquisition was from LSM510NLO/FCS confocal microscope (Carl Zeiss BV) with 40×/1.3 NA water objective and Vectashield medium (Vector Laboratories). LSM image software was used (Carl Zeiss BV). (H-I) Representative semiquantitative PCR analysis of hematopoietic tissue DNA 4 months after transplantation from (H upper panel) a primary recipient injected with 2 ee of E12 placenta CD41^{-} cells or (I upper panel) 0.1 ee of E14 FL. Representative semiquantitative PCR analysis of peripheral blood DNA from 6 secondary recipients injected with BM cells from the primary E12 placenta CD41^{-} recipient (H lower panel) and 5 recipients injected with BM cells from the primary E14 FL CD41^{-} recipient (I lower panel). Donor indicates the human β-globin PCR fragment, and Myo indicates the myogenin DNA normalization control PCR fragment. DNA dilution controls (0%-100%) were used to quantitate percentages of donor chimerism that are indicated below each lane. PB indicates peripheral blood; Th, thymus; LN, lymph node; Sp, spleen; M, myeloid (sorted from BM); E, erythroid (sorted from BM); L, lymphoid (sorted from BM); B, B lymphoid (sorted from spleen); and T, T lymphoid (sorted from spleen).

To examine whether HSCs during ontogeny express CD41, each sorted cell fraction from the distinct embryonic tissues was transplanted and donor cell engraftment examined at 4 months after transplantation. As expected, no mice were reconstituted with the CD41^{high} fraction. E11 AGM HSCs were found exclusively in the CD41^{int} fraction (Figure 1C) and were bona fide self-renewing HSCs as shown by high-level, multilineage engraftment of primary and secondary adult recipients (Figure 1J). CD41 expression colocalizes with expression of the Ly6A green fluorescent protein (GFP) HSC marker in some cells closely associated with the ventral aortic endothelium (Figure 1D), and multilineage self-renewing HSCs are enriched in the CD41^{int}Ly6A GFP^{+} fraction (supplemental Figure 1A-B). These data indicate, together with previous live imaging data,[13] that CD41 is a marker for the earliest emerging aortic HSCs as they are transiting from endothelial to hematopoietic fate. In contrast, all E12 AGM HSCs were restricted to the CD41^{-} fraction (Figure 1I), suggesting that CD41, as an AGM HSC marker, is developmentally time dependent. This is consistent with the data of McKinney-Freeman et al[25] showing that, at E11.5, AGM HSCs are in both CD41^{+} and CD41^{-} (CD150^{-}CD48^{-}) fractions.

CD41 expression on HSCs is not AGM restricted because, when sorted E11 (or E12, not shown) YS cells were transplanted, HSCs were found in both CD41^{-} and CD41^{int} fractions (Figure 1G). However, in E12 placenta (Figure 2C,H) and E14 FL (Figure 2G,I), HSCs were exclusively in the CD41^{-} fraction. The presence of HSCs in the E12.5 placenta CD41^{+} fraction was previously reported, but, as stated by the authors, this was probably because of contaminating CD41^{-} cells.[25] At E11.5, no repopulation was found with either the CD41^{int} or CD41^{-} placenta cell fractions (n = 2) because of the extremely low HSC frequency at this time point in the placenta. Thus, we cannot conclude whether the first placental HSCs are CD41 expressing. Immunostainings of E11 FL sections (and flow cytometric analysis of E14 FL) show no overlap in expression of CD41 and Ly6A GFP (Figure 2D; supplemental Figure 1C-D). Thus, CD41 is expressed on HSCs in a time-dependent manner. CD41 expression now adds a further possibility for HSC enrichment during development when used in combination with other known HSC markers (Ly6A, c-kit, CD45, CD34, and CD150; supplemental Figures 1-2).

CD41 as a marker of the earliest HSCs generated in the AGM, together with the finding that some YS HSCs are CD41 expressing, may indicate HSC generation in the YS or HSC migration from the early AGM. CD41 expression on HSCs is lost with developmental time and HSC amplification in placenta, and FL is independent of

CD41 expression. Hence, these data, showing that CD41 is a temporally restricted early HSC marker, are pivotal to future studies of its transcriptional regulation and role in HSC generation/migration.

Acknowledgments

The authors thank Henk Dronk and Experimental Dieren Centrum (Erasmus MC) for mouse care and Reinier van der Linden and Fredrik Wallberg for cell sorting.

This work was supported by The Netherlands Organisation for Scientific Research (VIDI grant 917-76-345, C.R.; and VICI grant 916-36-601, E.D.) and the National Institutes of Health (Merit Award R37 DK51077, E.D.).

Authorship

Contribution: C.R. performed experiments and wrote the paper; K.O., J.-C.B., and A.O. performed experiments; and E.D. wrote the paper.

Conflict-of-interest disclosure: The authors declare no competing financial interests.

The current affiliation of K.O. is Department of Haematology, Cambridge Institute for Medical Research, University of Cambridge, Cambridge, United Kingdom.

Correspondence: Elaine Dzierzak, Erasmus Medical Center, Erasmus MC Stem Cell Institute, Department of Cell Biology, PO Box 2040, 3000 CA Rotterdam, The Netherlands; e-mail: e.dzierzak@erasmusmc.nl.

References

1. Berridge MV, Ralph SJ, Tan AS. Cell-lineage antigens of the stem cell-megakaryocyte-platelet lineage are associated with the platelet IIb-IIIa glycoprotein complex. *Blood.* 1985;66(1):76-85.
2. Debili N, Robin C, Schiavon V, et al. Different expression of CD41 on human lymphoid and myeloid progenitors from adults and neonates. *Blood.* 2001;97(7):2023-2030.
3. Fraser JK, Leahy MF, Berridge MV. Expression of antigens of the platelet glycoprotein IIb/IIIa complex on human hematopoietic stem cells. *Blood.* 1986;68(3):762-769.
4. Ody C, Vaigot P, Quere P, Imhof BA, Corbel C. Glycoprotein IIb-IIIa is expressed on avian multilineage hematopoietic progenitor cells. *Blood.* 1999;93(9):2898-2906.
5. Mitjavila-Garcia MT, Cailleret M, Godin I, et al. Expression of CD41 on hematopoietic progenitors derived from embryonic hematopoietic cells. *Development.* 2002;129(8):2003-2013.
6. Emambokus NR, Frampton J. The glycoprotein IIb molecule is expressed on early murine hematopoietic progenitors and regulates their numbers in sites of hematopoiesis. *Immunity.* 2003;19(1):33-45.
7. Ferkowicz MJ, Starr M, Xie X, et al. CD41 expression defines the onset of primitive and definitive hematopoiesis in the murine embryo. *Development.* 2003;130(18):4393-4403.
8. Mikkola HK, Fujiwara Y, Schlaeger TM, Traver D, Orkin SH. Expression of CD41 marks the initiation of definitive hematopoiesis in the mouse embryo. *Blood.* 2003;101(2):508-516.
9. Yokota T, Huang J, Tavian M, et al. Tracing the first waves of lymphopoiesis in mice. *Development.* 2006;133(10):2041-2051.
10. Hashimoto K, Fujimoto T, Shimoda Y, Huang X, Sakamoto H, Ogawa M. Distinct hemogenic potential of endothelial cells and CD41+ cells in mouse embryos. *Dev Growth Differ.* 2007;49(4):287-300.
11. Li W, Ferkowicz MJ, Johnson SA, Shelley WC, Yoder MC. Endothelial cells in the early murine yolk sac give rise to CD41-expressing hematopoietic cells. *Stem Cells Dev.* 2005;14(1):44-54.
12. Corbel C, Salaun J. AlphaIIb integrin expression during development of the murine hemopoietic system. *Dev Biol.* 2002;243(2):301-311.
13. Boisset JC, van Cappellen W, Andrieu-Soler C, Galjart N, Dzierzak E, Robin C. In vivo imaging of haematopoietic cells emerging from the mouse aortic endothelium. *Nature.* 2010;464(7285):116-120.
14. Yokomizo T, Dzierzak E. Three-dimensional cartography of hematopoietic clusters in the vasculature of whole mouse embryos. *Development.* 2010;137(21):3651-3661.
15. Ottersbach K, Dzierzak E. The murine placenta contains hematopoietic stem cells within the vascular labyrinth region. *Dev Cell.* 2005;8(3):377-387.
16. Rhodes KE, Gekas C, Wang Y, et al. The emergence of hematopoietic stem cells is initiated in the placental vasculature in the absence of circulation. *Cell Stem Cell.* 2008;2(3):252-263.
17. de Bruijn MF, Ma X, Robin C, Ottersbach K, Sanchez MJ, Dzierzak E. Hematopoietic stem cells localize to the endothelial cell layer in the midgestation mouse aorta. *Immunity.* 2002;16(5):673-683.
18. de Bruijn MF, Speck NA, Peeters MC, Dzierzak E. Definitive hematopoietic stem cells first develop within the major arterial regions of the mouse embryo. *EMBO J.* 2000;19(11):2465-2474.
19. Medvinsky A, Dzierzak E. Definitive hematopoiesis is autonomously initiated by the AGM region. *Cell.* 1996;86(6):897-906.
20. Muller AM, Medvinsky A, Strouboulis J, Grosveld F, Dzierzak E. Development of hematopoietic stem cell activity in the mouse embryo. *Immunity.* 1994;1(4):291-301.
21. Chen MJ, Yokomizo T, Zeigler BM, Dzierzak E, Speck NA. Runx1 is required for the endothelial to haematopoietic cell transition but not thereafter. *Nature.* 2009;457(7231):887-891.
22. Zovein AC, Hofmann JJ, Lynch M, et al. Fate tracing reveals the endothelial origin of hematopoietic stem cells. *Cell Stem Cell.* 2008;3(6):625-636.
23. Dzierzak E, Speck NA. Of lineage and legacy: the development of mammalian hematopoietic stem cells. *Nat Immunol.* 2008;9(2):129-136.
24. Matsubara A, Iwama A, Yamazaki S, et al. Endomucin, a CD34-like sialomucin, marks hematopoietic stem cells throughout development. *J Exp Med.* 2005;202(11):1483-1492.
25. McKinney-Freeman SL, Naveiras O, Yates F, et al. Surface antigen phenotypes of hematopoietic stem cells from embryos and murine embryonic stem cells. *Blood.* 2009;114(2):268-278.
26. Strouboulis J, Dillon N, Grosveld F. Developmental regulation of a complete 70-kb human beta-globin locus in transgenic mice. *Genes Dev.* 1992;6(10):1857-1864.
27. Alvarez-Silva M, Belo-Diabangouaya P, Salaun J, Dieterlen-Lievre F. Mouse placenta is a major hematopoietic organ. *Development.* 2003;130(22):5437-5444.
28. Gekas C, Dieterlen-Lievre F, Orkin SH, Mikkola HK. The placenta is a niche for hematopoietic stem cells. *Dev Cell.* 2005;8(3):365-375.

Table S1. List of antibodies

Marker	Fluorochrome	Clone	Supplier
Staining for sorting and analysis			
CD41	PE	MwReg30	Santa Cruz Biotechnology
c-kit	APC-Alexa fluor 750	2B8	Caltag
CD45	FITC	30-F11	BD Pharmingen
CD34	Alexa fluor 647	RAM34	eBioscience
CD150	APC	9D1	eBioscience
Multilineage repopulation analysis			
CD4	PE	GK1.5	BD Pharmingen
CD8a	PE	53-6.7	BD Pharmingen
B220	FITC	RA3-6B2	BD Pharmingen
Ly6C	FITC	AL-21	BD Pharmingen
CD31	PE	MEC13.3	BD Pharmingen
Ly5.1	PE	A20	BD Pharmingen
Ly5.2	FITC	104	BD Pharmingen
Immunostaining			
CD41	purified	MwReg30	BD Pharmingen
rat IgG1	biotin	RG11/39.4	BD Pharmingen
Streptavidin	Cy5	-	Rockland Immunochemicals

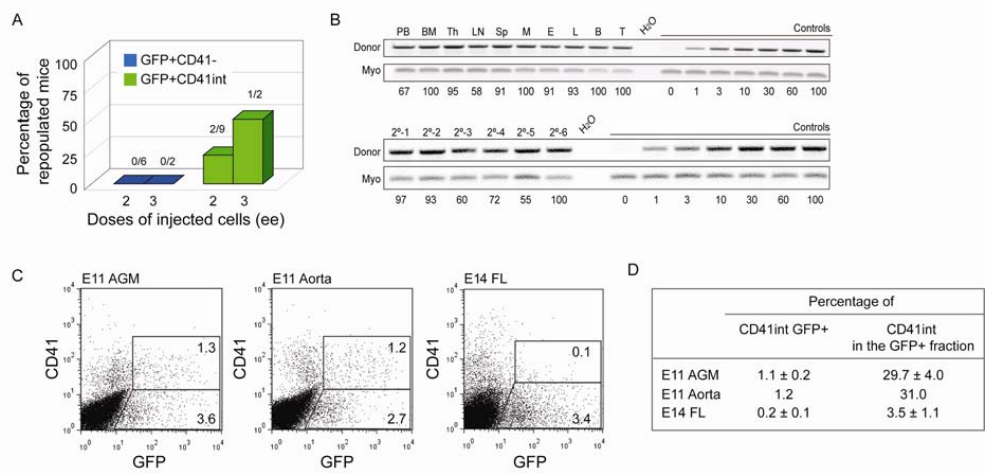

	Percentage of	
	CD41int GFP+	CD41int in the GFP+ fraction
E11 AGM	1.1 ± 0.2	29.7 ± 4.0
E11 Aorta	1.2	31.0
E14 FL	0.2 ± 0.1	3.5 ± 1.1

Figure S1. CD41 expression analysis in Ly6A GFP embryos. (A) In vivo hematopoietic repopulation analysis of CD41 sorted fractions of E11 Ly6A GFP AGM at four months post transplantation. Percentage of repopulated mice with greater than 10% donor chimerism in peripheral blood is shown. Numbers above columns indicate the number of mice repopulated/number of mice transplanted. Dose of injected cells is indicated as embryo equivalents (ee). n=3. (B) Representative semiquantitative PCR analysis (upper panel) of hematopoietic tissue DNA at 4 months post-transplantation from a primary recipient injected with 2ee of E11 AGM CD41^{int} Ly6A GFP^{+} cells. Representative semiquantitative PCR analysis (lower panel) of peripheral blood DNA from six secondary recipients injected with BM cells from the primary recipient. Donor indicates the *Ly6A GFP* PCR fragment and Myo indicates the *myogenin* DNA normalization control PCR fragment. DNA dilution controls (0 to 100%) were used to quantitate percentages of donor chimerism that are indicated below each lane. PB=peripheral blood; BM=bone marrow; Th=thymus; LN=lymph node; Sp=spleen, M=myeloid (sorted from BM); E=erythroid (sorted from BM); L=lymphoid (sorted from BM); B= B lymphoid (sorted from spleen); T=T lymphoid (sorted from spleen). (C) Flow cytometric analysis of E11 AGM, E11 aorta and E14 fetal liver (FL) cells obtained from Ly6A GFP embryos. Representative gates for CD41^{int}Ly6A GFP^{+}, CD41^{-}Ly6A GFP^{+} are shown. The percentage of cells in each fraction is indicated. (D) Table presenting the percentage of CD41^{int}Ly6A GFP^{+} cells and the percentage of CD41^{int} cells in the Ly6A GFP^{+} fraction.

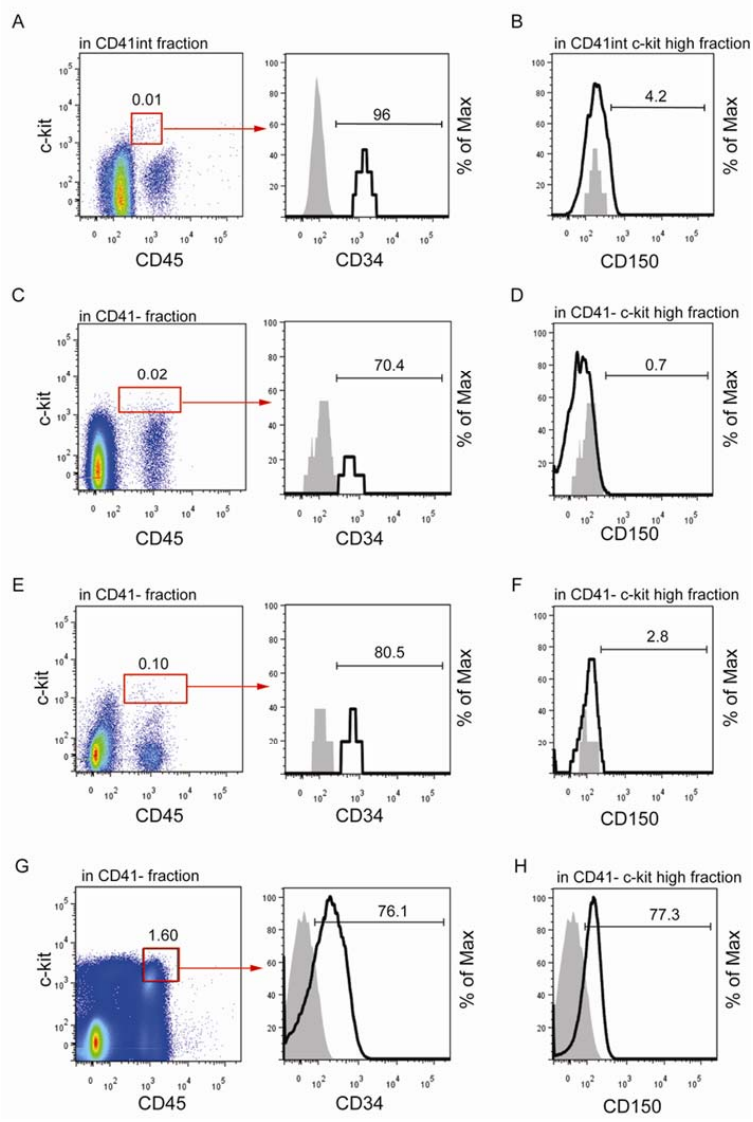

Figure S2. Multicolor staining analysis. Analyses of CD41 cell fractions in (A,B) E11 AGM, (C,D) E12 AGM, (E,F) E12 placenta and (G,H) E14 fetal liver (FL). (A,C,E,G, left panels) c-kit and CD45 expression in CD41^{int} fraction (E11 AGM) and CD41^{-} fraction (E12 AGM, E12 placenta, E14 FL). (A,C,E,G, right panels) CD34 expression in gated c-kit^{high}CD45$^{int/+}$ fractions (red gate in left panel). (B,D,F,H) CD150 expression in CD41^{int}c-kit^{high} (E11 AGM) and CD41^{-}c-kit^{high} (E12 AGM, E12 placenta, E14 FL) fractions. Percentages of cells are indicated. Gray histograms: controls. Bold black histogram: antibody staining. Note that populations are gated based on HSC marker expression found in our study and in the literature.
E11 AGM HSCs are CD41^{int}c-kit^{high}CD45^{int}CD34^{++}CD150^{-}
E12 AGM HSCs are CD41^{-}c-kit^{high}CD45$^{int/+}$CD34^{+}CD150^{-}
E12 placenta HSCs are CD41^{-}c-kit^{high}CD45^{int}CD34^{+}CD150^{-}
E14 FL HSCs are CD41^{-}c-kit^{high}CD45^{+}CD34^{+}CD150^{+}

Chapter 5 –
Integrin αIIb (CD41) plays a role in the maintenance of hematopoietic stem cells in the mouse embryo aorta

Submitted

Integrin αIIb (CD41) plays a role in the maintenance of hematopoietic stem cells in the mouse embryo aorta.

Jean-Charles Boisset, Thomas Clapes, Reinier van der Linden, Elaine Dzierzak and Catherine Robin

Erasmus University Medical Center, Dept. of Cell Biology, Erasmus MC Stem Cell Institute, PO Box 2040, 3000 CA Rotterdam, NL

ABSTRACT

Integrins play important roles as modulators of cell behaviour through their adhesion properties and the initiation of signaling cascades. αIIb subunit is one of the first cell surface markers indicative of hematopoietic commitment. αIIb pairs exclusively with β3 to form the αIIbβ3 integrin. β3 also pairs with αv to form the αvβ3 integrin. The expression and putative role of these integrins during mouse hematopoietic development is as yet unknown. We show here that hematopoietic stem cells (HSCs) differentially express αIIbβ3 and αvβ3 integrins throughout development. Whereas the first HSCs generated in the aorta at mid-gestation express both integrins, HSCs from the placenta only express αvβ3, and most fetal liver HSCs do not express either integrin. By using αIIb deficient embryos, we show that αIIb is not only a reliable HSC marker but it also plays an important and specific function in maintaining the HSC activity in the mouse embryonic aorta.

INTRODUCTION

Hematopoietic Stem Cells (HSCs) are at the foundation of the blood system and are the key cell type in transplantation protocols for blood-related disorders. The number of HSCs available for clinical applications and fundamental research is limited. It remains difficult at present to efficiently expand and/or generate HSCs in vitro mainly because the mechanisms underlying the generation and growth of HSCs, including the specific interactions between HSCs and the surrounding microenvironment occurring in vivo, are poorly understood.

Adult HSCs are initially generated during embryonic development[1]. They are first detected at embryonic day (E)10.5 of mouse development in the Aorta-Gonad-Mesonephros (AGM) region[2-3]. Starting at E11, HSCs are also found in the yolk sac (YS), placenta and fetal liver (FL). The pool of HSCs massively expands in the two later sites before colonizing in the bone marrow

(BM) from E17 onward[4-5]. Studies performed in the zebrafish, chicken and mouse models have clearly demonstrated that HSCs originate from specialized endothelial cells referred as hemogenic[1]. HSCs most likely reside in clusters of cells (Intra-Aortic Hematopoietic Clusters, IAHCs) that are tightly attached to the endothelium of the aorta, the vitelline and umbilical arteries, and the vascular labyrinth of the placenta[6-7]. In adult BM, HSCs localize in specialized niches that maintain the balance between HSC self-renewal, quiescence and differentiation. Adhesion molecules (including integrins) are important for the binding of HSCs to the niche microenvironment compounds[8-13]. In contrast to adult, the specific interactions and cell adhesion properties of HSCs in the aorta and within the successive developmental niches are still poorly described.

Integrins are transmembrane glycoproteins (gp) that play an important role in cell adhesion, survival, proliferation, differentiation, migration, gene regulation, and cytoskeletal arrangement. They form a family of 24 heterodimeric receptors composed of α (18 types) and β (8 types) subunits[14]. While some integrins are ubiquitously expressed, others are tissue or cell lineage specific[15]. Adult HSCs express several integrins important for homing and migration (e.g. α4β1, α5β1, α6β1)[8,16-18]. In embryo, αIIb (platelet (gp)IIb or CD41) is one of the earliest surface markers of hematopoietic commitment[19-24]. By performing time-lapse confocal imaging on live mouse embryo slices, we have shown that αIIb expression indeed coincides with the formation of Hematopoietic Stem/Progenitor Cells (HSPCs) from the hemogenic aortic endothelium[25-26]. Moreover, αIIb is located at the point of contact between the cells composing the IAHCs. αIIb expression is developmentally regulated since HSCs express αIIb in E11 AGM, but not in E12 AGM, E12 placenta or E14 FL[21,24,27]. αIIb deficient mice have no lineage commitment problems in the BM[28]. However, they have defective platelets and display bleeding disorders similar to those seen in β3 deficient mice[29] and in humans with Glanzmann thrombasthenia disease.

To date little is known about integrin expression and function in HSCs throughout embryonic development. Hence, we investigated the expression pattern of αIIb, β3 and v integrin subunits on HSCs in the main hematopoietic sites (AGM, YS, placenta, and FL). αIIb exclusively associates with β3 to form the major platelet integrin αIIbβ3 (gpIIb/IIIa or CD41/CD61). β3 also associates with αv to form the αvβ3 integrin (CD51/CD61). By performing stringent long-term transplantations of sorted populations based on integrin expression, we showed that newly generated HSCs in E11 AGM express αIIbβ3 integrins whereas HSCs from E12 placenta and E14 FL do not. AGM and placental HSCs express αvβ3 but most E14 FL HSCs do not. E12 YS contains all three types of HSCs (expressing or not αIIbβ3 and/or αvβ3). Finally, we observed a dramatic HSC defect in the AGM but not in the YS and FL of αIIb deficient embryos. Overall, our data show that αIIb plays a fundamental and

precise spatio-temporal role to maintain the HSC activity in the aorta of the mouse embryo.

METHODS

Mice and embryo generation

Embryos were generated from crosses of hβ-globin ln72 mice and wild-type (C57BL/10 x CBA)F1 females; Ly5.1 males and females; $\alpha IIb^{+/-}$ males and $\alpha IIb^{+/+}$ or $\alpha IIb^{+/tk}$ females; $\alpha IIb^{tk/tk}$ males and $\alpha IIb^{+/+}$ or $\alpha IIb^{+/tk}$ females; wild-type C57BL/6 females and males. The day of vaginal plug observation is embryonic day (E)0. ln72, YMT and αIIb genotypes were determined by DNA PCR. Mice were housed according to institutional guidelines and all animal procedures were carried out in compliance with the standards for human care and use of laboratory animals.

Dissections and cell preparation

E11-E14 embryos were isolated. Tissues (AGM, FL, YS, placenta) were dissected and dissociated as previously described[30]. Viable cells were counted (using trypan blue) and kept in phosphate-buffered saline (PBS), 10% fetal calf serum, and penicillin/streptomycin (PBS/FCS/PS) at 4°C for further analysis.

Explant culture

Whole AGMs were cultured as explants at 37°C for 3 days as previously described[2]. For the αIIb mutant AGM explant, the culture was performed with no added cytokines. To test the number of $CD41^{int}CD61^{int}CD45^{int}c\text{-}kit^{+}$ cells per wild-type AGM, the medium was supplemented or not with 200 ng/ml of recombinant murine IL-3[31] or 250 ng/ml of gremlin[32].

Hematopoietic progenitor assay

In vitro hematopoietic progenitor analysis was performed on dilutions of sorted cells plated in triplicates in methylcellulose medium (StemCell Technologies). Plates were incubated at 37°C in a humidified chamber under 5% CO2. Hematopoietic colonies were counted with an inverted microscope at day 12 of the culture.

In vivo transplantation assay and transplanted mice analysis

Intravenous injection of total or sorted cells into irradiated adult wild-type recipients was as previously described[31]. Recipient female mice ((129/SVxC57BL/6), C57BL/6 or (CBA x C57BL/10)) were exposed to a split dose of 9 Gy of γ-irradiation (^{137}Cs source) and injected with several cell doses (or embryo equivalent, ee). $2x10^5$ spleen cells (recipient background) were co-injected to promote short-term survival.

Blood was obtained at 1 and 4 months post-transplantation and DNA was analyzed for donor cell markers by semiquantitative PCR (hβ-globin, αIIb, Ymt). The percentage of donor contribution was calculated from a standard curve of DNA control dilutions (0 to 100% donor marker). Recipients were considered repopulated when the chimerism was greater than 10%. For multilineage repopulation analysis, thymus, lymph nodes, bone marrow and spleen were dissected from the repopulated recipients. T, B, erythroid, and myeloid cells were sorted from recipient BM and spleens after antibody staining (see below). Primary recipient BM cells were injected into secondary irradiated recipients to assess self-renewal capacity ($0.5x10^6$ or $2x10^6$ cells injected per recipient; Fig.5D). For the Ly5.2 recipients (C57BL/6) injected with Ly5.1 cells, the chimerism was determined by flow cytometry (see below). Recipients were considered repopulated when the chimerism was greater than 5%.

Flow cytometric analysis and sorting

Flow cytometry analysis and sorting were performed on a FACSscan and/or AriaIII (BD Bioscience) with CellQuest. Stainings were performed in PBS/FCS/PS for 30 minutes at 4°C. Cells were washed and resuspended in PBS/FCS/PS and 7AAD (Molecular Probes, Leiden, NL) or Hoechst 33258 (1 μg/ml, Molecular Probes) for dead cell exclusion. The positive gates were defined from staining with isotype-matched control antibodies. Monoclonal antibodies (BD Pharmingen, eBioscience, Invitrogen, Santa Cruz, Biolegends) used: FITC-anti-Ter119, FITC-anti-CD42 (Gp1bβ); PE-anti-CD41; APC-anti-CD61; APC-Cy7 or APC-AlexaFluor750-anti-c-kit; FITC, PE or PE-Cy7-anti-CD31; PerCP-Cy5.5-anti-CD45; APC or Pacific Blue-anti-CD34; Alexa-Fluor488-anti-CD51.

For the Ly5.2 recipients injected with Ly5.1 cells, the chimerism was determined by flow cytometry on blood after erythrocyte lysis (Beckman Coulter) and staining with FITC-anti-Ly5.2, PE-anti-Ly5.1 and 7-AAD. Flow cytometry data were analyzed with FlowJo.

For multilineage repopulation analysis, spleen cells were stained with FITC-anti-B220, PE-anti-CD8a and PE-anti-CD4; bone marrow cells were stained

with FITC-anti-Ly6C and PE-anti-CD31.

Whole-mount immunostaining

The whole-mount immunostaining was performed as previously described[7]. Rat anti-mouse primary antibodies for c-Kit (2B8) and biotinylated anti-CD31 (MEC13.3) were used (BD Biosciences). Secondary antibodies were goat anti-rat IgG-Alexa647 (Invitrogen) and streptavidin-Alexa594 (Invitrogen). Embryo caudal halves were imaged using a Leica SP5 confocal microscope.

Staining and Confocal Microscopy of non-fixed embryo and placenta slices

Non-fixed wild-type embryos were cut into thick transversal slices (200 μm) and stained with directly conjugated monoclonal antibodies as previously described[25-26]. The antibodies include: PE-anti-CD41 (MWreg30), Alexa488-anti-CD51 (RMV-7), APC-anti-CD61. Similarly, placentas isolated from E12 non-fixed wild-type embryos were cut into slices (200 μm) and were incubated with PE-anti-Tie-2, Alexa488-anti-CD51 (RMV-7) and APC-anti-CD61. Slices were immobilized into agarose gel and imaged by using a Leica SP5 confocal microscope.

RESULTS

Hematopoietic stem cells differentially express αIIbβ3 and αvβ3 integrins throughout development.

HSCs are restricted to the CD41intermediate (CD41int) fraction in E11 AGM[21,24]. However, HSCs in E12 AGM and placenta, and E14 FL, are exclusively in the $CD41^-$ fraction. In YS, HSCs are in both populations[24]. To further investigate integrin expression on HSCs, we performed flow cytometry analyses for αIIb (CD41), αv (CD51) and β3 (CD61) subunits. The expression profiles differed between tissues (Fig.1). $CD41^{int}CD61^-$ cells were only found in E11 AGM (Fig.1A), and not in E12 YS (Fig.1C), E12 placenta (Fig.1E) or E14 FL (Fig.1G). $CD41^-CD61^{high}$ cells were mainly in E12 placenta (Fig.1E) and to a less extent in E11 AGM (Fig.1A). Three distinct cell populations were present in all tissues: $CD41^-CD61^-$, $CD41^-CD61^{int}$ and $CD41^{int}CD61^{int}$.

To determine whether HSCs in E11 AGM expressed both αIIb and β3 subunits, $CD41^{int}CD61^-$ and $CD41^{int}CD61^{int}$ fractions were sorted and injected into adult wild-type irradiated recipients (n=2). Four months post-

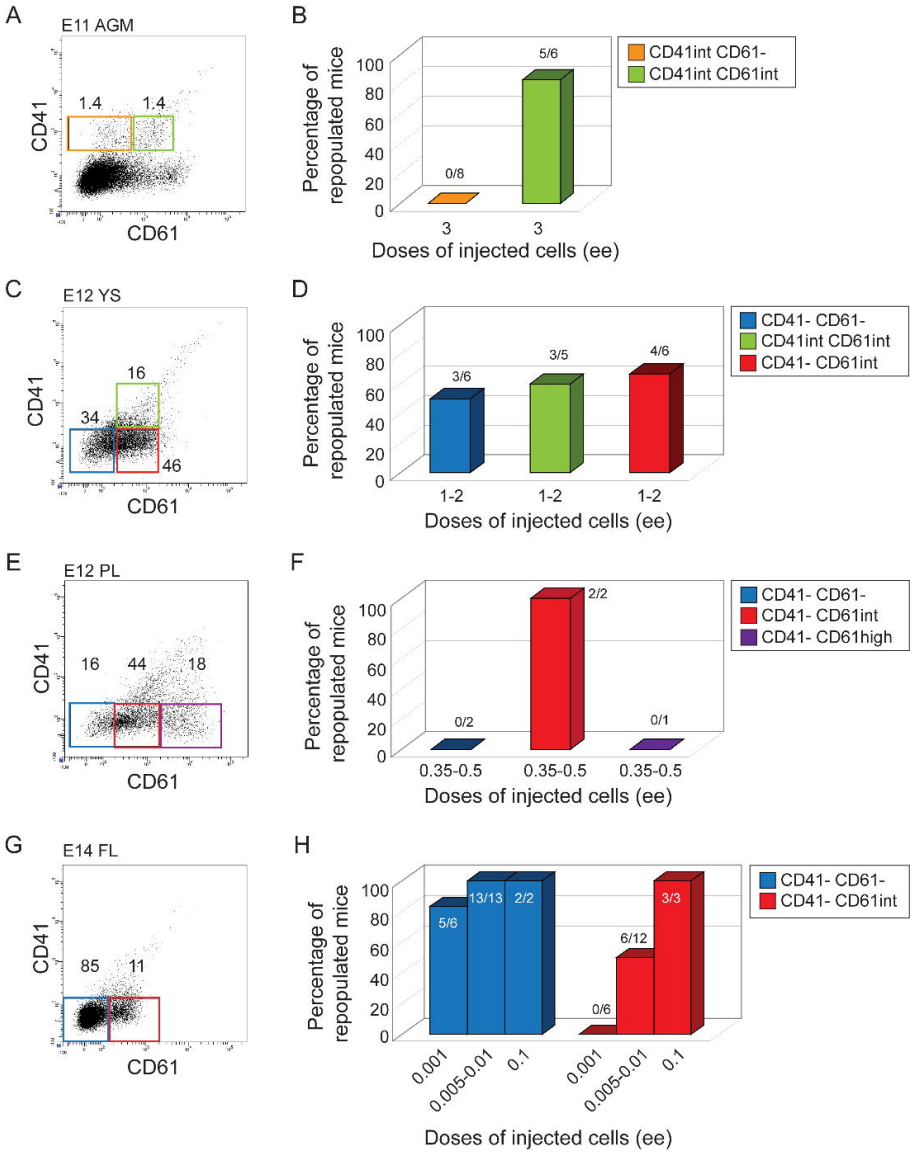

Figure 1. Phenotypic and functional analyses of integrin based sorted cell fractions isolated from embryonic tissues. (A,B) E11 Aorta-Gonad-Mesonephros (AGM), (C,D) E12 yolk sac (YS), (E,F) E12 placenta (PL) and (G,H) E14 fetal liver (FL). (A,C,E,G) Flow cytometric analysis of E11 AGM, E12 YS, E12 PL and E14 FL respectively. Representative sorting gates of each populations sorted based on CD41 (αIIb) and CD61 (β3) expression and tested in transplantation assays (orange: $CD41^{int}CD61^{-}$; green: $CD41^{int}CD61^{int}$; blue: $CD41^{-}CD61^{-}$; red: $CD41^{-}CD61^{int}$; purple: $CD41^{-}CD61^{high}$). The percentages of cells in each fraction are indicated next to the gates. (B,D,F,H) In vivo hematopoietic repopulation analysis of mice after the injection of integrin based sorted fractions of E11 AGM (n=2), E12 YS (n=4), E12 PL (n=2) and E14 FL (n=3) at 4 months post-transplantation. Percentage of repopulated mice showing greater than 10% donor chimerism in peripheral blood is shown. Numbers above columns indicate the number of mice repopulated/number of mice injected. Dose of injected cells is indicated as embryo equivalent (ee).

transplantation, the mice injected with $CD41^{int}CD61^{int}$ cells were reconstituted. No mice injected with $CD41^{int}CD61^{-}$ cells were reconstituted, even with a high cell dose (3 ee per mouse) (Fig.1B). The analysis of blood, BM, spleen, lymph nodes and thymus of the primary reconstituted recipients has shown that $CD41^{int}CD61^{int}$ cells were genuine HSCs as they provided high level multilineage engraftment (Supplemental Fig.1, top panel). The successful engraftment of the secondary recipients demonstrated the ability of the donor HSCs to self-renew (Supplemental Fig.1, bottom panel). 95% of the $CD41^{int}CD61^{int}$ cells expressed CD51 (Table 1). At E12, AGM HSCs were $CD41^{-}$ [24] but still expressed CD51 (Table 1). Thus, all newly generated HSCs in E11 AGM express both αIIbβ3 and αvβ3 integrins.

YS HSCs are found in both $CD41^{-}$ and $CD41^{int}$ fractions at E11 and E12[24]. In combination with CD61, three cell fractions were sorted from E12 YS ($CD41^{-}CD61^{-}$, $CD41^{-}CD61^{int}$ and $CD41^{int}CD61^{int}$ (Fig.1C)) and transplanted (n=4). Multilineage engraftment was obtained with all fractions (Fig.1D). Similar to E11 AGM HSCs, YS cells in the $CD41^{int}CD61^{int}$ and $CD41^{-}CD61^{int}$ fractions expressed CD51 (97% and 72% respectively) (Table 1). On the other hand, the majority of $CD41^{-}CD61^{-}$ cells did not express CD51 (Table 1). Thus, YS and AGM contain HSCs that express both αIIbβ3 and αvβ3 integrins, whereas some YS HSCs express solely αvβ3 integrin or none of these integrins.

HSCs in placenta and FL are $CD41^{-}$ [24]. $CD41^{-}CD61^{-}$, $CD41^{-}CD61^{int}$ and $CD41^{-}CD61^{high}$ (only present in placenta) fractions were sorted (Fig.1E, G) and transplanted (placenta: n=2, FL: n=3). The placental $CD41^{-}CD61^{int}$ fraction (but not the $CD41^{-}CD61^{-}$ fraction) contained HSCs (Fig.1F). Most of $CD41^{-}CD61^{int}$ cells expressed CD51 (86%) (Table 1). Thus, $CD41^{-}CD61^{int}$ HSCs in placenta express only αvβ3 integrin and therefore resemble $CD41^{-}CD61^{int}$ YS HSCs. In E14 FL, HSCs were in both $CD41^{-}CD61^{-}$ and $CD41^{-}CD61^{int}$ fractions (Fig.1H). Limiting cell dilution transplantations (0.001 to 0.1 ee) showed that HSCs were enriched in the $CD41^{-}CD61^{-}$ fraction (Fig.1H). Similarly to E12 placenta and YS, $CD41^{-}CD61^{int}$ FL cells also expressed CD51

Table I. Percentage of CD51+ cells in the cell fractions enriched in hematopoietic stem cells.

Tissue	Embryonic day	Cell fraction	Percentage of $CD51^{+}$ cells in the cell fraction
AGM	E11	$CD41^{int}CD61^{int}$	95
	E12	$CD41^{-}$	96
Placenta	E12	$CD41^{-}CD61^{int}$	86
YS	E12	$CD41^{int}CD61^{int}$	97
		$CD41^{-}CD61^{int}$	72
		$CD41^{-}CD61^{-}$	34
FL	E14	$CD41^{-}CD61^{int}$	98
		$CD41^{-}CD61^{-}$	8

(98%) (Table 1). In contrast, $CD41^{-}CD61^{-}$ FL cells did not express CD51 (Table 1). Thus all HSCs in the placenta express αvβ3 but not αIIbβ3 integrins, whereas most HSCs in the FL do not express these integrins.

E11 AGM hematopoietic stem cells are enriched in the $CD41^{int}$ $CD61^{int}$ $CD45^{int}$ $c\text{-}kit^{+}$ subpopulation.

To determine whether E11 AGM CD41intCD61int population could be further enriched in HSCs, integrin expression was used in combination with the pan-hematopoietic marker CD45 and the HSC marker c-kit[33]. All committed cells from erythroid (Ter119+) and megakaryocytic (Gp1bβ+) lineages were first excluded (Supplemental Fig.2A, left panel). The $CD41^{int}CD61^{int}$ fraction that contains all HSCs (Fig.1A,B) was further subdivided into four subfractions: $CD45^{-}c\text{-}kit^{-}$, $CD45^{-}c\text{-}kit^{+}$, $CD45^{int}c\text{-}kit^{+}$ and $CD45^{high}c\text{-}kit^{+}$ (Supplemental Fig.2A, middle and right panels). Each subfraction was injected into recipients that were analyzed at 1 month (for short-term repopulation, STR) and 4 months (for long-term repopulation, LTR) post-transplantation (n=8). As expected, $CD45^{-}c\text{-}kit^{-}$ and $CD45^{-}c\text{-}kit^{+}$ subfractions were not able to reconstitute mice, even with high doses of injected cells (5-10 ee) (Supplemental Fig.2C). Interestingly, $CD45^{int}c\text{-}kit^{+}$ and $CD45^{high}c\text{-}kit^{+}$ subfractions yielded short-term repopulation (Supplemental Fig.2C, left panel) but only the $CD45^{int}c\text{-}kit^{+}$ subfraction was capable of long-term repopulation (Supplemental Fig.2C, right panel). These cells provided high level multilineage reconstitution of the primary and secondary transplanted recipients (Supplemental Fig.2B). Thus, the $CD41^{int}CD61^{int}$ population contains both STR-HSCs and LTR-HSCs that both express CD45 and c-kit. However, STR-HSCs and LTR-HSCs can be discriminated based on the level of CD45 expression. STR-HSCs are $CD45^{high}$ while LTR-HSCs are $CD45^{int}$. There is as few as 96±31 $CD41^{int}CD61^{int}CD45^{int}c\text{-}kit^{+}$ cells per E11 AGM (n=6). Thus, the combination of integrin expression with other hematopoietic markers such as CD45 and c-kit can be used to discriminate cell populations highly enriched in STR-HSCs and LTR-HSCs in E11 AGM.

Interestingly, the number of $CD41^{int}CD61^{int}CD45^{int}c\text{-}kit^{+}$ cells per AGM was spectacularly increased when E11 AGMs were cultured as explant in presence of IL-3 and decreased in presence of Gremlin (when compared to the culture performed in non-supplemented medium) (Supplemental Fig.2D,E). It was consistent with our previous findings that IL-3 is a powerful amplification factor for embryonic HSCs[31] while Gremlin (a BMP antagonist) abolishes HSC activity in E11 AGM[32,34]. Therefore, our defined in vitro explant culture system can be used to rapidly test the effects of specific molecules/reagents on phenotypically defined HSC populations.

Localization of αIIb, αv and/or β3 integrin subunits expressing cells in the AGM and placenta.

To determine the precise location of the cells expressing αIIb, αv and/or β3, multicolour stainings were performed with directly labelled antibodies on non-fixed tissues. We used the technique that we previously developed to stain non-fixed embryo slices[26]. We observed CD41^{int}CD51^{int}CD61^{int} cells in the IAHCs attached to the aortic endothelium of E10.5 embryos (Fig.2A). Interestingly, the integrin subunits were concentrated at the junction between the cells forming the IAHCs.

We adapted the embryo slice staining technique to non-fixed placenta slices. E12 placentas were sliced and stained with directly labelled anti-Tie-2 antibodies (Fig.2B). This technique resulted in a very specific staining of both placental

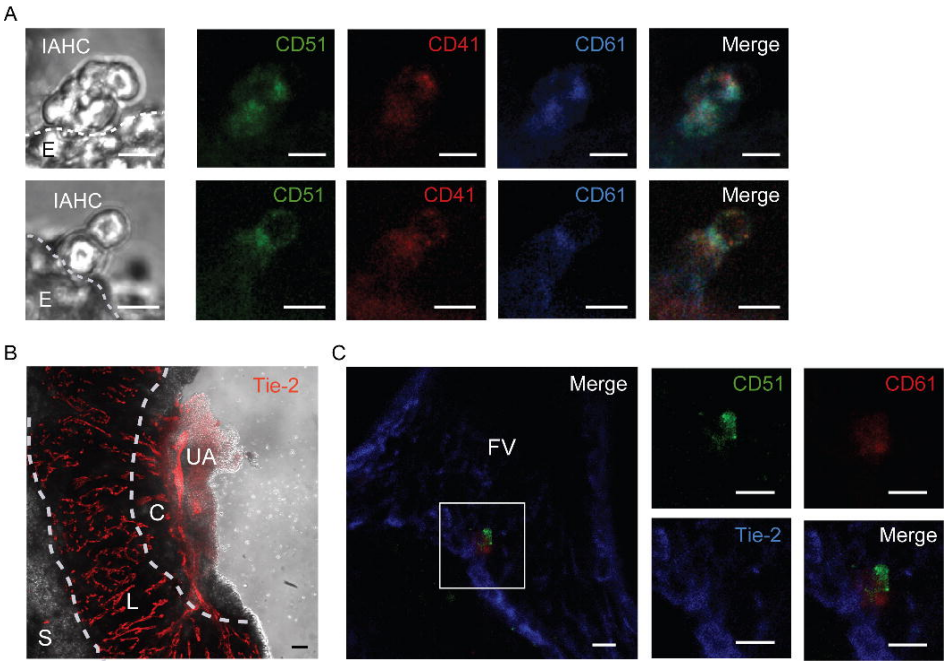

Figure 2. Location of phenotypically defined hematopoietic stem cells in AGM and placenta. (A) Examples of intra-aortic hematopoietic clusters attached to the aortic endothelium of E10.5 wild-type embryos. Non-fixed embryo slices were stained with directly labelled antibodies against CD51 (αv, green), CD41 (αIIb, red) and CD61 (β3, blue) and imaged with a confocal microscope. Transmitted light, individual and merged fluorescent images are shown. The right panel is a schematic representation of the cluster where the black lines indicate the concentrated expression of the CD41, CD51 and CD61. Scale bar: 10 μm. (B) Non-fixed placenta slices (E12) were stained with antibodies against Tie-2 (red) and imaged with a confocal microscope. Transmitted light and fluorescent images are merged. (C) Confocal stack image of an E12 non-fixed placenta slice stained with directly labelled antibodies against CD51 (green), CD61 (red) and Tie-2 (blue). Close up of the boxed area from the left panel shows a group of labelled cells (single and merged fluorescent channels are shown). Scale bar, 10 μm. UA: umbilical artery, C: chorionic plate, L: labyrinth, S: spongiotrophoblast layer, FV: fetal vessel.

vessels and umbilical artery (UA). This allowed delimitating the different parts of the placenta, including the chorionic plate (C), the vascular labyrinth (L) and the spongiotrophoblast layer (S) (Fig.2B). To localize phenotypically defined HSCs in the placental vessels (V), multicolour staining was performed with antibodies anti-Tie-2, CD51 and CD61 (Fig.2C). We observed groups of $CD51^{int}CD61^{int}$ cells in the vasculature of the chorionic plate. Similarly to the aorta, the integrin subunits were concentrated at the junction between the cells (Fig.2C). Thus, the staining of non-fixed embryo and placenta slices allows the precise localization of phenotypically defined HSCs in the IAHCs of the aorta and in the vasculature of the placental chorionic plate.

IIb deficient embryos have no qualitative or quantitative defects in hematopoietic progenitors or IAHCs in the AGM.

All hematopoietic progenitors are CD41int in E11 AGM[24]. To test whether the absence of αIIb has an effect on the production of hematopoietic progenitors, AGM cells from E11 wild-type ($\alpha IIb^{+/+}$) and αIIb mutant ($\alpha IIb^{+/tk}$ and $\alpha IIb^{tk/tk}$) embryos[28] were isolated and tested in a semi-solid clonogenic assay (n=3). As shown in Fig.3A, AGMs isolated from E11 mutant embryos contained all types of erythroid and/or myeloid progenitors. The numbers of total CFU-C and of each type of progenitor were similar in mutant and wild-type embryos. Thus, the absence of αIIb on the surface of the AGM cells does not influence the number or types of progenitors found in this region.

Whole embryo staining of $\alpha IIb^{+/+}$, $\alpha IIb^{+/tk}$ and $\alpha IIb^{tk/tk}$ E11 embryos for CD31 (to visualize the endothelium and IAHCs) and c-kit (to visualize all IAHCs) revealed no differences in IAHC cell number (Fig.3B) or in IAHC organization or shape (Fig.3C,D). In fact, it seems that there is slightly more IAHC cells in the αIIb mutant embryos than in the wild-type embryos (Fig.3B). Thus, either αIIb is not needed for the formation, organization and anchorage of the IAHCs or other integrins/adhesion molecules have a redundant effect and compensate for the absence of αIIb.

αIIb deficient embryos have a strong hematopoietic stem cell defect in the AGM.

To test whether αIIb plays a functional role on the surface of AGM HSCs, transplantations were performed with cells isolated from E11 wild-type ($\alpha IIb^{+/+}$) and αIIb mutants ($\alpha IIb^{+/tk}$ and $\alpha IIb^{tk/tk}$) AGMs (n=3). Whereas 72% of the mice injected with $\alpha IIb^{+/+}$ cells were reconstituted, only 29% and 38% of mice were reconstituted with $\alpha IIb^{+/tk}$ or $\alpha IIb^{tk/tk}$ cells, respectively, at four months post-transplantation (Fig.4A). Interestingly, the percentage of donor

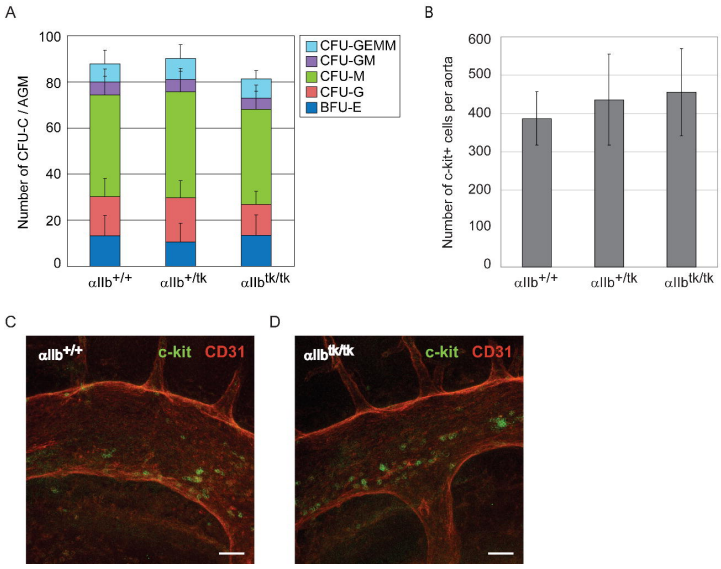

Figure 3. Intra-aortic hematopoietic clusters and in vitro clonogenic progenitor activity in E11 AGMs isolated from CD41 (αIIb) deficient embryos. (A) In vitro Colony-Forming Unit in Culture (CFU-C) analyses show the number of erythro-myeloid progenitors per AGM. AGM regions were isolated from E11 wild-type ($\alpha IIb^{+/+}$), haploinsufficient ($\alpha IIb^{+/tk}$) or deficient embryos for CD41 ($\alpha IIb^{tk/tk}$). Each sample was analysed in triplicate for each dilution. Error bars represent standard deviations for n=3 independent experiments. CFU-GEMM: CFU-Granulocyte-Erythroid-Macrophage-Megacaryocyte; CFU-GM: CFU-Granulocyte-Macrophage; CFU-M: CFU-Macrophage; CFU-G: CFU-Granulocyte; BFU-E: Burst-Forming Unit-Erythroid. (B) The graph represents the number of c-kit+ cells per of E11 $\alpha IIb^{+/+}$ (n=5 embryos), $\alpha IIb^{+/tk}$ (n=5 embryos) and $\alpha IIb^{tk/tk}$ (n=3 embryos) aorta. Error bars represent the standard deviations. Confocal stack images of the mouse aorta region of E11 $\alpha IIb^{+/+}$ (C) and $\alpha IIb^{tk/tk}$ (D) embryos after whole mount staining for c-kit (green) and CD31 (red). Scale bars: 50 μm.

chimerism was lower in the few mice repopulated with $\alpha IIb^{+/tk}$ or $\alpha IIb^{tk/tk}$ cells (10% average chimerism) as compared to the mice injected with $\alpha IIb^{+/+}$ cells (60% average chimerism) (Fig.4A, red bars). The reconstitution with $\alpha IIb^{tk/tk}$ cells resulted in multilineage engraftment (Supplemental Fig.3B,C), similar to the mice reconstituted with $\alpha IIb^{+/+}$ cells (Supplemental Fig.3A). To examine the self-renewal property of $\alpha IIb^{tk/tk}$ AGM HSCs, secondary transplantations were performed with BM cells isolated from two primary recipients repopulated with $\alpha IIb^{tk/tk}$ cells and one recipient repopulated with $\alpha IIb^{+/+}$ cells (Fig.4A, red arrows; Supplemental Fig.3A,B,C). Two doses of BM cells were injected ($0.5x10^6$ and $2x10^6$ cells per mouse) (Supplemental Fig.3D,E). $\alpha IIb^{tk/tk}$ AGM-derived cells successfully repopulated secondary recipients with similar chimerism as $\alpha IIb^{+/+}$ AGM-derived cells (Supplemental Fig.3D; Supplemental Fig.3E). These data show that $\alpha IIb^{+/tk}$ and $\alpha IIb^{tk/tk}$ embryos have fewer HSCs in the AGM as compared to $\alpha IIb^{+/+}$ embryos. However, the few $\alpha IIb^{+/tk}$ and $\alpha IIb^{tk/tk}$ HSCs remaining are functional since they provide long-term multilineage reconstitutions of primary and secondary recipients.

It was previously shown that the number of HSCs increases when intact or reaggregated wild-type AGMs are cultured in vitro for 3-4 days[2,35]. To determine whether HSCs can be maintained and expanded in the AGM region of αIIb mutant embryos, we performed explant cultures of intact AGMs before transplantations (n=3). Cells from $\alpha IIb^{+/tk}$ or $\alpha IIb^{tk/tk}$ explant AGMs were able to reconstitute 13% and 20% of the transplanted recipients, compared to 100% when cells from $\alpha IIb^{+/+}$ explant AGMs were injected (Fig. 4B). While as expected the HSC repopulation ability of the $\alpha IIb^{+/+}$ AGM cells was higher after explant culture (when compared to transplantations performed without pre-culture, Fig.4A), the HSC repopulation ability of the αIIb mutant AGM cells was lower. Altogether, the results support a role for αIIb in AGM HSC maintenance and/or proliferation.

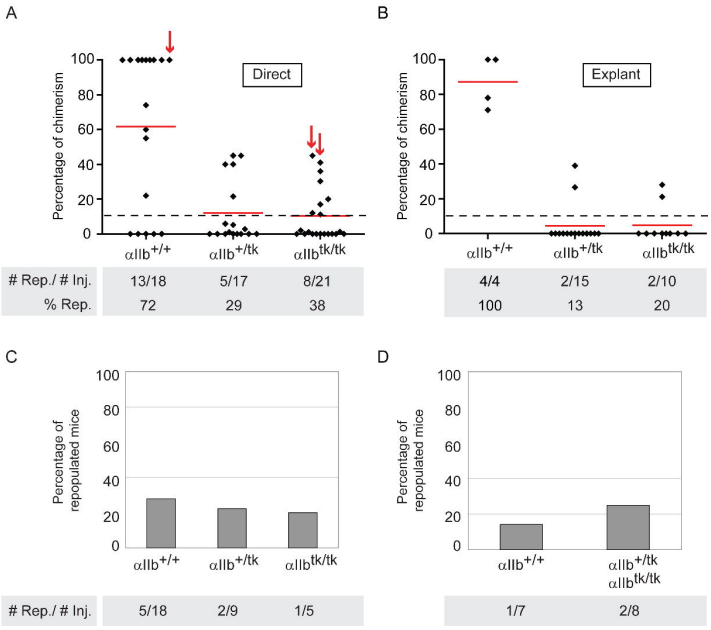

Figure 4. Functional analyses of AGM, yolk sac and fetal liver cells isolated from E11 CD41 (αIIb) deficient embryos. In vivo hematopoietic repopulation analysis of mice 4 months after the injection of (A,B) AGM, (C) yolk sac or (D) fetal liver cells isolated from E11 wild-type ($\alpha IIb^{+/+}$), haploinsufficient ($\alpha IIb^{+/tk}$) or deficient embryos for CD41 ($\alpha IIb^{tk/tk}$). (A,B) Percentage of chimerism in peripheral blood for each injected mice is shown. Each lozenge represents a transplanted mouse. Dash line: limit of positivity (>10% of chimerism in the peripheral blood). Red line: chimerism average. (A) Cells were injected directly after dissection and enzymatic dissociation of the AGMs (n=3) or (B) after 3 days of explant culture (n=3). The genotype of embryos is indicated below the graph (wild-type ($\alpha IIb^{+/+}$), haploinsufficient ($\alpha IIb^{+/tk}$) or deficient embryos for CD41 ($\alpha IIb^{tk/tk}$)), as well as the number of mice repopulated/number of mice transplanted (# Rep./# Inj.) and the percentage of repopulated mice (% Rep.). 1 embryo equivalent (ee) of AGM (n=3). (C, D) The mice, showing greater than 10% donor chimerism in peripheral blood, are considered as repopulated. Numbers above columns indicate the number of mice repopulated/number of mice transplanted. 1 ee of yolk sac (n=3) cells and, 3 to 4.5 ee of fetal liver cells (n=4) were injected per recipient. Due to the very low number of HSCs in E11 FL, $\alpha IIb^{+/tk}$ and $\alpha IIb^{tk/tk}$ cells were pooled.

αIIb knock-out embryos have no major hematopoietic stem cell defect in the YS and fetal liver.

To test whether the HSC activity was also affected in the YS (where part of HSCs express αIIb), we performed transplantations with YS cells isolated from E11 $\alpha IIb^{+/+}$, $\alpha IIb^{+/tk}$ and $\alpha IIb^{tk/tk}$ embryos (n=3). Four months post-transplantation, 28%, 22% and 20% of the mice injected with $\alpha IIb^{+/+}$, $\alpha IIb^{+/tk}$ or $\alpha IIb^{tk/tk}$ cells were reconstituted, respectively (Fig.4C). There was only a slight decrease in the number of reconstituted mice injected with $\alpha IIb^{+/tk}$ or $\alpha IIb^{tk/tk}$ cells when compared to the number of reconstituted mice injected with $\alpha IIb^{+/+}$ cells. Thus, while there is a strong HSC defect in the AGM of the αIIb mutant embryos, it is not the case in the YS.

We performed transplantations with FL cells isolated from E11 $\alpha IIb^{+/+}$, $\alpha IIb^{+/tk}$ and $\alpha IIb^{tk/tk}$ embryos (n=4), time when HSCs start to colonize the FL. The percentage of reconstituted mice after the injection of $\alpha IIb^{+/tk}$/$\alpha IIb^{tk/tk}$ cells (25%) was slightly higher than the percentage of reconstituted mice after the injection of $\alpha IIb^{+/+}$ cells (14%) (Fig.4D). Thus HSCs are able to colonize the FL of αIIb mutant embryos in vivo.

We further tested the HSC activity in the FL of E14 αIIb mutant embryos, time point when HSCs massively expand in vivo. FL cells isolated from $\alpha IIb^{+/+}$ and αIIb mutant embryos were isolated and injected in limiting dilution doses into recipients (0.001 [n=3] and 0.005 [n=3] ee per recipient). All mice transplanted with the high cell dose were reconstituted (Fig.5). However, the injection of the lower cell dose revealed a higher percentage of reconstituted mice when they were injected with αIIb mutant cells (62% and 83%) compared to wild-type cells (50%) (Fig.5). Thus, HSCs have no proliferative defect in the FL of the αIIb mutant embryos.

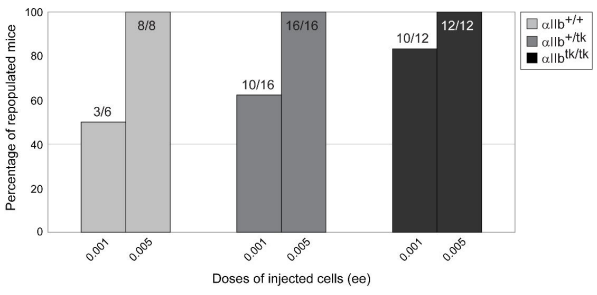

Figure 5. Functional analyses of E14 fetal liver cells isolated from CD41 (αIIb) deficient embryos. In vivo hematopoietic repopulation analysis of mice at 4 months after the injection of fetal cells isolated from E14 wild-type ($\alpha IIb^{+/+}$), haploinsufficient ($\alpha IIb^{+/tk}$), or deficient ($\alpha IIb^{tk/tk}$) embryos for CD41. Percentage of repopulated mice showing greater than 10% donor chimerism in peripheral blood is shown. Numbers above columns indicate the number of mice repopulated/number of mice transplanted. The number of embryo equivalent (ee) of cells injected per recipient is indicated. Light grey bar: cells from wild-type ($\alpha IIb^{+/+}$) embryos; Dark grey bar: cells from haploinsufficient ($\alpha IIb^{+/tk}$) embryos; Black bar: cells from deficient ($\alpha IIb^{tk/tk}$) embryos.

DISCUSSION

αIIb integrin subunit (CD41) is one of the first surface markers indicative of hematopoietic commitment[20-22,24]. It is notably expressed by the first hematopoietic cells emerging from the hemogenic endothelium in the aorta[25]. We found here that αIIb is not only a reliable HSC marker but it also plays an important role to maintain the HSC activity in the aorta. Moreover, we found that HSCs differentially express αIIb, β3 and αv integrin subunits during ontogeny, which can be used to enrich specific HSC populations throughout development.

Adult HSCs can be isolated to near purity by using a combination of several surface markers (e.g. $Lin^-Sca\text{-}1^+c\text{-}kit^+CD34^{low/-}$; $Lin^-Sca\text{-}1^+c\text{-}kit^+CD150^+CD244^-CD48^-$)[36-37]. Similar to adult HSCs, embryonic HSCs express c-kit and Ly6A (Sca-1)[33,35,38]. However, HSCs from the AGM and placenta do not express the SLAM marker CD150 and express CD34[21]. HSCs in the embryo also co-express most endothelial markers that are normally exclusively expressed by endothelial cells in adult[39-40]. Therefore, HSCs in the embryo are more difficult to isolate and localize in situ than adult HSCs. The only reliable identification of HSCs relies on their ability to provide long-term, high-level, multilineage reconstitution of primary and secondary adult irradiated recipients. By using such in vivo transplantation assay, we have shown that the first HSCs found in the AGM express both αIIbβ3 and αvβ3 integrins at E11. HSCs do not express αIIbβ3 but express αvβ3 integrins in E12 placenta. Most HSCs do not express both αIIbβ3 and αvβ3 integrins in E14 FL. Surprisingly, the YS contains HSCs with the different phenotypes observed in E11 AGM, E12 placenta and E14 FL. Therefore, HSCs differentially express three integrin subunits throughout development, which can be used to enrich in embryonic HSCs.

All HSCs express β3 until its expression decreases at the FL stage. However, adult BM HSCs ($CD34^{-/low}Lin^-Sca\text{-}1^+c\text{-}kit^+$) are further enriched in the $CD61^+$ (β3) subfraction[41], these cells also expressing αv[11]. This suggests that some HSCs re-express CD61 after the FL stage. During development, the expression pattern of αv closely follows the one of its partner β3. All HSCs downregulate αIIb and then part of them, also downregulate β3 and αv. Nevertheless, a substantial fraction of HSCs do not express αIIb or none of the integrin subunits in the YS at E11/E12. Such HSCs are not detectable in the AGM at the same time point. A possible explanation would be that the YS generate HSCs that would never express αIIb and/or β3. However it has been proposed, after performing in vivo CD41-Cre-mediated genetic tagging at embryonic stage that all/most HSCs go through an αIIb expressing phase, as it is reflected by a high percentage of labelled hematopoietic cells in the adult animals (35-65%)[42]. It is also possible that integrin expression on the surface of HSCs is regulated,

not only by their developmental stage, but also by the surrounding cells that compose the HSC niches. Altogether, we found that HSCs differentially express αIIb, β3 and αv with a progressive downregulation of these surface markers throughout development. Furthermore, they can be used in combination with other markers as CD45 and c-kit to enrich AGM cells either into short-term or long-term HSCs.

HSCs most likely reside in clusters (Intra-Aortic Hematopoietic Clusters or IAHCs) that are tightly attached to the endothelial layer of the embryonic aorta[43]. IAHC cells express αIIb[7,44]. However, visualizing the CD41 staining on embryo cryosections is rather difficult (due to low expression) and often leads to high background staining. In contrast, the labelling with directly conjugated antibodies of non-fixed embryo slices allows the visualization of low level of integrin expression in the aorta with good resolution[25-26]. We observed that IAHC cells co-express αIIb, β3 and αv. Interestingly, αIIb, β3 and αv were mainly localized at the junction between the cells that form the IAHCs. It is not possible to ascertain that β3 form dimers with αIIb or αv. However, the high co-localization of αv and β3, and the punctual co-localization of αIIb with β3 suggests that complete αIIbβ3 and αvβ3 integrins are present at the junctions between the IAHC cells. Similar direct labelling of live placenta slices allows a precise and reliable staining of both the placental vasculature and HSPCs. We observed groups of cells expressing both αv and β3 in the vasculature of the placental chorionic plate. Similar to the IAHCs, αv and β3 were mainly at the junction in between the cells. Thus, the intermediate expression level of integrin subunits can be nicely visualized at the junction in between the cells forming the IAHCs in the aorta and in group of cells located in the vascular labyrinth of the placenta.

We have previously shown that hematopoietic progenitors are $CD41^{int}$ in the AGM and YS (E11) whereas they are in both $CD41^{-}$ and $CD41^{int}$ fractions in the E12 placenta and E14 FL[24]. In addition, a study showed that the disruption of αIIb (null allele for the gpIIb gene) results in an increased number of hematopoietic progenitors in E9.5 YS, and in E12.5, E13.5 and E15.5 FL19, suggesting that αIIb plays a role in the regulation of some hematopoietic progenitors (CFU-Myeloid, BFU-E and CFU-Mk). To test whether αIIb plays a role in the progenitor activity in the AGM, we used mice in which the tk gene was knock-in into the *αIIb* locus, which resulted in the complete disruption of αIIb expression in homozygous $αIIb^{tk/tk}$ mice[28]. We observed no differences in the total number or types of progenitors in the AGM of E11 $αIIb^{+/+}$, $αIIb^{tk/+}$, or $αIIb^{tk/tk}$ embryos. Although surprising, such results indicate that αIIb does not play a role in the regulation of the hematopoietic progenitors in the AGM region. This difference in the requirement for αIIb on progenitors might depend on the surrounding microenvironment where they reside. Thus, αIIb does not

play a functional role on the progenitors despite the fact that all progenitors express this marker in the AGM[24].

We further tested whether IIb plays a role on HSC activity in the different embryonic sites where HSCs express this surface marker. We observed a dramatic decrease of the HSC activity in the AGMs of αIIb mutant embryos. Furthermore, the very few mice that were long-term multilineage reconstituted had a much lower donor cell chimerism. The successful secondary transplantations demonstrated that although there are fewer HSCs in the AGM of the αIIb mutant embryos, they are functional, multipotent and capable of self-renewal. This excludes the possibility that AGM HSCs in the αIIb mutant embryos have difficulties in homing to the adult BM niche after transplantation. Interestingly, the HSC defect was exclusive to the AGM since we did not find any differences in HSC activity in the YS and FL of αIIb mutant embryos at the same time point of development (E11). The HSC activity was also normal at a later stage (E14), when HSC expansion occurs in the FL, indicating that αIIb mutant HSCs can normally expand. The HSC defect is thus restricted to the AGM region, first site of adult-type HSC production. To determine the exact role of αIIb we pre-cultured the AGMs as explant before to perform transplantation. Such culture maintains and expand AGM HSCs from wild-type[2] but not from Runx-1$^{+/-}$ hematopoietic mutant embryos[31,45]. Similar to the Runx-1$^{+/-}$ embryos, the HSC activity was lower after explant culture of the αIIb mutant AGMs (when compared to the transplantation of cells isolated from freshly dissected AGMs). Thus, HSCs are not maintained in the AGM when αIIb is absent. The defect seems to be cell intrinsic since only IAHC cells (where HSCs reside) express αIIb in the dorsal aorta at this stage of development. An interesting observation is that the HSC defect is similar in the AGMs of αIIb$^{tk/+}$, or αIIb$^{tk/tk}$ embryos. A certain threshold of αIIb on the surface of HSCs is therefore necessary to maintain the HSC activity in the AGM.

Integrins are necessary for cell anchorage and also for cell signaling, as they act as bidirectional signaling molecules via inside-out and outside-in signaling between the intra- and extracellular spaces[46-47]. It remains puzzling how αIIb preserve the HSC activity in the AGM. αIIb, αv and β3 subunits are mainly localized at the junction between the IAHC cells, which suggest a role for these integrins in maintaining IAHC inner integrity, or IAHC attachment to the endothelium. If this is the case, fewer IAHCs should be present in the aorta of the αIIb mutant embryos. However, we found that the number of c-kit^{+} IAHC cells and the shape of the IAHCs were normal. Thus, either αIIb does not play a role in IAHC cells anchorage, or other adhesion molecules compensate for the absence of αIIb. The normal number of IAHCs also shows that αIIb, which is expressed by the emerging IAHCs and HSCs, is not required for the endothelial to hematopoietic transition (EHT). Very few HSCs are present in the aorta[4,31]

compared to the number of IAHCs at E11[7]. Therefore, the specific detachment of HSCs in absence of αIIb might not be quantifiable. The detached HSCs could eventually migrate into other hematopoietic sites where the HSC activity should then increase at that stage (E11). However, it does not seem to be the case as the HSC activity was comparable in the YS and FL of αIIb mutant and wild-type embryos.

Integrin binding to extra-cellular matrix compounds induces outside-in signaling through clustering of integrin heterodimers at focal adhesion sites[46-47]. This will recruit other cell surface receptors and many proteins that will activate intracellular signaling pathways. Therefore, the absence of αIIb might have direct or indirect consequences as for example the lack of recruitment of important receptors to the focal adhesion points (e.g. cytokine receptors) or the lack of signaling downstream of αIIbβ3 integrins. It was shown that platelet clot formation is mediated through phosphorylation of the c-Src kinase (regulating downstream effectors such as RhoA) after binding of αIIbβ3 to the Gα13 subunit[47]. It was also recently shown that outside-in signaling via pY747 of β3 (β3PY747) following activation of αvβ3 integrin by TPO-mediated inside-out signaling is indispensable for TPO-mediated maintenance of HSC activity in vitro and in vivo within the BM niche[48]. Whether such mechanisms also occur on E11 AGM HSCs will be the focus of further investigations.

Altogether our study shows that β3 and αv integrin subunits, in addition to αIIb, are reliable markers of the first HSCs found in the AGM. Such subunits are then differentially expressed by HSCs throughout embryonic development and can be used to isolate and localize HSCs. It has been shown that some integrin subunits are important for the retention of HSPCs in the adult BM niches (e.g. α4[49]) and/or for the colonization of HSPCs into the FL and BM (e.g. β1[9,50]). Here we highlight a new role of integrin subunits and provide evidences that αIIb is important to maintain the HSC activity in the aorta.

Acknowledgements

We thank Henk Dronk and Experimental Dieren Centrum (Erasmus MC) for mouse care. We thank Samly Srun for technical help at the beginning of the project. We thank Dr. Katrin Ottersbach, Dr. Charles Durand and Anna Klaus for helpful discussion. We thank Dr. Diana Tronik-Le Roux for giving us the authorization to use the αIIb$^{+/tk}$ mice that she generated. This work was supported by NWO (VIDI) grant 917-76-345 (C.R.), Landsteiner Foundation for Blood Transfusion Research (C.R.) and NIH RO37DKKD54077 (E.D) and FES Netherlands Institute for Regenerative Medicine (ED).

Authorship contributions

C.R. and J.C.B. conceived ideas and designed the research. C.R, J.C.B. and T.C. performed the experiments, analyzed the data, interpreted the experiments and made the figures. R. van L. performed the flow cytometry sorts. C.R., J.C.B., T.C. and E.D. wrote the manuscript.

Conflict of interest disclosures

The authors have no conflicting financial interests.

REFERENCES

1. Boisset JC, Robin C. On the origin of hematopoietic stem cells: Progress and controversy. Stem Cell Res. 2012;8:1-13.

2. Medvinsky A, Dzierzak E. Definitive hematopoiesis is autonomously initiated by the AGM region. Cell. 1996;86:897-906.

3. Muller AM, Medvinsky A, Strouboulis J, Grosveld F, Dzierzak E. Development of hematopoietic stem cell activity in the mouse embryo. Immunity. 1994;1:291-301.

4. Gekas C, Dieterlen-Lievre F, Orkin SH, Mikkola HK. The placenta is a niche for hematopoietic stem cells. Dev Cell. 2005;8:365-375.

5. Ottersbach K, Dzierzak E. The murine placenta contains hematopoietic stem cells within the vascular labyrinth region. Dev Cell. 2005;8:377-387.

6. Rhodes KE, Gekas C, Wang Y, et al. The emergence of hematopoietic stem cells is initiated in the placental vasculature in the absence of circulation. Cell Stem Cell. 2008;2:252-263.

7. Yokomizo T, Dzierzak E. Three-dimensional cartography of hematopoietic clusters in the vasculature of whole mouse embryos. Development. 2010;137:3651-3661.

8. Grassinger J, Haylock DN, Storan MJ, et al. Thrombin-cleaved osteopontin regulates hemopoietic stem and progenitor cell functions through interactions with alpha9beta1 and alpha4beta1 integrins. Blood. 2009;114:49-59.

9. Potocnik AJ, Brakebusch C, Fassler R. Fetal and adult hematopoietic stem cells require beta1 integrin function for colonizing fetal liver, spleen, and bone marrow. Immunity. 2000;12:653-663.

10. Wagers AJ, Weissman IL. Differential expression of alpha2 integrin separates long-term and short-term reconstituting Lin-/loThy1.1(lo)c-kit+ Sca-1+ hematopoietic stem cells. Stem Cells. 2006;24:1087-1094.

11. Umemoto T, Yamato M, Shiratsuchi Y, et al. Expression of Integrin beta3 is correlated to the properties of quiescent hemopoietic stem cells possessing the side population phenotype. J Immunol. 2006;177:7733-7739.

12. Qian H, Tryggvason K, Jacobsen SE, Ekblom M. Contribution of alpha6 integrins to hematopoietic stem and progenitor cell homing to bone marrow and collaboration with alpha4 integrins. Blood. 2006;107:3503-3510.

13. Notta F, Doulatov S, Laurenti E, Poeppl A, Jurisica I, Dick JE. Isolation of single human hematopoietic stem cells capable of long-term multilineage engraftment. Science. 2011;333:218-221.

14. Prowse AB, Chong F, Gray PP, Munro TP. Stem cell integrins: implications for ex-vivo culture and cellular therapies. Stem Cell Res. 2011;6:1-12.

15. Bouvard D, Brakebusch C, Gustafsson E, et al. Functional consequences of integrin gene mutations in mice. Circ Res. 2001;89:211-223.

16.Bonig H, Priestley GV, Wohlfahrt M, Kiem HP, Papayannopoulou T. Blockade of alpha6-integrin reveals diversity in homing patterns among human, baboon, and murine cells. Stem Cells Dev. 2009;18:839-844.

17. Bonig H, Watts KL, Chang KH, Kiem HP, Papayannopoulou T. Concurrent blockade of alpha4-integrin and CXCR4 in hematopoietic stem/progenitor cell mobilization. Stem Cells. 2009;27:836-837.

18. Lapidot T, Dar A, Kollet O. How do stem cells find their way home? Blood. 2005;106:1901-1910.

19. Emambokus NR, Frampton J. The glycoprotein IIb molecule is expressed on early murine hematopoietic progenitors and regulates their numbers in sites of hematopoiesis. Immunity. 2003;19:33-45.

20. Ferkowicz MJ, Starr M, Xie X, et al. CD41 expression defines the onset of primitive and definitive hematopoiesis in the murine embryo. Development. 2003;130:4393-4403.

21. McKinney-Freeman SL, Naveiras O, Yates F, et al. Surface antigen phenotypes of hematopoietic stem cells from embryos and murine embryonic stem cells. Blood. 2009;114:268-278.

22. Mikkola HK, Fujiwara Y, Schlaeger TM, Traver D, Orkin SH. Expression of CD41 marks the initiation of definitive hematopoiesis in the mouse embryo. Blood. 2003;101:508-516.

23. Mitjavila-Garcia MT, Cailleret M, Godin I, et al. Expression of CD41 on hematopoietic progenitors derived from embryonic hematopoietic cells. Development. 2002;129:2003-2013.

24. Robin C, Ottersbach K, Boisset JC, Oziemlak A, Dzierzak E. CD41 is developmentally regulated and differentially expressed on mouse hematopoietic stem cells. Blood. 2011;117:5088-5091.

25. Boisset JC, van Cappellen W, Andrieu-Soler C, Galjart N, Dzierzak E, Robin C. In vivo imaging of haematopoietic cells emerging from the mouse aortic endothelium. Nature. 2010;464:116-120.

26. Boisset JC, Andrieu-Soler C, van Cappellen WA, Clapes T, Robin C. Ex vivo time-lapse confocal imaging of the mouse embryo aorta. Nat Protoc. 2011;6:1792-1805.

27. Matsubara A, Iwama A, Yamazaki S, et al. Endomucin, a CD34-like sialomucin, marks hematopoietic stem cells throughout development. J Exp Med. 2005;202:1483-1492.

28. Tronik-Le Roux D, Roullot V, Poujol C, Kortulewski T, Nurden P, Marguerie G. Thrombasthenic mice generated by replacement of the integrin alpha(IIb) gene: demonstration that transcriptional activation of this megakaryocytic locus precedes lineage commitment. Blood. 2000;96:1399-1408.

29. Hodivala-Dilke KM, McHugh KP, Tsakiris DA, et al. Beta3-integrin-deficient mice are a model for Glanzmann thrombasthenia showing placental defects and reduced survival. J Clin Invest. 1999;103:229-238.

30. Robin C, Dzierzak E. Hematopoietic stem cell enrichment from the AGM region of the mouse embryo. Methods Mol Med. 2005;105:257-272.

31. Robin C, Ottersbach K, Durand C, et al. An unexpected role for IL-3 in the embryonic development of hematopoietic stem cells. Dev Cell. 2006;11:171-180.

32. Durand C, Robin C, Bollerot K, Baron MH, Ottersbach K, Dzierzak E. Embryonic stromal clones reveal developmental regulators of definitive hematopoietic stem cells. Proc Natl Acad Sci U S A. 2007;104:20838-20843.

33. Sanchez MJ, Holmes A, Miles C, Dzierzak E. Characterization of the first definitive hematopoietic stem cells in the AGM and liver of the mouse embryo. Immunity. 1996;5:513-525.

34. Robin C, Durand C. The roles of BMP and IL-3 signaling pathways in the control of hematopoietic stem cells in the mouse embryo. Int J Dev Biol. 2010;54:1189-1200.

35. Taoudi S, Gonneau C, Moore K, et al. Extensive hematopoietic stem cell generation in the AGM region via maturation of VE-cadherin+CD45+ pre-definitive HSCs. Cell Stem Cell. 2008;3:99-108.

36. Osawa M, Hanada K, Hamada H, Nakauchi H. Long-term lymphohematopoietic reconstitution by a single CD34-low/negative hematopoietic stem cell. Science. 1996;273:242-245.

37. Kiel MJ, Yilmaz OH, Iwashita T, Terhorst C, Morrison SJ. SLAM family receptors distinguish hematopoietic stem and progenitor cells and reveal endothelial niches for stem cells. Cell. 2005;121:1109-1121.

38. de Bruijn MF, Ma X, Robin C, Ottersbach K, Sanchez MJ, Dzierzak E. Hematopoietic stem cells localize to the endothelial cell layer in the midgestation mouse aorta. Immunity. 2002;16:673-683.

39. Taoudi S, Morrison AM, Inoue H, Gribi R, Ure J, Medvinsky A. Progressive divergence of definitive haematopoietic stem cells from the endothelial compartment does not depend on contact with the foetal liver. Development. 2005;132:4179-4191.

40. Baumann CI, Bailey AS, Li W, Ferkowicz MJ, Yoder MC, Fleming WH. PECAM-1 is expressed on hematopoietic stem cells throughout ontogeny and identifies a population of erythroid progenitors. Blood. 2004;104:1010-1016.

41. Umemoto T, Yamato M, Shiratsuchi Y, et al. CD61 enriches long-term repopulating hematopoietic stem cells. Biochem Biophys Res Commun. 2008;365:176-182.

42. Rybtsov S, Sobiesiak M, Taoudi S, et al. Hierarchical organization and early hematopoietic specification of the developing HSC lineage in the AGM region. J Exp Med. 2011;208:1305-1315.

43. North T, Gu TL, Stacy T, et al. Cbfa2 is required for the formation of intra-aortic hematopoietic clusters. Development. 1999;126:2563-2575.

44. Corbel C, Salaun J. AlphaIIb integrin expression during development of the murine hemopoietic system. Dev Biol. 2002;243:301-311.

45. Cai Z, de Bruijn M, Ma X, et al. Haploinsufficiency of AML1 affects the temporal and spatial generation of hematopoietic stem cells in the mouse embryo. Immunity. 2000;13:423-431.

46. Hynes RO. Integrins: bidirectional, allosteric signaling machines. Cell. 2002;110:673-687.

47. Gong H, Shen B, Flevaris P, et al. G protein subunit Galpha13 binds to integrin alphaIIbbeta3 and mediates integrin "outside-in" signaling. Science. 2010;327:340-343.

48. Umemoto T, Yamato M, Ishihara J, et al. Integrin-alphavbeta3 regulates thrombopoietin-mediated maintenance of hematopoietic stem cells. Blood. 2012;119:83-94.

49. Scott LM, Priestley GV, Papayannopoulou T. Deletion of alpha4 integrins from adult hematopoietic cells reveals roles in homeostasis, regeneration, and homing. Mol Cell Biol. 2003;23:9349-9360.

50. Hirsch E, Iglesias A, Potocnik AJ, Hartmann U, Fassler R. Impaired migration but not differentiation of haematopoietic stem cells in the absence of beta1 integrins. Nature. 1996;380:171-175.

SUPPLEMENTARY INFORMATIONS

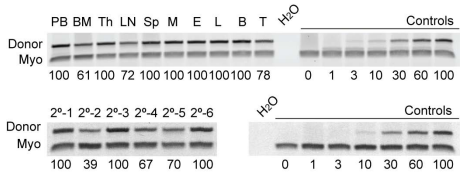

Supplementary Figure 1. Multilineage and self-renewal potential of CD41intCD61int cells sorted from E11 AGM. Representative semiquantitative PCR analysis of hematopoietic tissue DNA from (upper panel) a primary recipient injected with 3ee of E11 AGM CD41intCD61int cells and (lower panel) peripheral blood DNA from six secondary recipients injected with bone marrow cells from the primary recipient at 4 months post-transplantation. Donor indicates the human β-globin PCR fragment and Myo indicates the myogenin DNA normalization control PCR fragment. DNA dilution controls (0 to 100%) were used to quantify percentages of donor chimerism that are indicated below each lane. PB: peripheral blood; BM: bone marrow; Th: thymus; LN: lymph node; Sp: spleen, M: myeloid (sorted cells from bone marrow, BM); E: erythroid (sorted from BM); L: lymphoid (sorted from BM); B: B lymphoid (sorted from spleen); T: T lymphoid (sorted from spleen).

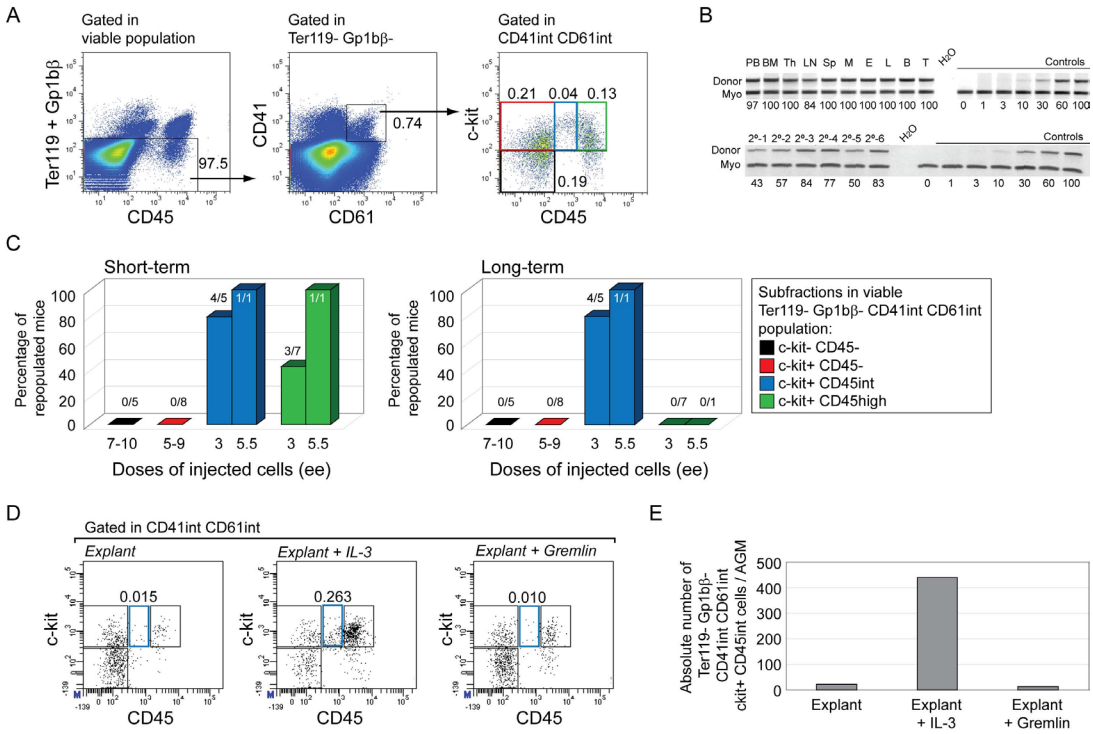

Supplementary Figure 2. Hematopoietic stem cell enrichment in integrin based sorted cell fractions isolated from E11 AGM. (A) Flow cytometric analysis of E11 AGM cells based on CD41, CD61, CD45 and c-kit expression. Flow cytometric plots show CD41 and CD61 expression (middle panel) on Ter119$^-$G1bβ$^-$ cells (left panel). Dot plots (right panel) show CD45 and c-kit expression of CD41^{int}CD61^{int} gated population shown in the middle panel. Representative sorting gates of the four populations of interest in the viable Ter119$^-$ G1bβ$^-$CD41^{int}CD61^{int} are indicated (black: c-kit$^-$CD45$^-$; red: c-kit$^+$CD45$^-$; blue: c-kit$^+$CD45^{int}; green: c-kit$^+$CD45^{high}). The percentages of cells in each fraction are indicated near the corresponding sorting gates. (B) Representative semiquantitative PCR analysis of hematopoietic tissue DNA from (upper panel) a primary recipient injected with 3ee of E11 AGM Ter119$^-$ G1bβ$^-$CD41^{int}CD61^{int}c-kit$^+$CD45^{int} cells and (lower panel) peripheral blood DNA from six secondary recipients injected with bone marrow cells from the primary recipient at 4 months post-transplantation. Donor indicates the human β-globin PCR fragment and Myo indicates the myogenin DNA normalization control PCR fragment. DNA dilution controls (0 to 100%) were used to quantify percentages of donor chimerism that are indicated below each lane. PB: peripheral blood; BM: bone marrow; Th: thymus; LN: lymph node; Sp: spleen, M: myeloid (sorted cells from bone marrow, BM); E: erythroid (sorted from BM); L: lymphoid (sorted from BM); B: B lymphoid (sorted from spleen); T: T lymphoid (sorted from spleen). (C) In vivo hematopoietic repopulation analysis of mice, one (short-term) and 4 (long-term) months after the injection of the four populations of interest gated in (A) (n=8). Percentage of repopulated mice showing greater than 10% donor chimerism in peripheral blood is shown. Numbers above columns indicate the number of mice repopulated/number of mice injected. Dose of injected cells is indicated as embryo equivalent (ee). (D) Flow cytometric plots showing CD45 and c-kit expression on Ter119$^-$G1bβ$^-$ CD41^{int}CD61^{int} cells from E11 AGM explants cultured without added molecules (left panel), in presence of IL-3 (middle panel) or in presence of gremlin (right panel). The percentages of the long-term HSC enriched population (Ter119$^-$G1bβ$^-$CD41^{int}CD61^{int}c-kit$^+$CD45^{int}) is indicated on the plot (Blue gate). (E) Absolute number of Ter119$^-$G1bβ$^-$ CD41^{int}CD61^{int}c-kit$^+$CD45^{int} cells per AGM after 3 days of explant culture without added molecules (explant), in presence of IL-3 (explant+IL-3) or in presence of gremlin (explant+gremlin).

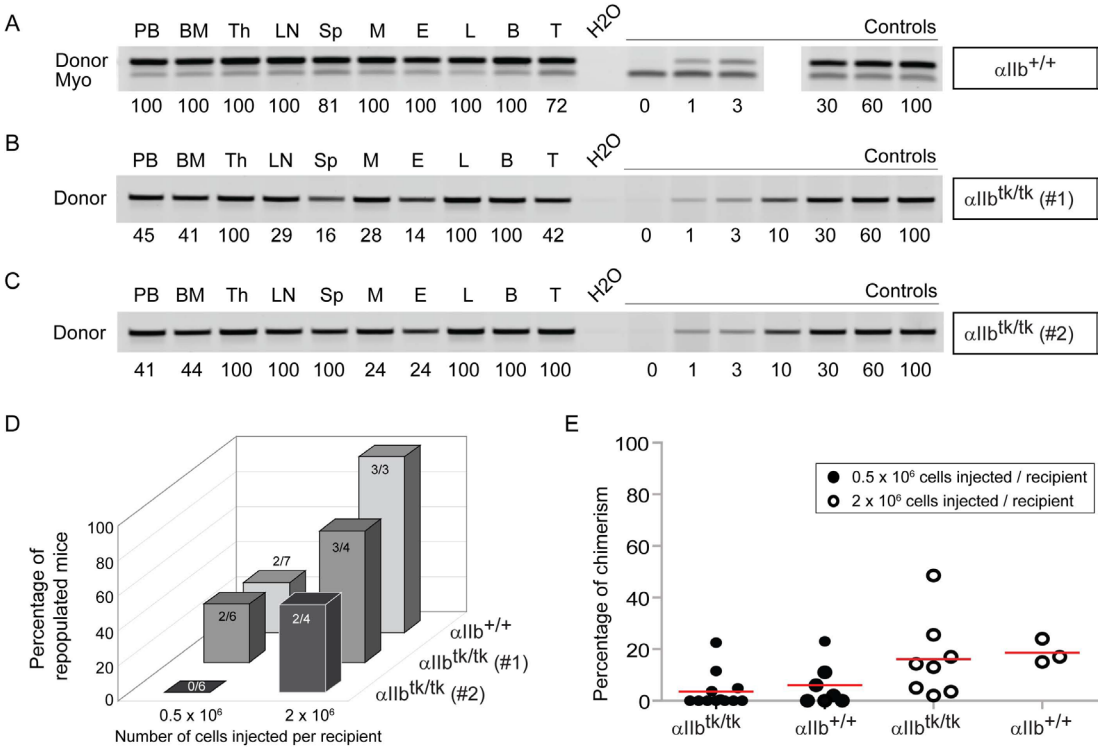

Supplementary Figure 3. Multilineage and self-renewal potential of AGM cells isolated from CD41 (αIIb) deficient embryos. Representative semiquantitative PCR analysis of hematopoietic tissue DNA from two primary recipient 4 months after the injection of AGM cells (1 ee) from (A,B) deficient embryos for CD41 ($\alpha IIb^{tk/tk}$) and (C) from wild-type embryo ($\alpha IIb^{+/+}$). Donor indicates the TK PCR fragment and Myo indicates the myogenin DNA normalization control PCR fragment. DNA dilution controls (0 to 100%) were used to quantify percentages of donor chimerism that are indicated below each lane. PB: peripheral blood; BM: bone marrow; Th: thymus; LN: lymph node; Sp: spleen, M: myeloid (sorted cells from bone marrow, BM); E: erythroid (sorted from BM); L: lymphoid (sorted from BM); B: B lymphoid (sorted from spleen); T: T lymphoid (sorted from spleen). (D) In vivo hematopoietic repopulation analysis of secondary recipients at 4 months after the injection of bone marrow cells isolated from the primary reconstituted recipient shown in (A), (B) and (C). Percentage of repopulated mice showing greater than 10% donor chimerism in peripheral blood is shown. Numbers above columns indicate the number of mice repopulated/number of mice transplanted. Recipients were injected with two different cell doses: $0.5x10^6$ and $2x10^6$ cells per recipients. (E) Percentage of chimerism in peripheral blood for each injected mice (shown in (D)) is shown. Each circle represents a transplanted mouse. Black circle: $0.5x10^6$ bone marrow cells injected per secondary irradiated recipient; White circle: $2x10^6$ cells per recipient. Red line: chimerism average.


INOX.
5/45
5
DUMOSTAR ®
NON - MAGNETIC
NON - CORROSIVE

Chapter 6 – Intra-aortic hematopoietic clusters contain pre-HSCs contributing to HSC production in the mouse embryo

In preparation

Intra-aortic hematopoietic clusters contain pre-HSCs contributing to HSC production in the mouse embryo

Boisset Jean-Charles[1], Clapes Thomas[1], Klaus Anna[1], Papazian Natalie[2], Onderwater Jos[3], Mommaas-Kienhuis Mieke[3], Cupedo Tom[2] and Robin Catherine[1]

[1]Department of Cell Biology, Erasmus MC Stem Cell Institute, Erasmus University Medical Center, Rotterdam, Netherlands
[2]Department of Hematology, Erasmus University Medical Center, Rotterdam, Netherlands
[3]Department of Molecular Cell Biology, Leiden University Medical Center, Leiden, Netherlands

SUMMARY

The exact nature and role of the Intra-Aortic Hematopoietic Clusters (IAHCs) described more than a century ago and found in the main arteries of all vertebrate species remain uncertain. IAHCs are derived from the underlying hemogenic endothelium and are presumed to contain the first Hematopoietic Stem Cells (HSCs) and progenitors. Here we show that IAHCs contains only very few Erythro-Myeloid progenitors. However, they contain pre-HSCs, *i.e.* capable of long-term multilineage reconstitution of newborn recipients, at a time when no HSCs are detected yet. We show by secondary transplantation and time-lapse confocal imaging that IAHC pre-HSCs can mature into HSCs. We propose that several successive steps of maturations are needed for the production of fully potent HSCs, with an endothelial into pre-HSC transition and further maturation into HSCs. Our data suggest a potential role for IAHC pre-HSCs in the massive HSC increase observed during embryonic development prior bone marrow colonization.

INTRODUCTION

The first adult-type Hematopoietic Stem Cells (HSCs) are generated during embryonic development. They start to be detected at mid-gestation at embryonic day (E)10.5 of mouse development in the Aorta-Gonad-Mesonephros (AGM) region (Medvinsky and Dzierzak, 1996; Muller et al., 1994). HSCs are defined by their ability to self-renew, and to give rise at the single cell level to all hematopoietic lineages. Both characteristics are tested by transplantation

into irradiated adult Wild-Type (WT) recipients. Long-term reconstitution of all blood lineages in primary and secondary recipients provides the ultimate proof that genuine HSCs were initially present in the injected cell population. After E10.5, in addition to the AGM, HSCs are also detected in the Yolk-Sac (YS), Fetal Liver (FL) and placenta (Gekas et al., 2005; Muller et al., 1994; Ottersbach and Dzierzak, 2005). It is only before birth that HSCs will migrate into the Bone Marrow (BM), the main adult HSC niche (Christensen et al., 2004).

From E9.5 onward, clusters of cells are observed in the vitelline artery, soon followed by their appearance in the dorsal aorta and umbilical artery (Yokomizo and Dzierzak, 2010). These so-called Intra-Aortic Hematopoietic Clusters (IAHCs) are attached to the endothelial layer facing the lumen of the main arteries. IAHCs are present in virtually all vertebrate species (Dieterlen-Lievre et al., 2006), in the floor of the dorsal aorta, but also in the roof part of the aorta in the mouse embryo (Taoudi and Medvinsky, 2007; Yokomizo and Dzierzak, 2010). The tight association of IAHCs with the endothelium has led to the hypothesis that they might be derived from it (Dantschakoff, 1909; Jordan, 1917). Multiple lines of evidence have now confirmed the so-called hemogenic endothelial origin of IAHCs and HSCs in chicken (Jaffredo et al., 2000; Jaffredo et al., 1998) and mouse (Chen et al., 2009; Eilken et al., 2009; Lancrin et al., 2009; Zovein et al., 2008). The direct observation of the endothelial to hematopoietic cell transition in the aorta by time-lapse confocal microscopy, notably *in vivo* in zebrafish embryos (Bertrand et al., 2010; Kissa and Herbomel, 2010; Lam et al., 2010) and *ex vivo* in thick non-fixed embryo slices (Boisset et al., 2010), definitively confirmed the endothelial origin of the hematopoietic stem/progenitor cells (HSPCs).

In the early 20th century, IAHCs were often described as lymphocytes, based on morphological examinations. Because HSCs were shown to emerge in the chicken embryo proper, it was therefore assumed that HSCs were most likely residing within IAHCs (Dieterlen-Lievre and Martin, 1981; Smith and Glomski, 1982). It was supported by the fact that both HSCs and IAHCs (1) express the same surface markers (e.g. c-kit, CD31, CD34, CD41)(Cumano and Godin, 2007), (2) are absent in *runx1* mutant embryos (North et al., 1999), and (3) are derived from the hemogenic endothelium (Chen et al., 2009; Zovein et al., 2008). Also hematopoietic progenitors are present in the AGM and might thus be part of the IAHCs (Ohmura et al., 1999). However, some discrepancies exist and raise questions on the exact cell composition and role of the IAHCs. Indeed IAHCs arise at E9.5 in the aorta (Yokomizo and Dzierzak, 2010), but the first HSCs only start to be detected at E10.5 (Muller et al., 1994), thus about 24 hours later. Also, there are around 2 HSCs present in the aorta at E11.5 (as calculated by transplantation of serial limiting cell dilutions) (Gekas et al., 2005;

Kumaravelu et al., 2002) whereas there are an average of 450 IAHC cells at the same time point (Yokomizo and Dzierzak, 2010). In addition, as described previously, IAHCs are present in both floor and roof parts of the dorsal aorta, but HSCs solely localize to the aortic floor side (Taoudi and Medvinsky, 2007).

Despite the impossibility to detect HSCs before E10.5 (<34 somite pairs, s.p.), by using conventional transplantation assay in adult irradiated WT recipients (Medvinsky and Dzierzak, 1996; Muller et al., 1994), it has been possible to uncover the existence of cells with HSC potential (*i.e.* self-renewal and multipotency) at earlier stages by using other in vivo assays. Such cells have been referred as HSC precursors or pre-HSCs. For example, E8 pre-circulatory Para-aortic Splanchnopleura (P-Sp) (prospective AGM area) pre-cultured as *in toto* explant, and then co-cultured as dissociated cells on S17 stromal cell line, could reconstitute adult irradiated *Rag2*$^{-/-}\gamma c^{-/-}$ recipients after transplantation (Cumano et al., 2001). Also, E9.0 YS and P-Sp cells could directly reconstitute busulfan conditioned WT newborn (long-term and multilineage) (Yoder and Hiatt, 1997; Yoder et al., 1997a; Yoder et al., 1997b). Secondary transplantations performed in WT adult irradiated recipients have confirmed the genuine HSC self-renewal potential of the transplanted cells (Yoder et al., 1997b). It is noteworthy that so far no direct connection has been established between pre-HSCs and the first HSCs detected in the AGM. Here, we hypothesized that IAHCs are mainly composed of pre-HSCs capable of maturation toward a true HSC state.

We performed an extensive study of the IAHCs to determine their exact morphology, phenotype and function. We found that IAHCs are heterogeneous in size, shape and surface marker expression, while all IAHC cells look similar in morphology. We designed a novel strategy to specifically label and isolate IAHC cells to purity for further phenotypic and functional analysis. We first reveal that IAHC cells contain no lymphoid progenitors and only very few erythro-myeloid progenitors (EMPs), which cannot account for the high number of IAHC cells present in the aorta at E10.0. We then showed that IAHCs contain pre-HSCs, able to sustain *in vivo* long-term hematopoiesis in primary newborn immunodeficient recipients. Finally, the successful long-term multilineage secondary transplantation of WT irradiated adult recipients, hallmark assay of adult type HSCs, proves the direct link existing between the IAHC pre-HSCs and HSCs. The maturation of pre-HSCs into HSCs in IAHCs was observed in the context of the AGM by performing time-lapse imaging of non-fixed slices of E10 Ly6A-GFP embryo. Therefore pre-HSCs residing in IAHCs are able to mature into functional HSCs, which suggest an *in vivo* role of IAHC's pre-HSCs in the massive increase in HSCs during embryonic development.

RESULTS

IAHCs are heterogeneous in shape but contain seemingly alike cells

To investigate the morphology of IAHCs, scanning electron microscopy of transversal thick slices of E10 (Figure 1A-D) and E11 (Figure 1E) embryos were performed. Before tissue fixation, the circulating blood was flushed out of the aorta to ascertain that attached IAHCs and not circulating cells were observed. On transversal sections, the delimitation between the different structures (IAHCs, single-layered endothelium and sub-aortic mesenchyme) was nicely visible (Figure 1A-C). The number of cells forming the IAHCs was highly variable, from single cells to massive agglutination of cells (Figure 1C and E). However, IAHCs with higher number of cells were more frequently observed at E10 than at E11. The shape of IAHCs was heterogeneous independently of the developmental stage and could be mainly organized within three categories: spheroid, stacks and 'mushroom like' structures (Figure 1C and 1E middle down panel). In all cases, the IAHC cells looked alike, with spherical shape and microvilli on the surface (Figure 1D). Although the function of these microvilli is unclear, close-up views suggest a possible role for cell-cell junction and communication (Figure 1D). Interestingly, the microvilli are absent on the underlying endothelial cells, although they are the direct IAHC cell precursors (Figure 1E).

Defective IAHC formation in *runx1*$^{-/-}$ embryos might result from apoptosis occurring during the endothelial to hematopoietic transition.

To observe in details the structure of the aorta in hematopoietic mutants, transversal slices of *runx1*$^{-/-}$ (Figure S1A-G) and *runx1*$^{+/-}$ (Figure S1H) embryos were observed. As expected, no IAHCs were found in the dorsal aorta of *runx1*$^{-/-}$ embryos (Figure S1A). The endothelial cells were often seen disorganized (Figure S1B) and covered of cell debris, which was not observed in WT embryos (Figure S1 C, D and Figure 1). Many dying cells were also observed attached to the endothelium of *runx1*$^{-/-}$ (Figure S1E) and *runx1*$^{+/-}$ (Figure S1H) embryos (in pink). A close observation of the *runx1*$^{-/-}$ endothelium shows that some cells started to round up, and displayed microvilli (Figure S1F and G). This suggests that the endothelial to hematopoietic transition took place in *runx1* mutant embryos but eventually failed, resulting in apoptosis. Also, only few single IAHC cells could be observed in *runx1*$^{+/-}$ embryos (Figure S1H, in yellow). Noteworthy, it seems that the aorta and the cardinal veins of *runx1*$^{-/-}$ embryos were slightly bigger in diameter than in WT embryos of the same age (Figure S1A).

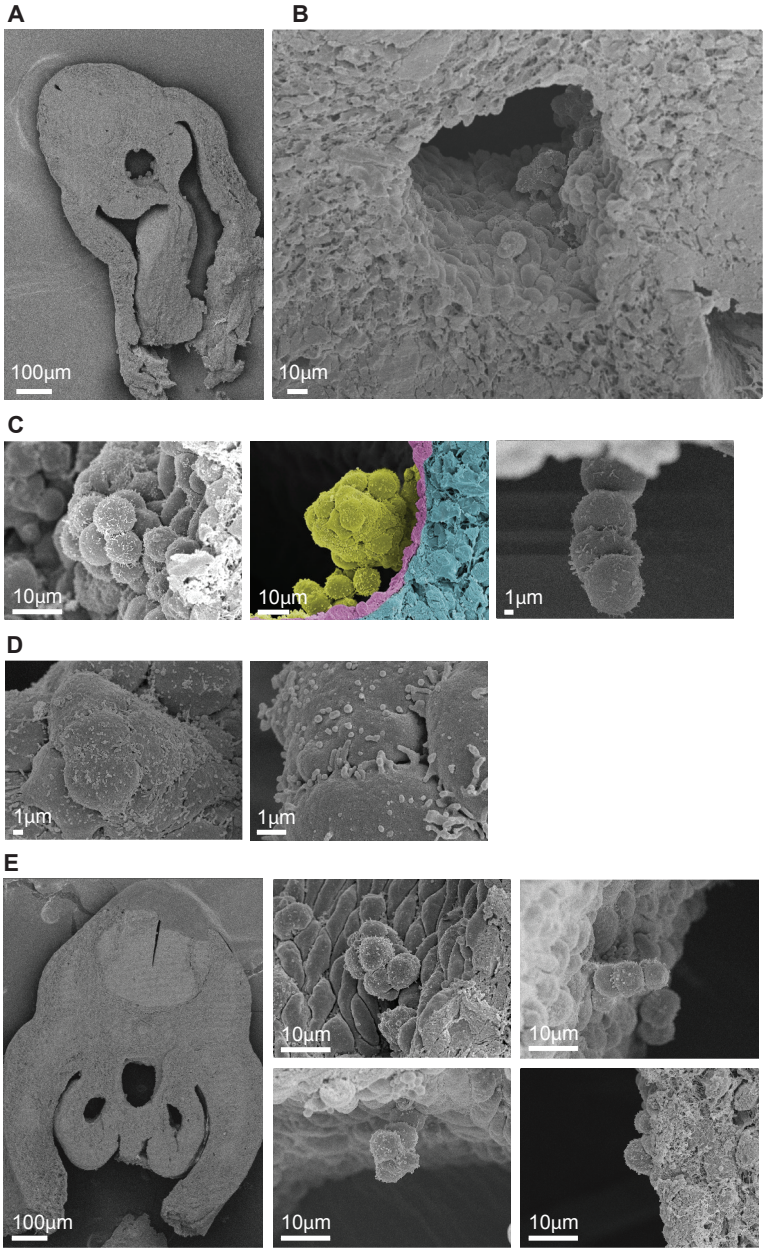

Figure 1. Cells forming the intra-aortic hematopoietic clusters (IAHC) seem identical but form heterogeneous IAHCs at E10 and E11. Scanning electron microscopy observation of 200 µm vibratome transversal sections of E10 (A-D) and E11 (E) WT embryos. (A) Global view of an E10 embryo slice and (B) close-up view of the dorsal aorta (different slices). (C) Examples of E10 IAHCs. Note in the middle panel the different tissue layers: IAHC in yellow, endothelium in pink and mesenchyme in cyan (artificial colors). (D) Close-up view of IAHC cell interactions and microvilli. Left panel in (D) is a higher magnification of middle panel in (C). (E) Global view of an E11 embryo slice (left panel), and different examples of IAHCs at higher magnification. Upper middle panel in (E) is a 200 µm sagittal slice, which allows an 'en face' view of the aortic lumen and therefore of the endothelium. Scales are as indicated on each pictures. E10 were 28-34 somite pairs (s.p.). Top: dorsal side; bottom: ventral side.

IAHC cells, although phenotypically heterogeneous, can be isolated to purity.

Others and we have shown that all IAHCs specifically express high levels of c-kit. However, other cells, in the circulating blood or outside the aorta (e.g. primordial germ cells), also express c-kit. To exclusively label IAHC cells for further isolation, we injected directly labeled antibodies against c-kit directly into the aorta of non-fixed embryo trunk. With this approach, circulating blood was flushed out of the aorta and the attached IAHCs were stained in a single procedure. We could then observe IAHCs expressing c-kit in live thick transversal embryo slices (Figure 2A and E), as previously shown (Boisset et al., 2011; Boisset et al., 2010). To test whether the intra-aortic injection of c-kit antibody procedure could help isolating a clear IAHC population, flow cytometry analysis were performed after dissection and dissociation of the AGMs. We compared the c-kit staining performed directly on dissociated AGM cells (standard procedure) (Figure 2B) with the c-kit staining performed intra-aorta prior to dissociation (Figure 2C). In standard staining, all c-kit expressing cells in the total AGM were stained. However, many cells expressing c-kit at an intermediate level blurred the definition of the c-kithigh expressing IAHC population. On the other hand, when c-kit was injected inside the aorta, the IAHC population was sharply defined as shown by flow cytometry. In addition, we controlled that the intra-aortic staining procedure did not detach IAHCs, the flush pressure being higher than natural blood circulation. We performed whole-embryo c-kit staining of flushed compared to non-flushed embryos. We found no significant differences in the number of c-kit (IAHC) cells in the aorta or in the shape of IAHCs (data not shown). Therefore, intra-aortic staining allows to label and to isolate to purity IAHC cells based on c-kit^{high} expression.

We then investigated whether IAHC cells differentially expressed certain surface molecules indicating an inner heterogeneity. We previously observed on embryo sections that IAHC cells differentially expressed Ly6A (Sca1)-GFP at E10 (Boisset et al., 2010), result that was confirmed here by confocal observation of thick non-fixed *Ly6A-GFP* embryos slices (Figure 2D, E and F). Furthermore, we examined on live slices the expression of classical surface markers expressed by endothelial or hematopoietic cells (Figure 2F and G). All endothelial and IAHC cells expressed VE-Cadherin, Tie2 and CD31. On the other hand, Flk1 was only expressed by endothelial cells while CD45 was only expressed by some IAHC cells. The same observations could be drawn from E11 embryo slices (Figure S2A-D). However, at E9, cells expressing Ly6A-GFP were very rare and mostly located in the endothelium (Figure S2E-I). At such early stages, we did not observe c-kit or CD45 expressing cells in the aorta, according to the fact that there are no IAHCs present yet (Figure S2E-G).

To further investigate the phenotype of the IAHC cells, we focused on the

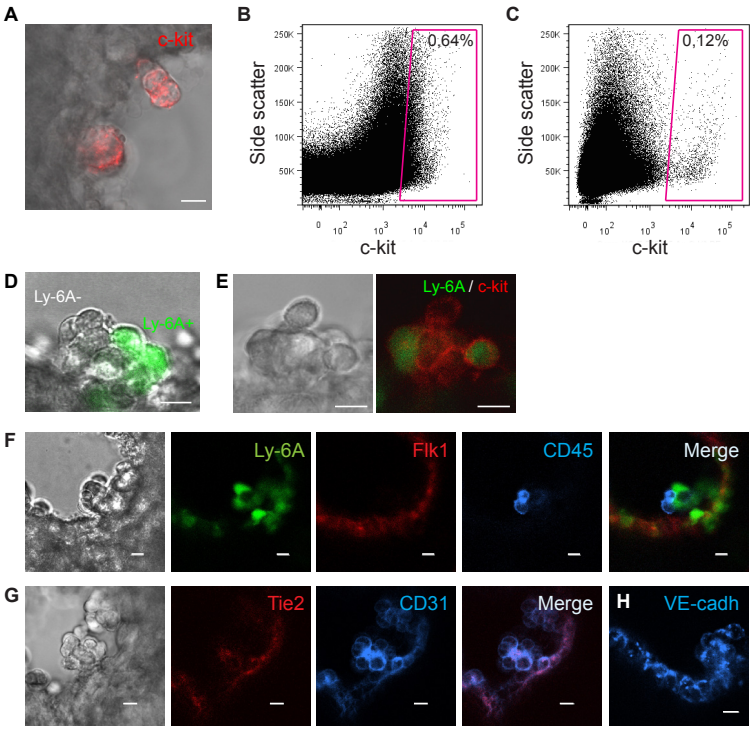

Figure 2. Isolation of IAHCs to purity after intra-aortic injection of c-kit antibodies. (A and D-H) Confocal microscopic observation of non-fixed E10 embryo transversal slices. WT embryos were used in (A, G and H), and Ly6A-GFP embryos in (D-F). (A and E) Intra-aortic staining and (F and G) staining by incubation of the thick slices with different directly conjugated antibodies as indicated on the different panels. Green=GFP, Red=PE; blue=APC or AlexaFluor 647. (A and D) Fluorescent channel is merged with the transmitted light channel. (E-G) Left panel=transmitted light channel, other panels=single fluorescence or merge of the fluorescent signals. Scale bar=10 µm. (B and C) Flow cytometry analyses of E10 AGM cells stained with a PE anti-c-kit antibody after enzymatic dissociation (B), or by intra-aortic injection before AGM dissociation (C). Note that IAHC c-kithigh population (pink gate) is better defined in (C). Percentages of the IAHC population are indicated in the corresponding gates.

two markers Ly6A-GFP and CD45, found to be differentially expressed by the c-kit^{high} IAHC cells. Confocal microscopy of non-fixed *Ly6A-GFP* embryos (thick transversal slices or whole embryo trunk) were done in parallel with flow cytometry analysis of dissociated *Ly6A-GFP* AGM cells, in both cases after staining with the same c-kit and CD45 conjugated antibodies. At E10 and E11, c-kit expressing IAHCs contain cells with four different phenotypes: c-kit^{high} {Ly6A-GFP $^{-\text{ or }+}$ CD45 $^{-\text{ or }+}$} (Figure 3A-C (E10 embryo slices), F-H (E11 embryo slices); figure S3 (E10 whole embryo trunk); supplementary video1). The observed heterogeneity of phenotype within and between the IAHCs was independent of the IAHC size and shape (Figure3A-C). Sometimes, only a single cell in a cluster was expressing CD45 or Ly6A-GFP (Figure3A and B). We also observed in the aorta putative macrophages as single cells only expressing CD45 but not c-kit (Sharp sign in figure 3C). The same four

different phenotypes were identified within the c-kit^{high} expressing cells at E10 and E11 by flow cytometry (Figure 3D and 3I). The staining was performed after dissociation, which explained the high percentage of intermediate c-kit expressing cells. However the blood was initially flushed out of the aorta, which ensured that the c-kit^{high} cells that we observed were the IAHC cells. The aortic circulating blood from E10 and E11 embryos was collected and also analyzed by flow cytometry (Figure 3E and J, respectively). c-kit^{high} cells were present in the circulation as a well defined population. However, in contrast to IAHC cells, in the circulating blood, they were mostly Ly6A-GFP^{-} CD45$^{-\text{ or }+}$ at E10 and Ly6A-GFP$^{+\text{ or }-}$ CD45^{+} at E11 but not Ly6A-GFP^{+} CD45^{-} at both stages. In addition, the percentage of c-kit^{high} Ly6A-GFP^{-} CD45^{+} was much higher than in the IAHCs. Therefore, although IAHC cells look alike they are phenotypically heterogeneous. However, all IAHC cells can be easily isolated to purity based on c-kit^{high} expression after in situ intra-aortic staining.

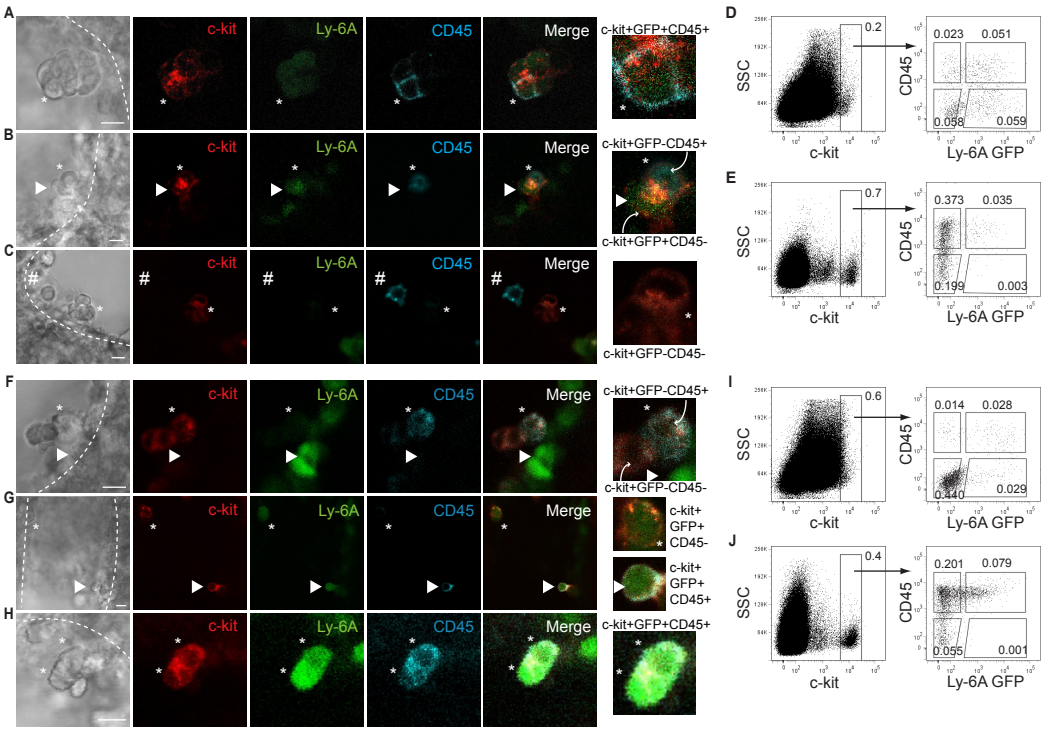

Figure 3. IAHC cells differentially express Ly6A-GFP and CD45 at E10. Confocal microscopic observation of E10 (A-C) and E11 (F-H) non-fixed ***Ly6A-GFP*** embryo transversal slices stained with PE anti-c-kit (red), and APC anti-CD45 (blue) antibodies. Left panel is the transmitted light channel. The following panels are the fluorescent channels. The endothelium position is depicted as a dotted line. The extreme right panels are close-ups of IAHC cells shown in the fluorescent merged images. Asterisk and arrowhead mark the cells of interest in the different channels. The phenotype of each cell is indicated. The sharp sign refers to a putative c-kit-Ly6A-GFP^{-} CD45^{+} macrophage. Scale bars=10 µm. (D, E, I and J) Flow cytometry analyses of E10 (D and E) or E11 (I and J) ***Ly6A-GFP*** embryonic cells stained with PE anti-c-kit and APC anti-CD45 antibodies. (D and I) are AGM cells, and (E and J) are AGM flushed blood cells. Ly6A-GFP and CD45 expression are shown in the gated c-kit^{high} population. Percentages of each viable population are indicated for each gate.

IAHCs contain few erythro-myeloid progenitors

To functionally characterize the different sub-populations identified phenotypically, they were first sorted and tested *in vitro*. To determine whether IAHCs contained Erythro-Myeloid Progenitors (EMPs), E10 AGM cells (blood was removed) sorted from *Ly6A-GFP* embryos were tested in a clonogenic (methylcellulose-based) assay (Figure S4A). EMPs were highly enriched in the Ly6A-GFP^{+} (Ly6A^{+}) population (Figure S4B). However, the same number and type of EMPs were found, proportionally to the Ly6A^{+} and Ly6A^{-} fractions found in the AGM (Figure S4C). To determine whether Ly6A-GFP is a marker of EMPs in the adult bone marrow (all HSCs being Ly6A^{+}), negative, low and high Ly6A-GFP expressing cells were sorted and tested in vitro (Figure S4D and E). All EMPs were exclusively in the Ly6A^{+} population (with a higher number in the Ly6A^{high} fraction). Thus, while all EMPs express Ly6A-GFP in the adult bone marrow, only part of them express Ly6A-GFP in E10 AGM.

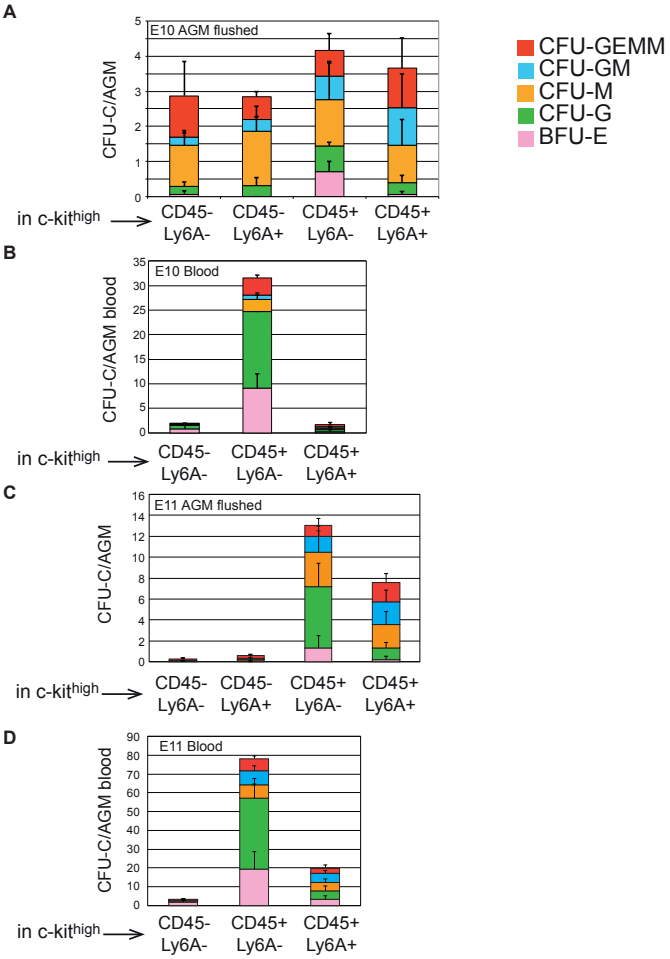

Figure 4. Most erythroid-myeloid progenitors are circulating in E10/E11 AGMs. (A-D) Bar graphs show the number of colony-forming units in culture (CFU-C) per AGM (A and C) or per 1 equivalent of AGM flushed blood (B and D), at E10 (A and B) and E11 (C and D). The different IAHC subpopulations tested are depicted under each graph (c-kit^{high} {CD45$^{+ \text{ or } -}$ Ly6A$^{+ \text{ or } -}$}). Colors correspond to all different types of progenitors observed. Error bars are the standard deviations calculated for n=3 independent experiments. CFU-GEMM=CFU-granulocyte-erythroid-macrophage-megakaryocyte; CFU-GM=CFU-granulocyte-macrophage; CFU-M=CFU-macrophage; CFU-G=CFU-granulocyte; BFU-E=Burst-forming unit-erythroid.

We analyzed the EMP potential of the four sorted IAHC cell populations based on c-kit, Ly6A-GFP and CD45 expression, as described previously (Figure 3D and I). At E10 all types of EMPs were present in all subpopulations of IAHC cells (c-kit^{high} {Ly6A-GFP $^{-\text{ or }+}$ CD45 $^{-\text{ or }+}$}) (Figure 4A). However, the number of EMPs was very low, representing in total an average of 14 EMPs per AGM. At E11, EMPs were mainly in the CD45$^+$ subpopulation, and were in higher number in the Ly6A$^-$ subfraction (Figure 4C). However, at E10 and E11 in the AGM circulating blood, EMPs were highly enriched in the Ly6A$^-$ CD45$^+$ subpopulation (Figure 4B,D, respectively). Importantly there were many more EMPs in the aortic flushed blood than in the IAHCs. Thus, IAHCs contain very few EMPs that cannot account for the high number of IAHC cells observed at E10/E11. Based on the same phenotypes, the EMP content was also examined at E10 in other hematopoietic organs. The YS, FL and placenta contained high numbers of EMPs, enriched in the c-kit^{high} Ly6A$^-$ CD45$^+$ (Figure S5A,B,C respectively), similarly to E10-E11 circulating blood.

In addition, E10 c-kit^{high} IAHC cells (1045 cells), 3ee of unsorted cells, or 2x10^4 c-kit^{high} sorted cells from E10 YS were unable to provide any pre-B progenitors in specially designed clonogenic assay (data not shown). Thus, EMPs are highly enriched in the c-kit^{high} Ly6A$^-$ CD45$^+$ population in all hematopoietic tissues, at the exception of the E10 aorta, where EMPs are found equally in all populations. Importantly, IAHCs contain very few EMPs since they are mainly in the circulation. Also, EMPs differentially express CD45 and Ly6A in the IAHCs.

Table 1. Summary of reconstitution experiments

A

Cells injected	Populations sorted	Number repopulated/Number injected
E9 YS (n=4)	-	5/8
E10 AGM (n=2)	c-kit^{high} intra-aorta	2*/2
E10 AGM (n=3)	c-kit^{high} CD45$^-$ Ly6A$^-$	3/3
	c-kit^{high} CD45$^-$ Ly6A$^+$	3/4
	c-kit^{high} CD45$^+$ Ly6A$^-$	1/4
	c-kit^{high} CD45$^+$ Ly6A$^+$	3/4
E11 FL (n=1)	c-kit^{high} CD45$^-$ Ly6A$^-$	1/1
	c-kit^{high} CD45$^-$ Ly6A$^+$	0/1
	c-kit^{high} CD45$^+$ Ly6A$^-$	1/1
	c-kit^{high} CD45$^+$ Ly6A$^+$	1/1

B

c-kit^{high} cells from primary	Bone marrow		Spleen	
Secondary recipient	*Rag2*$^{-/-}\gamma$***c***$^{-/-}$	WT	Rag2$^{-/-}\gamma$c$^{-/-}$	WT
Number repopulated/ Number injected	2/2	1$^{\#}$/2	2/2	1$^{\#}$/2

Long-term reconstitution (4-5 months) of (A) primary injected *Rag2*$^{-/-}\gamma$***c***$^{-/-}$ newborns, or (B) secondary injected *Rag2*$^{-/-}\gamma$***c***$^{-/-}$ or WT adult recipients. Mice were considered positive when donor derived cells were detected in the BM and spleen of the recipient by both flow cytometry of the H2k^k and Ly6A-GFP donor markers, and semi-quantitative PCR of the *Ly6A-GFP* transgene.

* 1 recipient was injected with 783 cells, 1 recipient with 1372 cells.

$^{\#}$ The reconstituted secondary recipient was injected with cells from the primary recipient initially injected with 783 cells.

IAHCs contain pre-HSCs

Since IAHCs contain very few EMPs, we further tested their in vivo potential. HSC potential is identified by classical transplantations only in embryos older than E10.5 (>33 s.p.) (Medvinsky and Dzierzak, 1996; Muller et al., 1994). However, transplantation in busulfan conditioned (Yoder et al., 1997b) or W^{41} newborn liver (Peeters et al., 2005) reveals HSC-like (thereafter referred as pre-HSC) potential in E9 and E10 YS or P-Sp. Also, explant culture of E8 P-Sp yield long-term chimerism in irradiated adult *Rag2*$^{-/-}\gamma c^{-/-}$ recipients (Cumano et al., 2001). We took advantages of both models and tested pre-HSC potential by transplanting IAHC cells into the liver of irradiated *Rag2*$^{-/-}\gamma c^{-/-}$ newborns.

To test our in vivo model, E9 YS cells were first transplanted. Four months post-transplant 5 out of 8 recipients transplanted were reconstituted (Table 1A). Reconstitution levels were determined by flow cytometry analysis of $H2k^k$ and Ly6A-GFP expression (donor) (Figure S6B-G, J-O), and confirmed by semi-quantitative PCR of the *Ly6A-GFP* transgene (Data not shown). The chimerism was comprised between 0.5% and 1.1% in the BM, 3.45-41% in the spleen, and 0.4-10.9% in the blood (Figure S6A). After 4 months, donor cells had mainly differentiated to the myeloid lineage, as shown by MAC1/Gr1 expression (representative experiment showing the chimerism in BM

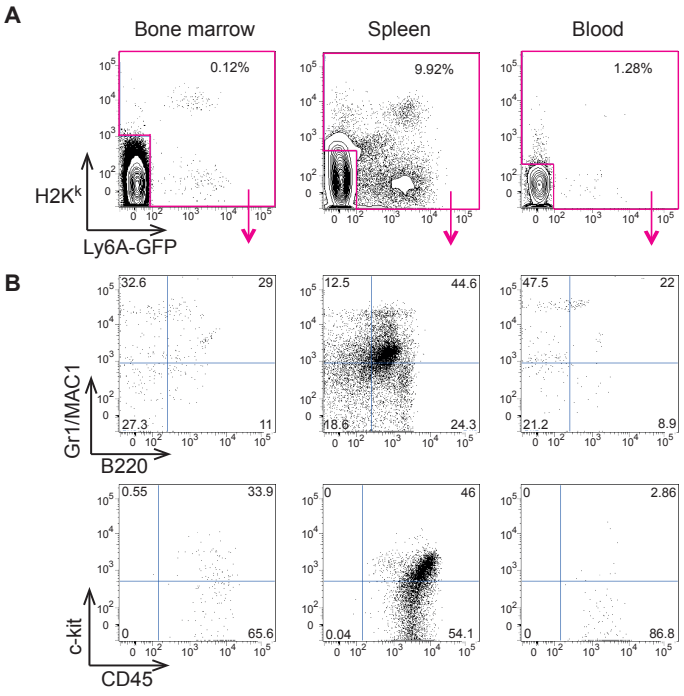

Figure 5. E10 IAHCs contain pre-HSCs before HSC production. Flow cytometry analyses at 5 months of a *Rag2*$^{-/-}\gamma c^{-/-}$ grown-up newborn initially injected with 783 E10 (<33 s.p.) IAHC cells. (A) Percentage of viable $H2K^{k+}$ and/or Ly6A-GFP^{+} (donor markers) cells in BM, spleen and peripheral blood of the recipient (pink gate). (B) Gr1/MAC1, B220, c-kit and CD45 expression in the donor cell fractions gated in (A). In each quadrant is depicted the percentages of donor viable cells for each indicated cell surface markers.

and spleen, S6D and H respectively), and a high percentage of cells had an immature hematopoietic phenotype as shown by CD45 and c-kit expression (Figure S6E and I). We performed secondary transplantations in irradiated adult *Rag2*$^{-/-}\gamma c^{-/-}$ with BM cells isolated from a primary reconstituted mouse. Donor cells were present after 4 months in the BM and spleen (respectively 0.22% and 1.3%) (data not shown). We also transplanted spleen cells from the primary reconstituted recipient shown in Figure S6B-I. After 4 months, chimerism (although low) was present in the BM and spleen of the transplanted recipients (Figure S6 J-Q), mainly as c-kit^{+} stem/progenitor cells (Figure S6 M and Q). Therefore, pre-HSCs can be probed in our transplantation model.

To test whether IAHCs contain pre-HSCs, intra-aortic c-kit^{high} cells were sorted and transplanted into the livers of irradiated *Rag2*$^{-/-}\gamma c^{-/-}$ newborns. Two newborns were reconstituted after injection of 1372 and 783 cells, (Table 1A). Respectively, reconstitution levels were 0.06% and 0.1% in the BM, 2.4% and 9.9% in the spleen, and 0.4% and 1.3% in the peripheral blood after 5 months (Table 1A and Figure 5A (shows the results obtained with the mouse injected with 783 cells)). Secondary transplantations were performed with BM and spleen cells isolated from both reconstituted primary recipients in irradiated adult *Rag2*$^{-/-}\gamma c^{-/-}$ recipients. In both cases, reconstitution (albeit at low levels) in the BM, spleen and peripheral blood of the secondary recipients were obtained after 4 additional months (Table 1B). The reconstitution was multilineage in primary and secondary recipients, but similarly to E9 YS cell transplantations, most donor cells were expressing c-kit, thus remaining and/or producing immature stem/progenitor cells (Figure 5B).

To determine whether IAHC cells could mature toward cells with a true HSC potential, secondary transplantations were this time performed in irradiated adult WT recipients. The analysis was here solely based on PCR detection of the *Ly6A-GFP* transgene since the secondary recipients and donor cells were both H2K^{k+}. The BM and the spleen of one mouse out of two injected provided long-term reconstitution of the secondary WT recipients (Table 1B). The mouse injected with the BM cells of the first recipient had 3.2% chimerism in the spleen and 4% in the peripheral blood. The mouse injected with the spleen cells had 17% chimerism in the spleen and 5.3% in the peripheral blood. The donor marker was not detectable in the BM of both mice, probably due to a low level of chimerism and little sensitivity of the semi-quantitative PCR. Overall, IAHCs contain pre-HSCs capable of maturation toward adult type HSCs.

To test whether pre-HSCs were present in all subpopulations of IAHCs (sorted based on c-kit, Ly6A-GFP and CD45 expression), transplantations in newborns were performed with the 4 different populations (c-kit^{high} {Ly6A-GFP$^{+\text{ or }-}$ CD45$^{+\text{ or }-}$}). We found that all subpopulations contained pre-HSCs, but at a lower frequency in the c-kit^{high} Ly6A-GFP^{-} CD45^{+} sub-fraction (Table

1A). The reconstitution was multilineage but in most cases biased toward the myeloid lineage with a large donor stem/progenitor compartment (c-kit^{+} CD45^{+}) (data not shown). We performed secondary transplantations of the BM and spleen cells of the primary reconstituted recipients into irradiated adult *Rag2*$^{-/-}\gamma c^{-/-}$ and WT mice. Only the original c-kit^{high} {Ly6A^{+} CD45$^{+\text{ or }-}$} IAHC populations could reconstitute secondary recipients (*Rag2*$^{-/-}\gamma c^{-/-}$ or WT) (data not shown, n=1).

A general idea is that IAHC cells are progressively detaching from the aorta and would start to colonize the FL via the circulation. We indeed find the 4 phenotypically defined IAHC populations in the FL (c-kit^{high} {Ly6A-GFP$^{-\text{ or }+}$ CD45$^{-\text{ or }+}$}) although the Ly6A-GFP^{+} CD45^{-} subpopulation was almost absent) (Data not shown). To test whether pre-HSCs were still present in E11 FL, the 4 phenotypically defined IAHC populations present in the FL were transplanted (2.7-3.3 ee for each population). Reconstitutions were obtained with the Ly6A-GFP^{-} CD45$^{-\text{ or }+}$, and Ly6A-GFP^{+} CD45^{+}, but not with the Ly6A-GFP^{+} CD45^{-} subpopulations (table 1A). Reconstitution from the c-kit^{high} Ly6A-GFP^{+} CD45^{+} population was expected since this is the phenotype of HSCs at E11 in the

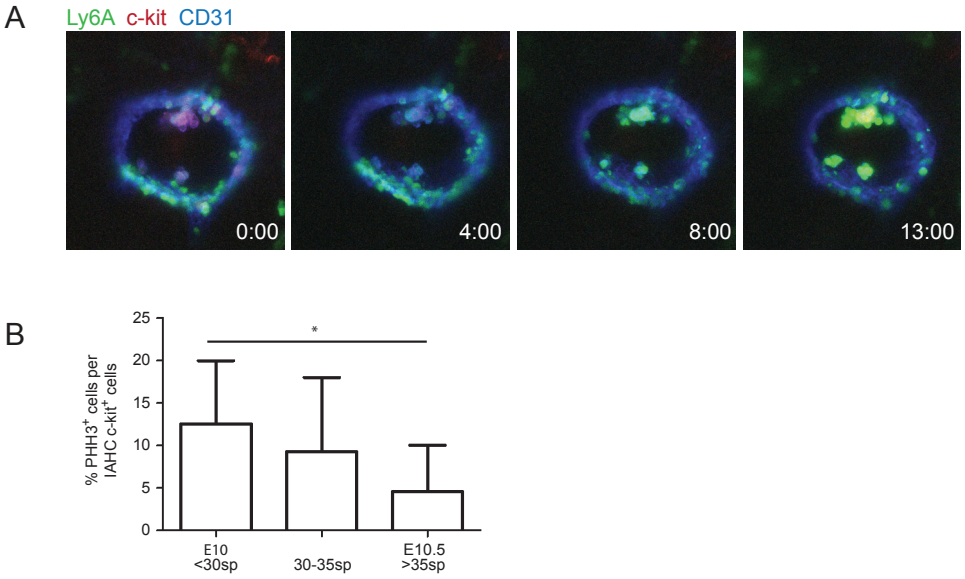

Figure 6. IAHC cells become phenotypically defined HSCs with little proliferation. (A) Still pictures from a three-dimensional time-lapse movie (See supplementary video 2) performed on 200 µm live ***Ly6A-GFP*** (green) embryo transversal slices, stained with PE anti-c-kit (red) and AlexaFluor 647 anti-CD31 (blue) antibodies injected intra-aorta. The video is a maximal projection of a stack of 120 µm. Time is indicated in hour : min. (B) Percentage of PHH3^{+} cells per IAHC cells at different developmental periods, counted by microscopic observation of thick embryo slices, as shown in (Figure S7B and C). 14 slices (409 c-kit cells) isolated from E10 embryos at <30 s.p., 27 slices (769 c-kit cells) at 30-35 s.p. and 7 slices (362 c-kit cells) at >35 s.p. were analyzed. Stages are indicated below the stack area chart. * indicate p<0,05

AGM. Nevertheless, repopulation with the Ly6A-GFP$^-$ subfractions shows that pre-HSCs are present in E11 FL. It thus suggest that pre-HSC populations might colonize the FL.

IAHC cells mature into HSCs during development

The transplantations performed in newborns indicate that IAHCs contain pre-HSCs able to mature into HSCs in vivo, since they are able to reconstitute secondary WT adult recipients. However, it is unclear whether this maturation happens during the short time course of embryonic development. Only some E10 IAHC cells already expressed Ly6A-GFP and/or CD45, but both markers are not exclusive of pre-HSCs. On the other hand, all HSCs at E11.5 express c-kit (Sanchez et al., 1996), Ly6A-GFP (de Bruijn et al., 2002) and CD45 (North et al., 2002). To test whether IAHC cells could mature into phenotypically defined HSCs from E10 onward, time-lapse confocal microscopy was performed to image thick non-fixed slices of E10 *Ly6A-GFP* embryos. The aorta was specifically stained with CD31 and c-kit antibodies prior to imaging. All Ly6A-GFP$^-$ IAHC cells started to express Ly6A-GFP during the course of imaging (13 hours) (Figure 6A, Supplementary video 2). After imaging, the slices were stained with a CD45 antibody. No apparent CD45 expression was observed in the IAHC (data not shown). This suggests that expression of CD45 is a late event in the maturation of IAHCs. To test whether cell proliferation occurs in the IAHCs, thick non-fixed embryo slices were fixed and stained for phospho-Histone H3.3 (PHH3, proliferation marker), CD31 and c-kit (Figure S7A,B). The number of PHH3$^+$ cells in the IAHCs was counted as well as the total number of IAHC cells (Figure S7C). Only a small proportion of IAHC cells were positive for PHH3 at early (13.7%), mid (9.3%) and late (4.6%) E10 stages (Figure 6B). Thus, the majority of IAHC cells are not actively proliferating during their maturation toward a putative true HSC state.

DISCUSSION

IAHCs have been observed since more than a century, but a precise and clear description of their phenotype and function has been lacking up to now. First, we were able to provide high-resolution images of IAHC cells by scanning electron microscopy. IAHCs with the highest number of cells were observed at E10.5. They were reduced in size and number by E11.5. This is in accordance with previous confocal microscopy observations showing that the number of IAHC cells, and IAHC cells per IAHC, peaks at E10.5 (Yokomizo and Dzierzak, 2010). We also observed microvilli on the surface of IAHC cells (Medvinsky et

al., 1996). These microvilli might function as junctions for cell communication and/or anchorage. Another possibility is that they might be necessary for IAHC cell migration and attachment to other hematopoietic organs. Indeed, these structures are reminiscent of what can be observed on immune cells, in which presenting adhesion molecules on microvilli is important for tethering during rolling on vascular endothelium (Abitorabi et al., 1997; Majstoravich et al., 2004).

It was shown in the zebrafish embryo that the endothelial to hematopoietic transition lead to a shrinkage of the aorta, because the transition happens without cell division, which thus deplete the aortic endothelial population (Kissa and Herbomel, 2010). Therefore, the observation of a slightly bigger aorta diameter in *runx1*$^{-/-}$ embryos suits a lack of emergence in these mutant embryos.

The functional characterization of IAHCs has so far been hindered by the lack of methods to specifically purify these cells. By injecting c-kit antibodies directly into the aorta before tissue dissociation, we could specifically and solely label the IAHC cells that face the lumen of the aorta. These cells could be sorted to purity as they represent a well-defined c-kit^{high} population. With this approach, the c-kit cells located outside of the aorta (Yokomizo and Dzierzak, 2010; Yokomizo et al., 2011; Zovein et al., 2010) were not labeled. In addition, we identified and sorted sub-populations of IAHC cells, based on their differential expression of Ly6A-GFP and CD45, which proved useful for further characterization. It was already known that IAHC cells differentially express both markers (Boisset et al., 2010; Mizuochi et al., 2012; Yokomizo and Dzierzak, 2010). However, they were never used in combination to characterize the IAHC cells.

The AGM contains the first HSCs at mid-gestation, but in very low number (Gekas et al., 2005; Kumaravelu et al., 2002). A massive increase of the HSC pool happens rapidly after, mainly in the FL. Indeed, the number goes from an average of 11 to 152 HSCs in the total conceptus in 24h, from E11 to E12 (Gekas et al., 2005; Kumaravelu et al., 2002). This could be due to intensification of HSC self-renewal (FL HSCs are highly cycling (Bowie et al., 2006; Morrison et al., 1995)), and/or to a maturation of cells toward HSCs. This later idea was proposed after a massive HSC increase was observed in an *in vitro* re-aggregation culture while most HSCs were slow-cycling (at E11.5) (Taoudi et al., 2008). However, the *in vivo* relevance of this idea has been lacking so far. Here we demonstrate that the IAHCs located in the aorta are (at least in part) a reservoir of very immature cells (pre-HSCs) able to mature in vivo into adult engrafting HSCs. Indeed pure IAHC cells sorted from the aorta before HSC production (<34 s.p.), successfully reconstitute primary (immunodeficient newborns) and secondary (WT) recipients. Moreover, we witnessed by confocal imaging the first maturation steps of IAHC cells into phenotypically defined HSCs *ex vivo* in live embryo slices.

HSPCs are believed to compose the IAHCs. However, the early appearance of IAHCs and their excess compared to the number of HSCs indicate that hematopoietic cells with a different function compose the IAHCs. Here we show that the number of EMPs was very low in IAHCs, about 15 EMPs per AGM (containing ~600 IAHC cells at E10 (Yokomizo and Dzierzak, 2010)). In fact, most AGM EMPs were circulating, and are most likely coming from the YS, the biggest reservoir of EMPs at E10, which is in accordance to previous data (Ohmura et al., 1999). In addition, it has been shown that the embryo proper generates only very few EMPs on its own, whereas most of them are YS derived (Lux et al., 2008). Although B progenitors were reported previously in the AGM by using *in vitro* culture on stromal cell line TSt-4, we here did not observe any late B progenitors (pre-B, tested in methylcellulose without co-culture step) (Ohmura et al., 1999). Thus, hematopoietic progenitors represent a very minor fraction of IAHCs. Therefore IAHCs that express c-kit, a marker of HSPCs, contain very few hematopoietic progenitors and no HSCs at early E10, but they contain pre-HSCs (at least 1 in 284 IAHC cells, the lowest number of cells injected per recipient).

Maximov, one of the first to report the existence of IAHCs, hypothesized in the early 20th century that IAHC cells would progressively detach from the aorta to colonize other hematopoietic organs (Maximov, 1909). Indeed, after E10.5, the number of IAHC cells present in the mouse aorta is progressively decreasing (Yokomizo and Dzierzak, 2010). Such events have been followed in the zebrafish embryo where the hematopoietic cells emerging from the aortic endothelium detached in the sub-aortic mesenchyme to finally migrate into the underlying cardinal vein (Kissa and Herbomel, 2010). In the mouse, we observed that the cell emergence from the endothelium happened toward the aortic lumen, but the possible detachment of the IAHC cells and their journey could not be observed since blood circulation was absent in our *ex vivo* conditions (Boisset et al., 2010). The FL is known to be colonized by hematopoietic cells generated in other organs, but is not capable to autonomously produce them (Houssaint, 1981; Johnson and Moore, 1975). Here we found that the FL contained pre-HSCs at E11, potentially coming from the IAHCs and hypothetically contributing, after maturation, to the massive increase in the number of HSCs observed after mid-gestation in the FL (Gekas et al., 2005). It has been shown that pre-HSCs are also present in the YS at E9 and E10. To which extent each population contributes to the FL HSC pool still needs to be determined.

In a previous study, we used the Ly6A-GFP reporter as a marker to trace the HSCs. The emergence of Ly6A-GFP$^+$ IAHC cells from Ly6A-GFP$^+$ endothelial cells was observed *ex vivo* in non-fixed thick embryo slices (Boisset et al., 2010). In addition, it was suggested that the *Ly6A* transgene exclusively marks

hemogenic endothelial cells producing HSCs (Chen et al., 2011). Nevertheless, here we showed that IAHCs contain pre-HSCs and EMPs in the Ly6A-GFP$^+$ fraction as well as in the GFP$^-$ fraction, which indicates that Ly6A-GFP is very unlikely to be an exclusive marker of hemogenic endothelial cells. In fact, the potential of Ly6A-GFP$^-$ endothelial cells to produce EMPs and/or HSCs has never been tested. Therefore no marker specifically identifies hemogenic from non-hemogenic endothelial cells to date.

We observed that early E10 IAHC cells (no HSC yet) provided long-term and multilineage reconstitution upon transplantation in irradiated *Rag2*$^{-/-}\gamma c^{-/-}$ newborn. Therefore IAHC cells have an HSC potential. However, the modality of engraftment raises several questions. Indeed, the level of chimerism was low (especially in the blood), high in the spleen, and biased toward the stem/progenitor compartment and also often to the myeloid compartment. This could be due to the low number of cells injected, and/or the properties of pre-HSCs. In a previous study, it was shown that as low as 100 CD34$^+$ c-kit$^+$ cells from E9 YS or P-Sp could reconstitute at high level a busulfan conditioned WT newborn in a competitive setting (Yoder et al., 1997a). Nevertheless, chimerism levels are difficult to compare to our study because of the different methods used for experiment and analysis. However, similar levels of reconstitution in adult *Rag2*$^{-/-}\gamma c^{-/-}$ recipients were observed previously after injection of E10 AGM cells (Bertrand et al., 2005; Cumano et al., 2001). Thus, it seems plausible that IAHC's pre-HSCs need some maturation processes, to gain the full properties of adult HSCs, which were bypassed in our transplantation protocol. It has been proposed that pre-HSCs miss the expression of the MHC class I (Cumano et al., 2001; Kieusseian et al., 2012), and/or of other receptors (Yoder et al., 1997b), which precludes their engraftment in the adult BM. Whether the maturation of a pre-HSC toward an HSC depends solely on these molecules or on more complex processes is still unknown. However, it seems that the maturation process depends on the close interactions of pre-HSCs with the surrounding microenvironment. Indeed, it is only after 33 s.p. that the first HSCs are detectable in the embryo (Muller et al., 1994). It is also after this time point that the HSC activity increases in AGM explants (Medvinsky and Dzierzak, 1996), mainly through maturation as shown in AGM cell reaggregate cultures (Taoudi et al., 2008). Therefore, the AGM microenvironment seems to change after 33 s.p. since it allows IAHC's pre-HSCs to mature into HSCs. However, in vivo, this maturation process does not happen in the AGM since so few HSCs are detected there (Kumaravelu et al., 2002), but most likely outside of the AGM, in the FL and/or placenta.

Therefore, we propose a model where hemogenic endothelial cells do not form adult HSCs directly after the endothelial to hematopoietic transition. The IAHC cells derived from the endothelium would be an intermediate

cell population referred to as pre-HSCs that most likely mature later on into fully potent HSCs (most likely in the FL and placenta, the two main HSC reservoirs at mid-gestation) (Kieusseian et al., 2012). This has important clinical significance. One of the goals in the field of regenerative medicine is to reprogram somatic cells into HSCs by expression of transcription factors. So far, success has been limited, but understanding what drives endothelial cells to become fully competent HSCs, *in vivo* during development, would certainly help in defining experimental conditions to mimic this process *in vitro*.

EXPERIMENTAL PROCEDURES

Embryo generation

Mouse embryos were generated from timed matings. Observation of vaginal plugs was considered as day 0 of embryonic development. WT embryos were generated in the C57BL/6, Ly5.1 or FVB/NJ backgrounds. *Ly6A-GFP* embryos (Ma et al., 2002) were generated by crossing *Ly6A-GFP*$^{+/-}$ males with (C57Bl10 x CBA) females, *runx1*$^{-/-}$ embryos by crossing *runx1*$^{+/-}$ males and females, and *Rag2*$^{-/-}\gamma c^{-/-}$ pups by crossing *Rag2*$^{-/-}\gamma c^{-/-}$ males and females.

Scanning electron microscopy

E10.5 WT C57BL/6 embryos were separated from placenta, YS and amnion. Head and tail were cut. Blood in the aorta of the remaining caudal half was removed through injection of PBS/FCS (PBS supplemented with 10% fetal calf serum, penicillin (100 U/ml) and streptomycin (100 mg/ml)) inside the dorsal aorta using a pulled glass capillary and a glass syringe. Next, the embryo caudal parts were fixed overnight in osmium tetroxide, washed several times in PBS and subsequently sectioned with a Lancer Vibratome Series 1000 (Technical Products International) into transversal sections of 200 μm. Sections were fixed in 1.5% glutaraldehyde in 0.1M cacodylate buffer, dehydrated in a graded ethanol series, critical point dried over CO_2, sputter-coated with gold-palladium and viewed in a Jeol JSM 7600F Scanning Electron Microscope at 5 kV.

Confocal microscopy of non-fixed embryos (slices or whole)

The tissue preparation was as previously described (Boisset et al., 2011; Boisset et al., 2010). Briefly, E10 *Ly6A-GFP* embryos (32-35 somite pairs, s.p.) were freed from placenta, YS, amnion, head and tail. Non-fixed embryo trunks were stained by intra-aortic injection of antibodies or only PBS/FCS (to remove blood), and either cut into 200 μm transversal live slices with a tissue chopper

or dissected to remove the dorsal tissues (for live whole aorta observation). Tissues were embedded in agarose gel and observed by confocal microscopy (Leica Microsystem). In the case of ex vivo time-lapse imaging, embryos were first stained with an AlexaFluor647 anti-CD31 and PE anti-c-kit antibodies, or only AlexaFluor647 anti-c-kit antibody (in case of staining after imaging). After slicing and embedding, live slices were observed during 13 h. Following time-lapse imaging, slices (still in agarose gel) were stained with a PE anti-CD45 antibody, and observed again by confocal microscopy. Time-lapse videos were reconstructed using ImageJ. For multicolor z-stack pictures, thick embryo slices were stained after cutting by incubation with Pacific Blue anti-CD34 (RAM34), PE anti-c-kit (2B8), PE anti-flk-1 (Avas12 1), APC anti-CD45 (30-F11), PE anti-CD41 (MWReg30), PE anti-Tie2 (TEK4), APC anti-CD34 (RAM34), AlexaFluor 647 anti-CD31 (MEC13.3), AlexaFluor 647 anti-VE-Cadherin (eBioBV13) antibodies, and observed by confocal microscopy. Images were edited with the Leica Analysis Software, or with Volocity (Perkin Elmer) for 3D images or video reconstructions.

Embryonic tissue isolation and cell preparation

Pregnant mice were sacrificed by cervical dislocation to collect E9-E11 tissues. *Ly6A-GFP* embryos were checked under the fluorescent microscope for GFP expression. All embryonic tissues were dissected and enzymatically dissociated as previously described (Robin and Dzierzak, 2005). Briefly, after removal of the mother uterus, YS and placenta were separated from the embryo. Intra-embryonic AGM and FL were further carefully dissected away from all other embryonic tissues. YS, placenta and AGM were enzymatically digested in a 0.125% collagenase solution in PBS/FCS for 1 hour (1.5h for YS and placenta) at 37°C. FL were crushed through a 40 μm nylon cell strainer. Single cell suspensions were used for flow cytometry analysis, clonogenic assays and transplantations as previously described (Robin and Dzierzak, 2005). For AGM, the intra-aortic blood was removed by intra-aortic injection of PBS/FCS, or by the injection of antibodies (in the case of intra-aortic staining). The flushed blood was collected and filtered on a 40 μm mesh for further analyses.

Flow cytometry analysis and sorting

For flow cytometry analysis and sorting, cells were counted after Trypan Blue staining, to exclude the dead cells, in a Bürker Türk counting chamber. Cells were then stained with PE anti-c-kit (2B8) and APC anti-CD45 (30-F11) antibodies for 30 minutes at 4°C and washed. Alternatively PE anti-c-kit antibodies were injected intra-aorta prior to AGM dissection and dissociation. Cells were analyzed and sorted with an Aria III flow cytometer (Becton

Dickinson). 7-aminoactinomycin D (7-AAD) (Invitrogen) or Hoechst 33258 (Invitrogen, Molecular probes) were added to the cell suspension to discriminate dead from alive cells.

Hematopoietic progenitor assays

For Erythroid-Myeloid Progenitor (EMP) clonogenic assay, different doses of cells were plated in methylcellulose (M3434; StemCell Technologies). After 12 days of culture, colonies were identified and counted by microscopic observation. For pro-B progenitor clonogenic assay, different doses of cells were plated in methylcellulose (M3630; StemCell Technologies) and the colonies were counted after 7 days of culture.

Intra-liver newborn transplantations, analysis, and secondary transplantations

Cells were washed and resuspended in 15-20 µL of PBS before injection in the liver of 1-5 days old *Rag2*$^{-/-}\gamma c^{-/-}$ irradiated newborns (3 Gy, ^{137}Cs-source). After 4-5 months, donor chimerism was analyzed on BM, spleen and peripheral blood (red blood cells were lysed with IOTest® 3 Lysing Solution, Beckman Coulter) of the grown-up pups. The presence of donor contribution was determined by flow cytometry (LSR II, Becton Dickinson) after staining with an APC anti-H2k^{k} H100-27.R55 antibody and by Ly6A-GFP expression (both of donor origin). Dead cells were excluded with DAPI or Hoechst 33258 (Invitrogen, Molecular probes). Expression of H2k^{d} (recipient) and H2k^{k} (donor) were tested in BALB/c mice (same background as the recipient *Rag2*$^{-/-}\gamma c^{-/-}$ mice) (data not shown). In addition, BM, spleen and peripheral blood cells were analyzed by semi-quantitative Polymerase Chain Reaction (PCR) for the presence of the *Ly6A-GFP* transgene (data not shown). Multilineage analyses were carried out on BM, spleen and peripheral blood of the transplanted grown-up pups by using APC-Cy7 or APC efluor780 anti-MAC1 (M1/70), APC-Cy7 anti-Gr1 (RB6-8C5), AlexaFluor 700 anti-B220 (RA3-6B2), PE-Cy7 anti-CD45 (30-F11), and Per-CP-Cy5.5 anti-c-kit (2B8) antibodies.

For secondary transplantations, BM and spleen cells from primary recipients were isolated and suspended in PBS for injection (up to 31x10^{6} BM cells and 58x10^{6} spleen cells were injected per recipients) in either adult irradiated *Rag2*$^{-/-}\gamma c^{-/-}$ or WT (C57Bl10 x CBA) recipients (respectively 3Gy or 9Gy split dose, ^{137}Cs-source). 2x10^{5} (C57Bl10 x CBA) spleen cells were co-injected in the later recipient. After 4-5 months, secondary recipients were analyzed as described previously for primary recipients. (C57Bl10 x CBA) recipients were only analyzed by semi-quantitative PCR on BM, spleen and peripheral blood since

they express $H2k^k$ as the donor cells.

Confocal microscopy of thick fixed embryo slices

FVB/NJ embryos were dissected, the head and tail removed and the aortic blood flushed away. The remaining non-fixed embryo trunk was cut into 200 μm slices with a tissue chopper. Slices were fixed 30 minutes in 2% Para-Formaldhyde at 4˚C, washed in PBS and dehydrated in methanol. After rehydration, slices were sequentially incubated with anti-c-kit (2B8)/AlexaFluor 647 anti-rat IgG, biotin anti-CD31 (MEC13.3)/AlexaFluor 594 streptavidin and Anti-phospho-Histone H3.3 (PHH3)/AlexaFluor 488 anti-rabbit IgG antibodies as previously described (Yoko 2012). Slices were cleared with a benzyl alcohol benzyl benzoate (BABB) solution and observed by confocal microscopy (Leica Microsystem). *z*-stack images of the aorta were obtained with a 20x Epiplan-Neofluar dry lens. The number of intra-aortic c-$kit^{high}PHH3^-$ (non proliferative) and c-$kit^{high}PHH3^+$ (proliferative) cells was manually counted using the Leica Analysis Software. Student's *t* test was used to determine statistical significance. *P* values <0.05 were considered significant.

ACKNOWLEDGMENTS

We thank Henk Dronk and Experimental Dieren Centrum (Erasmus MC) for mouse care. This work was supported by NWO (VIDI) grant 917-76-345 (C.R.) and Landsteiner Foundation for Blood Transfusion Research (C.R.).

REFERENCES

Abitorabi, M.A., Pachynski, R.K., Ferrando, R.E., Tidswell, M., and Erle, D.J. (1997). Presentation of integrins on leukocyte microvilli: a role for the extracellular domain in determining membrane localization. The Journal of cell biology 139, 563-571.

Bertrand, J.Y., Chi, N.C., Santoso, B., Teng, S., Stainier, D.Y., and Traver, D. (2010). Haematopoietic stem cells derive directly from aortic endothelium during development. Nature 464, 108-111.

Bertrand, J.Y., Giroux, S., Golub, R., Klaine, M., Jalil, A., Boucontet, L., Godin, I., and Cumano, A. (2005). Characterization of purified intraembryonic hematopoietic stem cells as a tool to define their site of origin. Proc Natl Acad Sci U S A 102, 134-139.

Boisset, J.C., Andrieu-Soler, C., van Cappellen, W.A., Clapes, T., and Robin, C. (2011). Ex vivo time-lapse confocal imaging of the mouse embryo aorta. Nature protocols 6, 1792-1805.

Boisset, J.C., van Cappellen, W., Andrieu-Soler, C., Galjart, N., Dzierzak, E., and Robin, C. (2010). In vivo imaging of haematopoietic cells emerging from the mouse aortic endothelium. Nature 464, 116-120.

Bowie, M.B., McKnight, K.D., Kent, D.G., McCaffrey, L., Hoodless, P.A., and Eaves, C.J. (2006). Hematopoietic stem cells proliferate until after birth and show a reversible phase-specific engraftment defect. J Clin Invest 116, 2808-2816.

Chen, M.J., Li, Y., De Obaldia, M.E., Yang, Q., Yzaguirre, A.D., Yamada-Inagawa, T., Vink, C.S., Bhandoola, A., Dzierzak, E., and Speck, N.A. (2011). Erythroid/myeloid

progenitors and hematopoietic stem cells originate from distinct populations of endothelial cells. Cell Stem Cell 9, 541-552.

Chen, M.J., Yokomizo, T., Zeigler, B.M., Dzierzak, E., and Speck, N.A. (2009). Runx1 is required for the endothelial to haematopoietic cell transition but not thereafter. Nature 457, 887-891.

Christensen, J.L., Wright, D.E., Wagers, A.J., and Weissman, I.L. (2004). Circulation and chemotaxis of fetal hematopoietic stem cells. PLoS Biol 2, E75.

Cumano, A., Ferraz, J.C., Klaine, M., Di Santo, J.P., and Godin, I. (2001). Intraembryonic, but not yolk sac hematopoietic precursors, isolated before circulation, provide long-term multilineage reconstitution. Immunity 15, 477-485.

Cumano, A., and Godin, I. (2007). Ontogeny of the hematopoietic system. Annual review of immunology 25, 745-785.

Dantschakoff, V. (1909). Untersuchungen uber die Entwickelung von Blut und Bindegewebe bei Vogeln. Das lockere Bindegewebe des Huhnchens in Fetalen Leben. Arch f mikr Anat 73, 117-181.

de Bruijn, M.F., Ma, X., Robin, C., Ottersbach, K., Sanchez, M.J., and Dzierzak, E. (2002). Hematopoietic stem cells localize to the endothelial cell layer in the midgestation mouse aorta. Immunity 16, 673-683.

Dieterlen-Lievre, F., and Martin, C. (1981). Diffuse intraembryonic hemopoiesis in normal and chimeric avian development. Dev Biol 88, 180-191.

Dieterlen-Lievre, F., Pouget, C., Bollerot, K., and Jaffredo, T. (2006). Are intra-aortic hemopoietic cells derived from endothelial cells during ontogeny? Trends Cardiovasc Med 16, 128-139.

Eilken, H.M., Nishikawa, S., and Schroeder, T. (2009). Continuous single-cell imaging of blood generation from haemogenic endothelium. Nature 457, 896-900.

Gekas, C., Dieterlen-Lievre, F., Orkin, S.H., and Mikkola, H.K. (2005). The placenta is a niche for hematopoietic stem cells. Dev Cell 8, 365-375.

Houssaint, E. (1981). Differentiation of the mouse hepatic primordium. II. Extrinsic origin of the haemopoietic cell line. Cell differentiation 10, 243-252.

Jaffredo, T., Gautier, R., Brajeul, V., and Dieterlen-Lievre, F. (2000). Tracing the progeny of the aortic hemangioblast in the avian embryo. Dev Biol 224, 204-214.

Jaffredo, T., Gautier, R., Eichmann, A., and Dieterlen-Lievre, F. (1998). Intraaortic hemopoietic cells are derived from endothelial cells during ontogeny. Development 125, 4575-4583.

Johnson, G.R., and Moore, M.A. (1975). Role of stem cell migration in initiation of mouse foetal liver haemopoiesis. Nature 258, 726-728.

Jordan, H.E. (1917). Aortic Cell Clusters in Vertebrate Embryos. Proc Natl Acad Sci U S A 3, 149-156.

Kieusseian, A., Brunet de la Grange, P., Burlen-Defranoux, O., Godin, I., and Cumano, A. (2012). Immature hematopoietic stem cells undergo maturation in the fetal liver. Development.

Kissa, K., and Herbomel, P. (2010). Blood stem cells emerge from aortic endothelium by a novel type of cell transition. Nature 464, 112-115.

Kumaravelu, P., Hook, L., Morrison, A.M., Ure, J., Zhao, S., Zuyev, S., Ansell, J., and Medvinsky, A. (2002). Quantitative developmental anatomy of definitive haematopoietic stem cells/long-term repopulating units (HSC/RUs): role of the aorta-gonad- mesonephros (AGM) region and the yolk sac in colonisation of the mouse embryonic liver. Development 129, 4891-4899.

Lam, E.Y., Hall, C.J., Crosier, P.S., Crosier, K.E., and Flores, M.V. (2010). Live imaging of Runx1 expression in the dorsal aorta tracks the emergence of blood progenitors from endothelial cells. Blood 116, 909-914.

Lancrin, C., Sroczynska, P., Stephenson, C., Allen, T., Kouskoff, V., and Lacaud, G. (2009). The haemangioblast generates haematopoietic cells through a haemogenic endothelium stage. Nature 457, 892-895.

Lux, C.T., Yoshimoto, M., McGrath, K., Conway, S.J., Palis, J., and Yoder, M.C. (2008). All primitive and definitive hematopoietic progenitor cells emerging before E10 in the mouse embryo are products of the yolk sac. Blood 111, 3435-3438.

Ma, X., Robin, C., Ottersbach, K., and Dzierzak, E. (2002). The Ly-6A (Sca-1) GFP transgene is expressed in all adult mouse hematopoietic stem cells. Stem Cells 20, 514-521.

Majstoravich, S., Zhang, J., Nicholson-Dykstra, S., Linder, S., Friedrich, W., Siminovitch, K.A., and Higgs, H.N. (2004). Lymphocyte microvilli are dynamic, actin-dependent structures that do not require Wiskott-Aldrich syndrome protein (WASp) for their morphology. Blood 104, 1396-1403.

Maximov, A.A. (1909). Der Lymphozyt als gemeinsame Stammzelle

der verschiedenen Blutelemente in der embryonalen

Entwicklung und im postfetalen Leben der Säugetiere. Folia Haematologica 8, 125-134.

Medvinsky, A., and Dzierzak, E. (1996). Definitive hematopoiesis is autonomously initiated by the AGM region. Cell 86, 897-906.

Medvinsky, A.L., Gan, O.I., Semenova, M.L., and Samoylina, N.L. (1996). Development of day-8 colony-forming unit-spleen hematopoietic progenitors during early murine embryogenesis: spatial and temporal mapping. Blood 87, 557-566.

Mizuochi, C., Fraser, S.T., Biasch, K., Horio, Y., Kikushige, Y., Tani, K., Akashi, K., Tavian, M., and Sugiyama, D. (2012). Intra-aortic clusters undergo endothelial to hematopoietic phenotypic transition during early embryogenesis. PloS one 7, e35763.

Morrison, S.J., Hemmati, H.D., Wandycz, A.M., and Weissman, I.L. (1995). The purification and characterization of fetal liver hematopoietic stem cells. Proc Natl Acad Sci U S A 92, 10302-10306.

Muller, A.M., Medvinsky, A., Strouboulis, J., Grosveld, F., and Dzierzak, E. (1994). Development of hematopoietic stem cell activity in the mouse embryo. Immunity 1, 291-301.

North, T., Gu, T.L., Stacy, T., Wang, Q., Howard, L., Binder, M., Marin-Padilla, M., and Speck, N.A. (1999). Cbfa2 is required for the formation of intra-aortic hematopoietic clusters. Development 126, 2563-2575.

North, T.E., de Bruijn, M.F., Stacy, T., Talebian, L., Lind, E., Robin, C., Binder, M., Dzierzak, E., and Speck, N.A. (2002). Runx1 expression marks long-term repopulating hematopoietic stem cells in the midgestation mouse embryo. Immunity 16, 661-672.

Ohmura, K., Kawamoto, H., Fujimoto, S., Ozaki, S., Nakao, K., and Katsura, Y. (1999). Emergence of T, B, and myeloid lineage-committed as well as multipotent hemopoietic progenitors in the aorta-gonad-mesonephros region of day 10 fetuses of the mouse. J Immunol 163, 4788-4795.

Ottersbach, K., and Dzierzak, E. (2005). The murine placenta contains hematopoietic stem cells within the vascular labyrinth region. Dev Cell 8, 377-387.

Peeters, M., Ling, K.W., Oziemlak, A., Robin, C., and Dzierzak, E. (2005). Multipotential hematopoietic progenitor cells from embryos developed in vitro engraft unconditioned W41/W41 neonatal miceB. Haematologica 90, 734-739.

Robin, C., and Dzierzak, E. (2005). Hematopoietic stem cell enrichment from the AGM region of the mouse embryo. Methods in molecular medicine 105, 257-272.

Sanchez, M.J., Holmes, A., Miles, C., and Dzierzak, E. (1996). Characterization of the first definitive hematopoietic stem cells in the AGM and liver of the mouse embryo. Immunity 5, 513-525.

Smith, R.A., and Glomski, C.A. (1982). “Hemogenic endothelium” of the embryonic aorta: Does it exist? Developmental and comparative immunology 6, 359-368.

Taoudi, S., Gonneau, C., Moore, K., Sheridan, J.M., Blackburn, C.C., Taylor, E., and Medvinsky, A. (2008). Extensive hematopoietic stem cell generation in the AGM region via maturation of VE-cadherin+CD45+ pre-definitive HSCs. Cell Stem Cell 3, 99-108.

Taoudi, S., and Medvinsky, A. (2007). Functional identification of the hematopoietic stem cell niche in the ventral domain of the embryonic dorsal aorta. Proc Natl Acad Sci U S A 104, 9399-9403.

Yoder, M.C., and Hiatt, K. (1997). Engraftment of embryonic hematopoietic cells in conditioned newborn recipients. Blood 89, 2176-2183.

Yoder, M.C., Hiatt, K., Dutt, P., Mukherjee, P., Bodine, D.M., and Orlic, D. (1997a). Characterization of definitive lymphohematopoietic stem cells in the day 9 murine yolk sac. Immunity 7, 335-344.

Yoder, M.C., Hiatt, K., and Mukherjee, P. (1997b). In vivo repopulating hematopoietic stem cells are present in the murine yolk sac at day 9.0 postcoitus. Proc Natl Acad Sci U S A 94, 6776-6780.

Yokomizo, T., and Dzierzak, E. (2010). Three-dimensional cartography of hematopoietic clusters in the vasculature of whole mouse embryos. Development 137, 3651-3661.

Yokomizo, T., Ng, C.E., Osato, M., and Dzierzak, E. (2011). Three-dimensional imaging of whole midgestation murine embryos shows an intravascular localization for all hematopoietic clusters. Blood 117, 6132-6134.

Zovein, A.C., Hofmann, J.J., Lynch, M., French, W.J., Turlo, K.A., Yang, Y., Becker, M.S., Zanetta, L., Dejana, E., Gasson, J.C., et al. (2008). Fate tracing reveals the endothelial origin of hematopoietic stem cells. Cell Stem Cell 3, 625-636.

Zovein, A.C., Turlo, K.A., Ponec, R.M., Lynch, M.R., Chen, K.C., Hofmann, J.J., Cox, T.C., Gasson, J.C., and Iruela-Arispe, M.L. (2010). Vascular remodeling of the vitelline artery initiates extravascular emergence of hematopoietic clusters. Blood 116, 3435-3444.

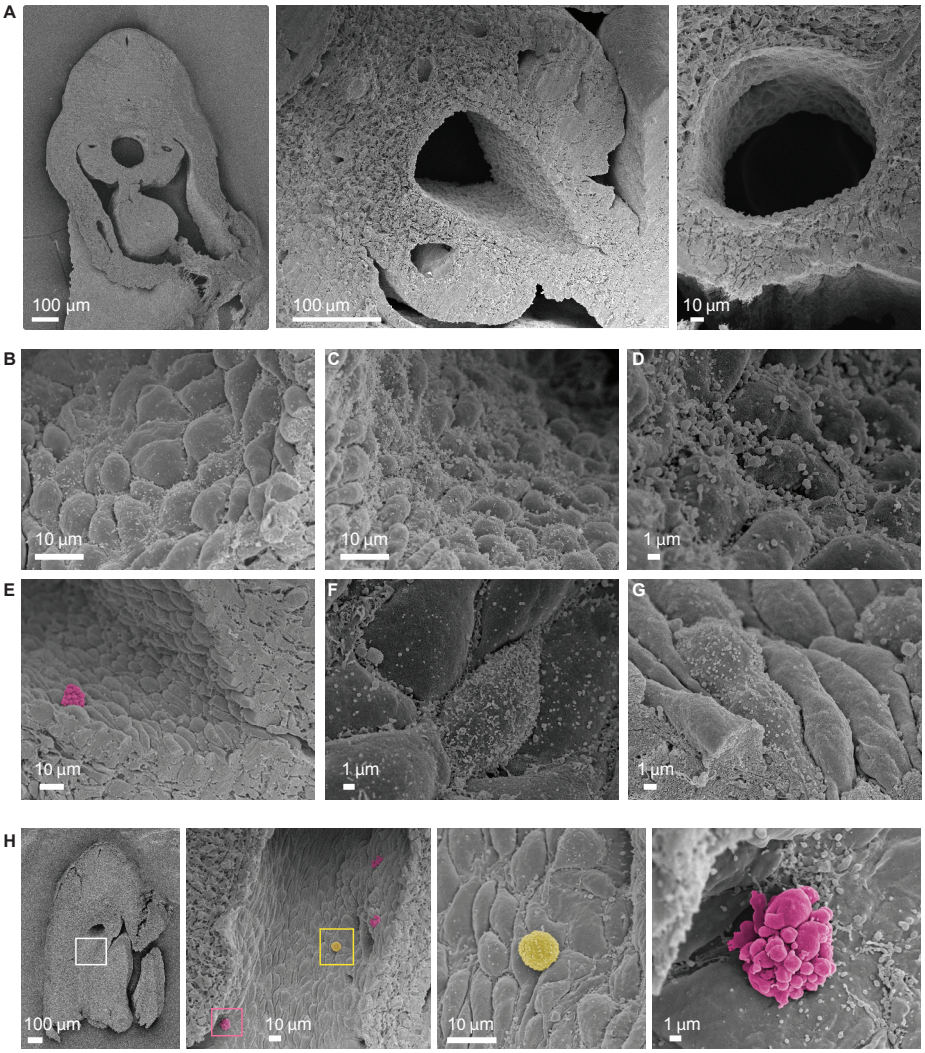

Figure S1. Runx1 deficiency might lead to abortive endothelial to hematopoietic transition. Scanning electron microscopy observation of 200 µm vibratome transversal sections of E10 *runx1*$^{-/-}$ (A-G) and *runx1*$^{+/-}$ embryos (H). (A) Global view of E10 *runx1*$^{-/-}$ embryo slices and aortas. (B-G) Close-up views of the *runx1*$^{-/-}$ aortic endothelium. (H) Left panel is a global view of a *runx1*$^{+/-}$ embryo section. The white-boxed region is shown enlarge in the middle left panel. Note that on this section the aorta is connected to the vitelline artery. The yellow-boxed region is shown enlarged in the middle right panel, and the pink one is in the right panel. Yellow artificial color represents a single IAHC cell, and pink represents apoptotic cells. Scales are as indicated on each pictures. E10=26-31 somite pairs (s.p.). Top: dorsal side; bottom: ventral side.

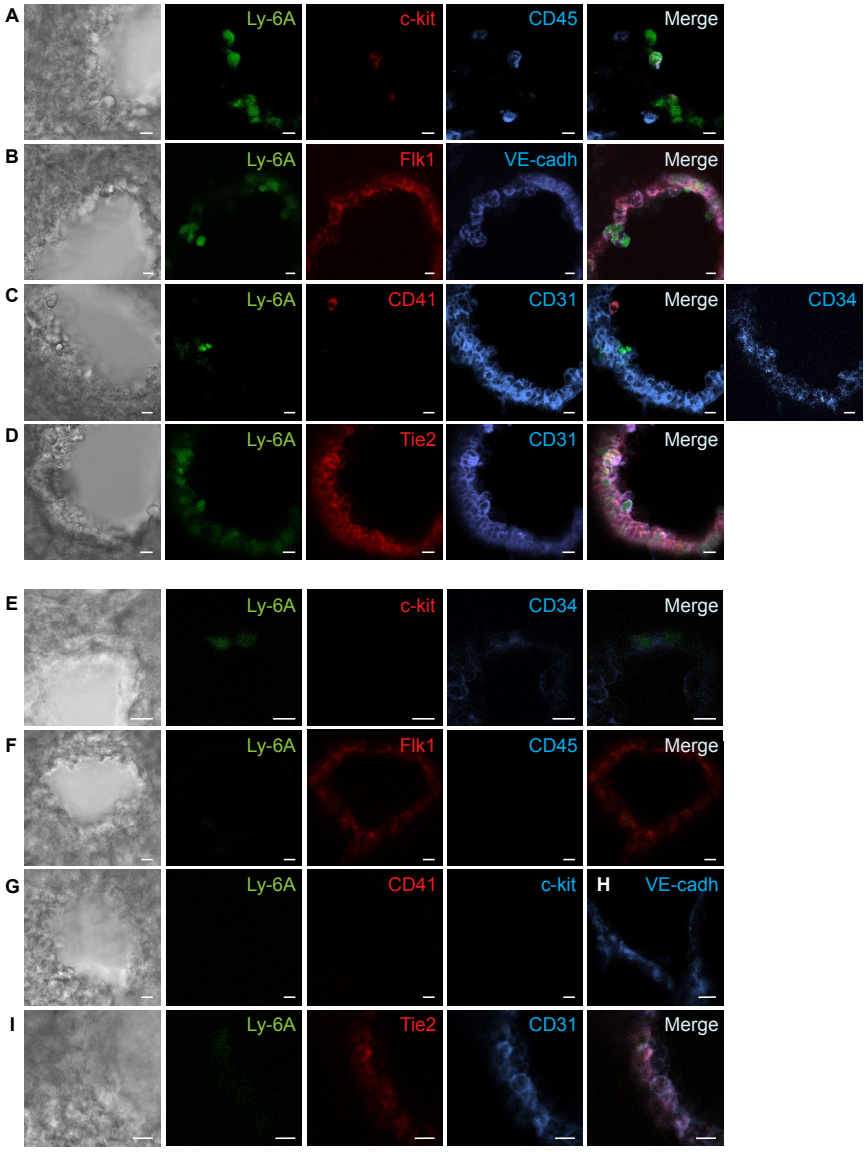

Figure S2. Expression of Ly6A-GFP and different surface markers in E9 and E11 aortas. Confocal microscopic observation of E11 (A-D) or E9 (E-I) non-fixed *Ly6A-GFP* embryo transversal slices. Green=GFP, Red=PE, Blue=APC or AlexaFluor 647. Left panel=transmitted light, middle panels=fluorescence, right panel=merge of the fluorescent signals. (C) Pacific Blue anti-CD34 was used as a third color (blue). Scale bar=10 µm.

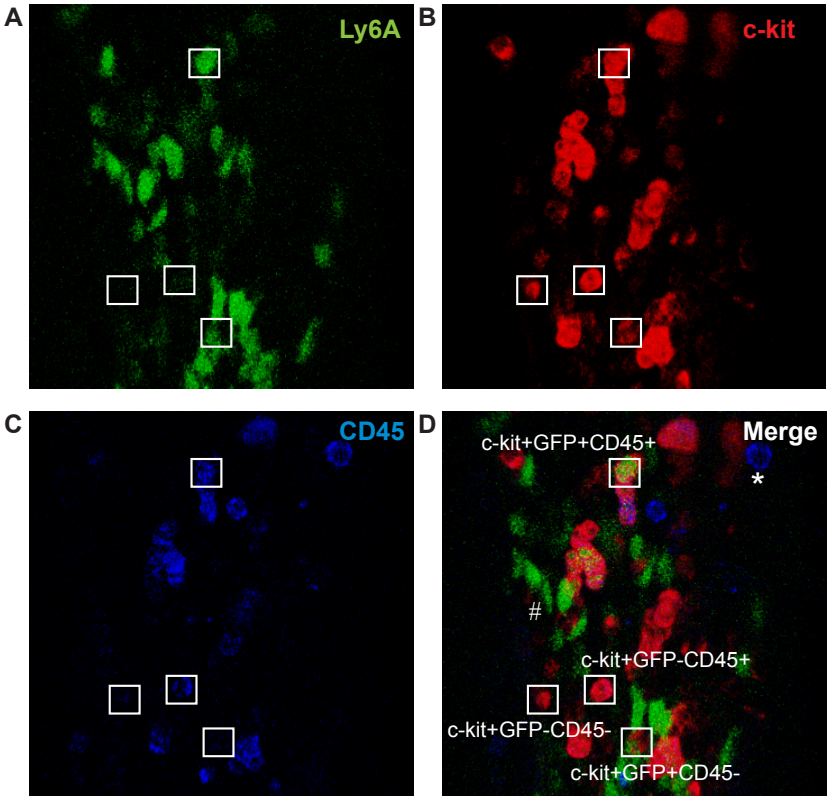

Figure S3. IAHC cells differentially express Ly6A-GFP and CD45 as shown in whole aorta. (A-D) Confocal observation of the aortic floor of an E10 *Ly6A-GFP* (A) embryo stained intra-aortic with PE anti-c-kit (B) and APC anti-CD45 (C) antibodies. Pictures are the maximum projection of a *z*-stack. (D) Merge of the different fluorescent signals shown in (A-C). The boxes track cells of interest over the different fluorescent channels (each cell phenotype is indicated near the corresponding boxes). The sharp sign in (D) notes an example of Ly6A-GFP^{+} endothelial cells that do not express c-kit and CD45. The asterisk sign designates a putative macrophage (c-kit^{-} Ly6A-GFP^{-} CD45^{+}). A 3D reconstruction of the *z*-stack is shown in Supplementary video 1 (the CD31 channel is not shown here for better clarity).

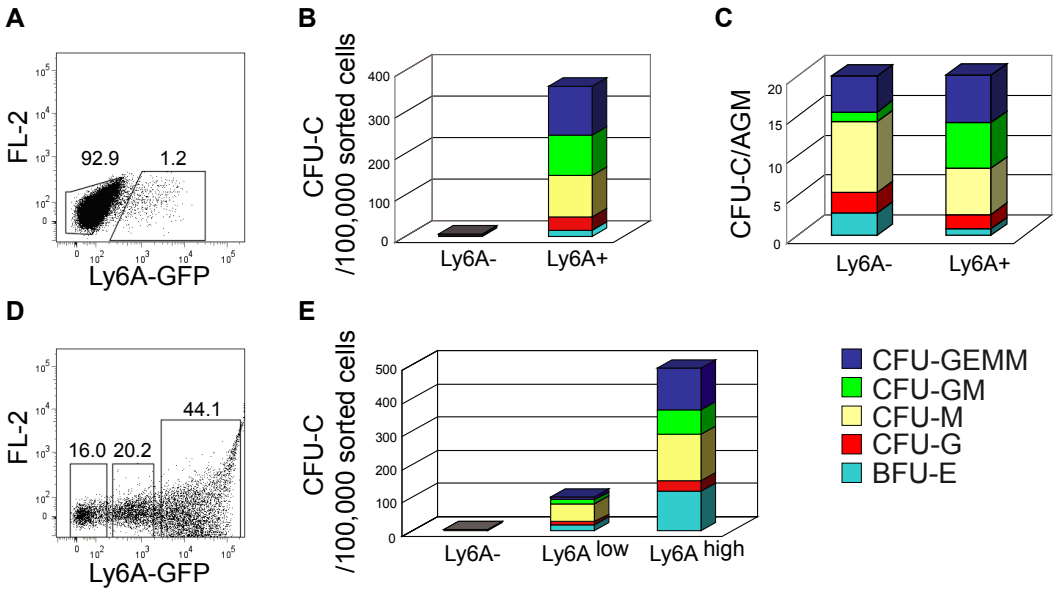

Figure S4. Ly6A-GFP marks all adult but not all E10 embryonic EMPs. E10 Ly6A-GFP^{-} and Ly6A-GFP^{+} AGM cells were sorted (A) and tested in an erythroid-myeloid clonogenic assay (B and C). The number of colony forming units in culture (CFU-C) present in both Ly6A-GFP populations is shown per 100,000 sorted cells (B) and per AGM (C), n=1. Adult *Ly6A-GFP* BM cells were sorted based on no, low and high GFP expression (D) and tested in a clonogenic assay (E), n=1. The number of CFU-C present in the different populations is shown per 100,000 sorted cells. The percentages of each sorted populations are indicated above the gates (A,D). The colors correspond to the different types of hematopoietic progenitors (B,C,E). CFU-GEMM=CFU-granulocyte-erythroid-macrophage-megakaryocyte; CFU-GM=CFU-granulocyte-macrophage; CFU-M=CFU-macrophage; CFU-G=CFU-granulocyte; BFU-E=Burst-forming unit-erythroid.

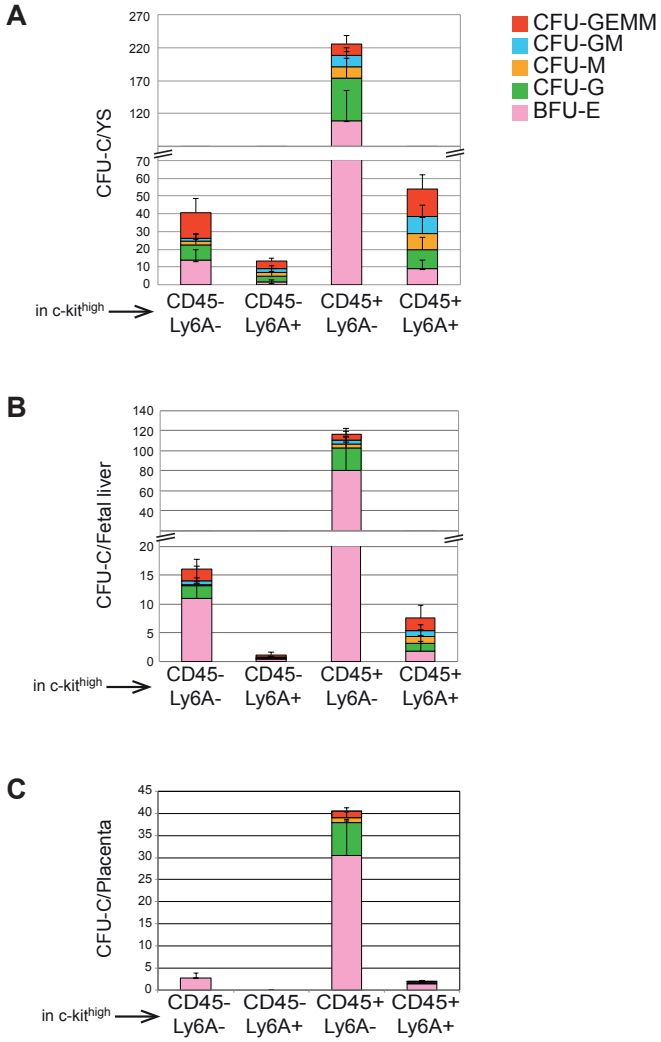

Figure S5. EMPs in E10 YS, FL and placenta are enriched in the c-kit^{high} Ly6A^{-} CD45^{+} cell subfraction. (A-C) Bar graphs show the number of colony forming units in culture (CFU-C) per E10 YS (A), FL (B) and placenta (C). The different subpopulations tested are depicted under each graph. Colors correspond to the different types of progenitors counted. Error bars are the standard deviations calculated for n=3 experiments (A and B) and n=2 (C). CFU-GEMM=CFU-granulocyte-erythroid-macrophage-megakaryocyte; CFU-GM=CFU-granulocyte-macrophage; CFU-M=CFU-macrophage; CFU-G=CFU-granulocyte; BFU-E=Burst-forming unit-erythroid.

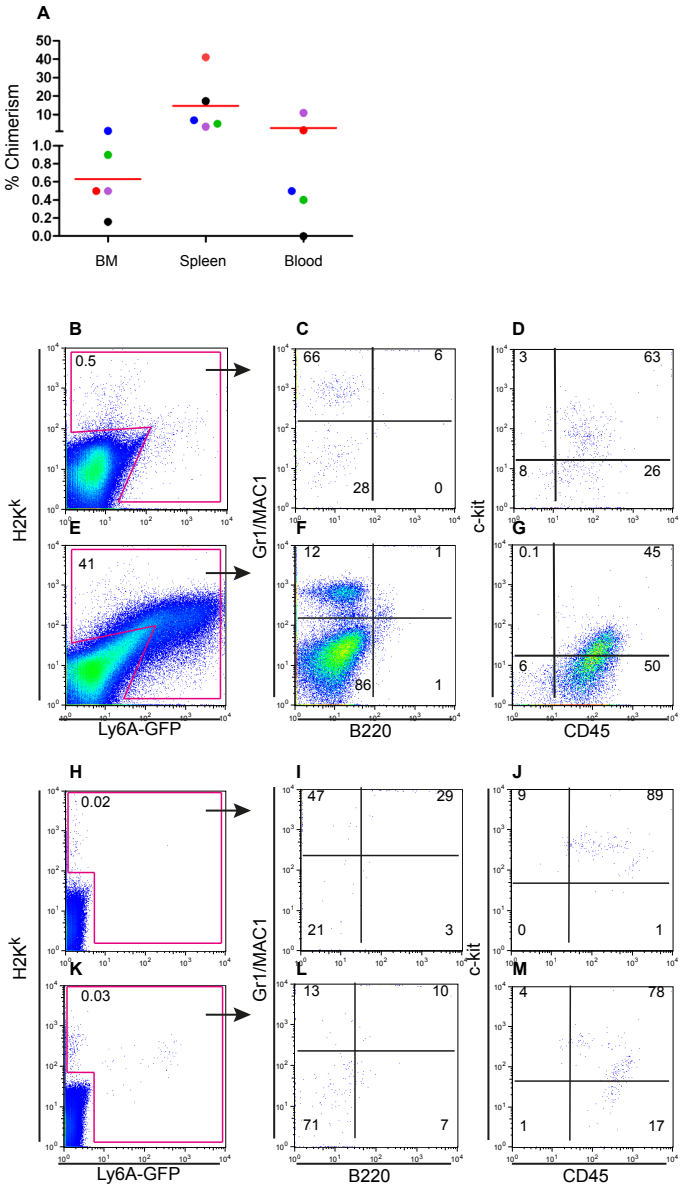

Figure S6. E9 YS cells can multilineage and long-term reconstitute *Rag2*$^{-/-}$γ*c*$^{-/-}$ newborns. E9 YS cells (5.5-13 embryo equivalent) were injected in the liver of *Rag2*$^{-/-}$γ*c*$^{-/-}$ newborns and analyzed 4 months after transplantation. The percentages of chimerism in the BM, spleen and peripheral blood of the 5 reconstituted recipients out of 8 transplanted are shown in (A). Each color corresponds to one mouse. Red bar=average chimerism. Flow cytometry analyses of a primary reconstituted *Rag2*$^{-/-}$γ*c*$^{-/-}$ grown-up newborn (B-G) (shown in red in (A)), and a secondary recipient injected with the BM of the primary recipient (H-M). (B, E, H and K) Percentages of viable H2K^{k+} and/or Ly6A-GFP^{+} donor cells in BM (B and H) and spleen (E and K) are indicated in the pink gates. The analysis of non-transplanted recipients was used to define positivity. (C, D, F, G, I, J, L and M) Gr1/MAC1, B220, c-kit and CD45 expression in the BM and spleen of the recipients is shown in the donor cell fractions (pink gates). In each quadrant is depicted the percentages of donor viable cells for each indicated cell surface markers.

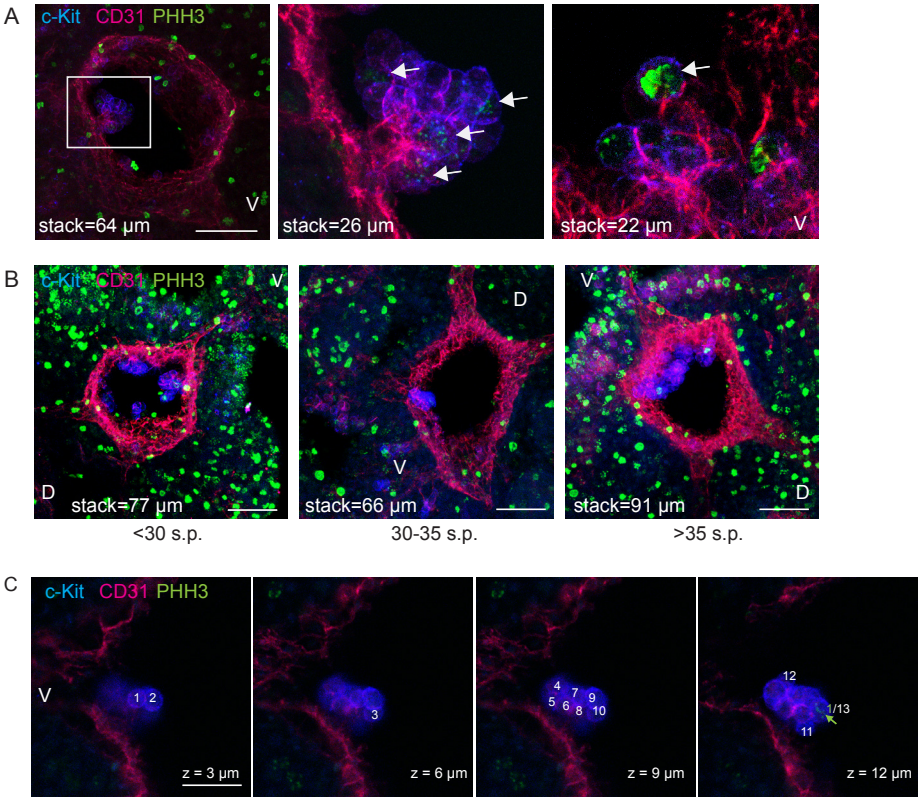

Figure S7. IAHC cells have limited proliferative activity. (A, B and D) Confocal microscopic observation of transversal 200 µm fixed and cleared thick embryo slices stained with anti-c-kit (blue), anti-CD31 (red) and anti-phospho-Histone H3.3 (PHH3) (green) antibodies. Pictures in (A and B) are maximum projections of a *z*-stack (the depth of the stack is indicated on each pictures). (A) Examples of PHH3$^+$ IAHC cells (arrows). The middle panel is a close-up of the boxed region shown in the left panel. (B) Representative pictures of PHH3$^+$ IAHC cells at different developmental time points (staged in somite pairs, s.p.). (C) Different *z*-planes of a single *z*-stack show one PHH3$^+$ cell (green arrow) within 13 c-kit^{high} IAHC cells. The aortic endothelium and IAHCs are CD31$^+$ (red). Scale bars are 50 µm (A,B) and 25 µm (D). V=ventral aspect of the aorta; D=dorsal aspect of the aorta.

Supplementary video 1. Three-dimensional reconstitution of the floor of E10 *Ly6A-GFP* embryo after intra-aortic injection of Pacific Blue anti-CD31, PE anti-c-kit, and APC anti-CD45 antibodies.

Supplementary video 2. Time-lapse video of a maximal projection of E10 *Ly6A-GFP* non-fixed embryo slice after intra-aortic injection of AlexaFluor 647 anti-CD31 and PE anti-c-kit. Images were taken every 15min for up to 13h.

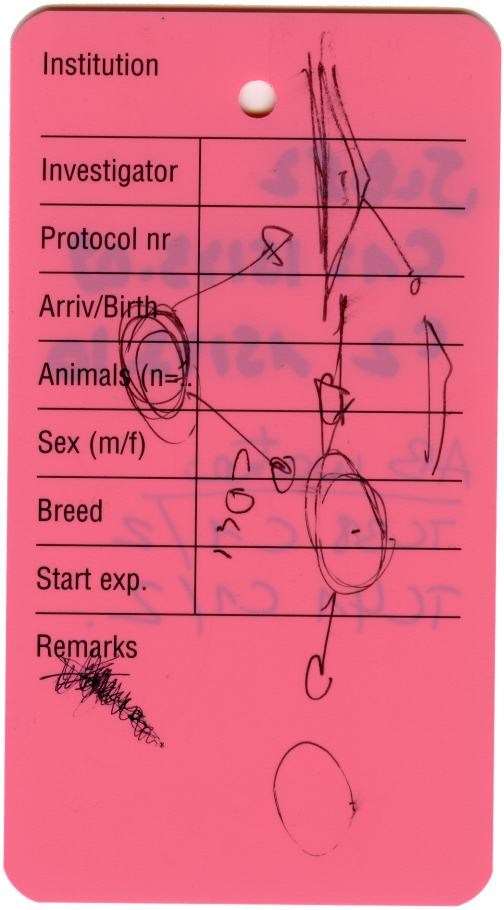
Institution
Investigator
Protocol nr
Arriv/Birth
Animals (n=..
Sex (m/f)
Breed
Start exp.
Remarks

Chapter 7 – Discussion

The central theme of this thesis could be summed up in essence by a simple question: how to make a blood stem cell? Development in general could be compared to a complex chain reaction system, *i.e.* a trigger (in that case fecundation) initiates a self-maintaining chain of events (cell division/ differentiation/migration/secretion …). The beauty of the system (but also its complexity) is that every part of the structure and corresponding actions are heavily dependent on each other, and influenced by their position in time and space. If placed in the context of making a blood (or Hematopoietic) Stem Cell (HSC), then what cell(s) precedes HSCs, in what state and environment, and eventually what triggered the change? In addition, decades of research in molecular biology have shown that the sequence of events leading to a particular state – and for stem cells, the maintenance of the state – during development is deeply conditional on the cell genome and its expression. The work presented in this thesis shows (or at least defends the idea) that the cells preceding HSCs are pre-HSCs, as we could observe and test them in their intra-aortic location, in the Intra-Aortic Hematopoietic Clusters (IAHCs) (Chapter 6). It also shows that the cells preceding IAHCs are endothelial cells (Chapter 2 and 3). And finally that the integrin subunit αIIb helps to maintain/promote HSC activity in the AGM (Chapter 4 and 5) (Figure 1).

Three other studies performed in the zebrafish embryo have also shown an endothelial origin for hematopoietic cells, including HSCs (Bertrand et al., 2010; Kissa and Herbomel, 2010; Lam et al., 2010). In one study, the mechanism of endothelial into hematopoietic transition (EHT) was particularly well described by careful time-lapse confocal microscopy imaging (Kissa and Herbomel, 2010). Some ventral elongated endothelial cells bent toward the sub-aortic space, the neighboring cells closing the newly formed gap. Then, the cells rounded up and detached to reach the nearby axial vein. Despite some structural differences, like for example the absence of IAHCs in the zebrafish, and the emergence toward the sub-aortic space, the global process is strikingly similar to what is observed in the chicken or the mouse embryo: the aortic endothelium gives rise to blood (Figure 2). The developmental time needed to reach the EHT is obviously different between the three species (~36 h for zebrafish, ~72 h for chicken, and ~9.5 days for mice). However, the morphology of the embryos is quite similar when the process starts (e.g. development of the aorta, gonads and mesonephros). This again emphasizes the importance of the environmental cues that drive, if not trigger, the EHT.

It has been hypothesized that IAHCs and HSCs could derive from the sub-aortic mesenchyme without taking characteristics of the endothelium (Bertrand et al., 2005). Interestingly, although it is now clear that most blood cells and HSCs are formed via an endothelial intermediate, none of the data produced up to now can completely rule out this other theory.

The process of emergence is unique in itself. The endothelium, a differentiated cell type, gives rise to a self-renewing cell of a different lineage type, which is at the foundation of the whole blood system. This raises multiple questions. For example, is the hemogenic endothelium indeed a genuine differentiated endothelium, which is able to give rise to blood when instructed by the right cues? Or is it an intermediate state of embryonic development that takes the characteristics of an endothelial cell but will only exist in one place and time? In other words, are endothelial cells intrinsic- or extrinsically hemogenic. Of course, this is important in a clinical context, as adult endothelial cells could be a source of HSCs.

The general model for the origin of adult stem cells is that they are remnants of embryonic tissue rudiments, and retain at adult stage their embryonic properties (propensity to divide/multipotency), hypothetically because they lie in an environment that maintains these properties (the niche). The rest of the embryonic tissue will differentiate to form the final adult tissue, later replenished by the remaining stem cells (Slack, 2008). The formation of HSCs during embryonic development sets a new paradigm to understand how adult stem cells are produced. Indeed, as discussed before, HSCs arise from a different (although related) cell type, and from seemingly differentiated cells, which would thus not be "in a similar state of developmental commitment to the embryonic rudiment that produced them" (Slack, 2008). Hemogenic endothelial cells express Runx1, like HSCs (embryonic (North et al., 2002) and adult (North et al., 2004)), but until proven otherwise, do not share the same self-renewal properties. Moreover, before the emergence of HSCs, the hemogenic endothelium already produces

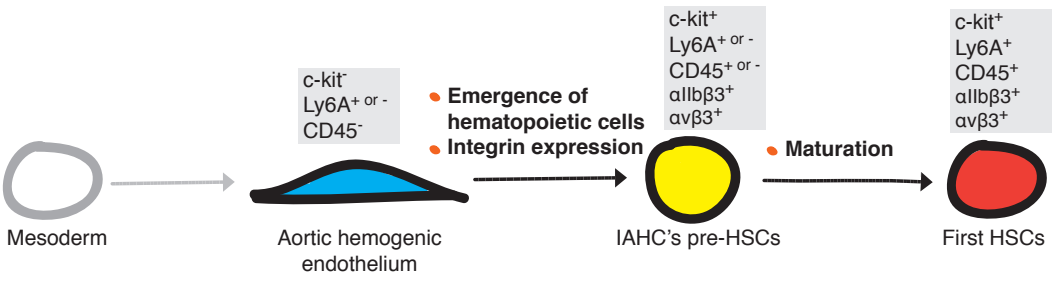

Figure 1. Graph summarizing the different findings of this thesis.

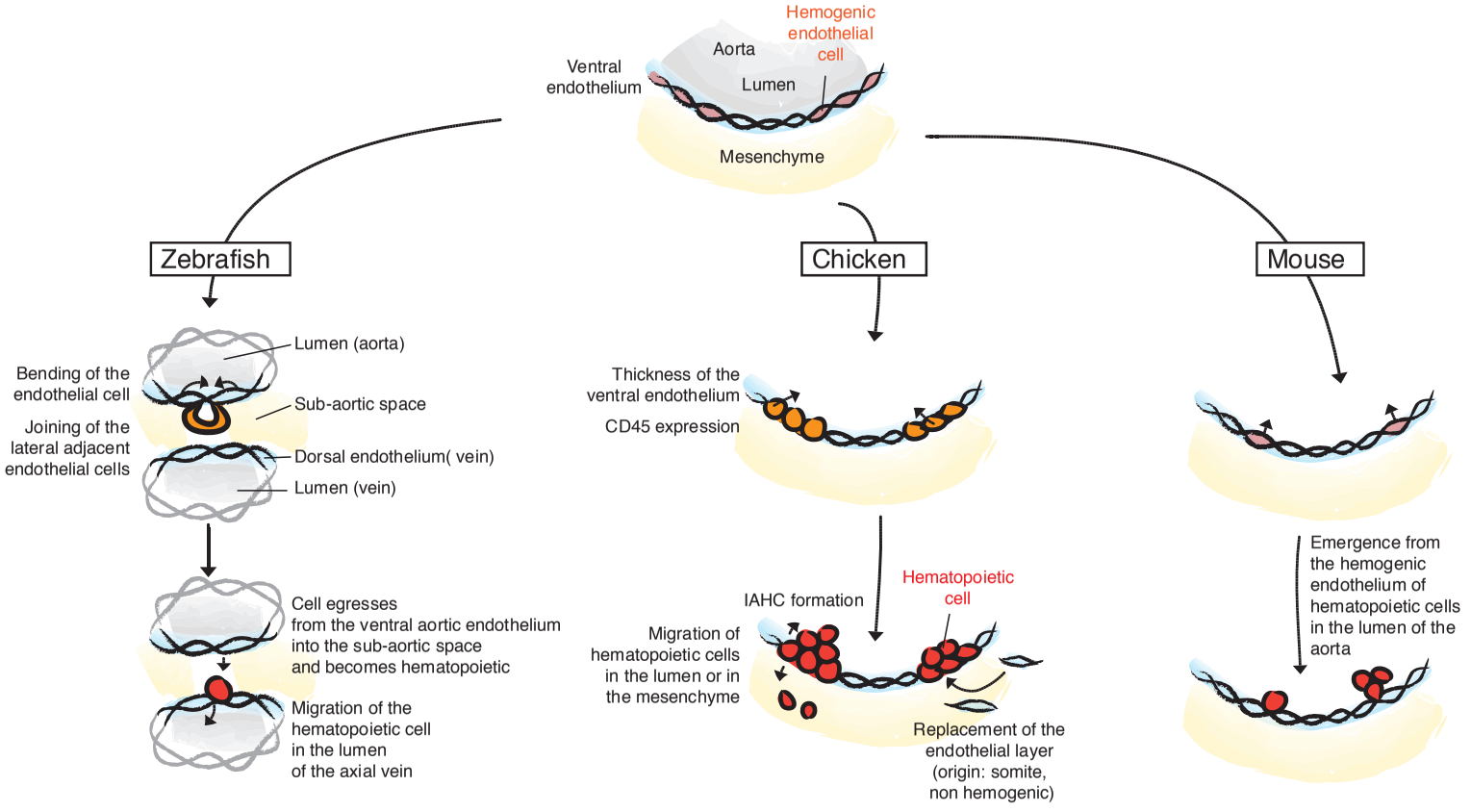

Figure 2. Formation of hematopoietic stem/progenitor cells in the aorta of the zebrafish, chicken and mouse embryos. Hematopoietic cells and intra-aortic hematopoietic clusters (IAHCs) are generated from hemogenic endothelial cells located in the ventral aspect of the aorta. It is important to note that the process leading to the transition from hemogenic endothelial cells into hematopoietic cells differs between fish, avian and mouse species.

(in the YS, and possibly in the placenta) differentiated blood cells (erythrocytes/ macrophages/ megakaryocytes) and hematopoietic progenitors that do not last until adulthood (Eilken et al., 2009; Yoshimoto et al., 2011; Yoshimoto et al., 2012). This is often called the first wave or primitive hematopoiesis. Thus, it seems again that the product of emergence is dependent on the environment in which endothelial cells are located. However, to add to complexity, it has been shown that microglia (myeloid population present in the brain) are composed of primitive macrophages, thus not HSC derived (Ginhoux et al., 2010; Schulz et al., 2012). These macrophages are present in the adult brain, and so must possess some sort of self-renewal capabilities, although unipotent.

Pre-HSCs (also referred as pre-definitive HSCs, meta-definite HSCs or newborn reconstituting HSCs) appear before adult transplantable HSCs. These cells have been identified in the YS and the P-Sp of E9.0 embryos, but were present in higher numbers in the YS (Yoder et al., 1997). A YS origin for these pre-HSCs is very conceivable although still controversial. Nevertheless, only the AGM is eventually able to concentrate the HSC potential at E10.5, again emphasizing its singular microenvironment (Medvinsky and Dzierzak, 1996; Muller et al., 1994). Whether these early YS pre-HSCs contribute to E10 IAHC pre-HSCs remains to be determined.

There are ~1500 HSCs in the FL at maximum as calculated by transplantation of limiting cell dilutions (Ema and Nakauchi, 2000; Gekas et al., 2005). Maturation of the ~600 IAHC's putative pre-HSCs (Yokomizo and Dzierzak, 2010; and this thesis) and the undetermined number of YS pre-HSCs (but also others) present at E10 (Yoder et al., 1997) would easily account for the number of HSCs present in the FL at mid-gestation. Studies focusing on HSC self-renewal in the FL are mainly based on the analysis of their cell-cycle status (Bowie et al., 2006; Morrison et al., 1995), and eventually only indicate that a number of HSCs are indeed cycling, but not necessarily amplifying, *i.e.* one HSC would give one HSC and a progenitor after division. In other words, the plateau of HSCs is not inevitably reached through high HSC symmetric self-renewal leading to amplification of a small pool of HSCs, but could also be through maturation of a consistent pre-existing pool of pre-HSCs. The data presented in this thesis would fit that model. We have shown for example that pre-HSCs are present in E11 FL. It would be interesting to determine whether some of these cells are also present later on at E12 and E13, when the number of FL HSCs is still increasing, or even later in the adult BM. We have shown that CD41 (αIIb integrin chain) marks all HSCs in the AGM as well as the IAHC cells. But interestingly, αIIb deficiency leads to a higher number of IAHC cells at E11 and of HSCs in the E14 FL, but harboring less HSCs in the E11 AGM. This apparent paradox is resolved if αIIb is a repressor of emergence and a facilitator of pre-HSC maturation, in fact a balance keeper. The absence of

αIIb would lead to an increased pool of pre-HSCs (as seen for example by an increased number of IAHC cells), delayed in their maturation, explaining the higher number of FL HSCs seen later during development. The concept of maturation is relatively new, but it is crucial to understand and decipher it. Indeed, it makes a difference whether the FL microenvironment promotes the amplification of the HSC pool at mid-gestation via symmetric self-renewal or via the maturation of pre-HSCs. It is especially interesting to understand the embryonic HSC expansion process in a clinical context where one of the main goals is the amplification of HSCs for enhanced therapeutic engraftment.

In conclusion, it is clear that many facets of HSC production remain to be clarified. One approach in order to better comprehend how HSCs with full potential are generated would be to purify very enriched populations of aortic endothelium, pre-HSCs and HSCs at different time-points of development and to analyze their transcriptome (proteome if technically possible). Especially, this would maybe help to grasp the internal mechanism that causes an endothelial cell to undertake such a drastic morphologic and phenotypic transformation as to eventually become an HSC. Single cell transcriptome analysis could reveal whether IAHC cells are heterogeneous or already fated to all become HSCs. In addition, this could show what differences exist between pre-HSCs and fully potent HSCs. Finally, getting to know where HSC ancestors reside will be of great interest to understand the important extrinsic factors ruling their commitment toward HSCs.

REFERENCES

Bertrand, J.Y., Chi, N.C., Santoso, B., Teng, S., Stainier, D.Y., and Traver, D. (2010). Haematopoietic stem cells derive directly from aortic endothelium during development. Nature 464, 108-111.

Bertrand, J.Y., Giroux, S., Golub, R., Klaine, M., Jalil, A., Boucontet, L., Godin, I., and Cumano, A. (2005). Characterization of purified intraembryonic hematopoietic stem cells as a tool to define their site of origin. Proc Natl Acad Sci U S A 102, 134-139.

Bowie, M.B., McKnight, K.D., Kent, D.G., McCaffrey, L., Hoodless, P.A., and Eaves, C.J. (2006). Hematopoietic stem cells proliferate until after birth and show a reversible phase-specific engraftment defect. J Clin Invest 116, 2808-2816.

Eilken, H.M., Nishikawa, S., and Schroeder, T. (2009). Continuous single-cell imaging of blood generation from haemogenic endothelium. Nature 457, 896-900.

Ema, H., and Nakauchi, H. (2000). Expansion of hematopoietic stem cells in the developing liver of a mouse embryo. Blood 95, 2284-2288.

Gekas, C., Dieterlen-Lievre, F., Orkin, S.H., and Mikkola, H.K. (2005). The placenta is a niche for hematopoietic stem cells. Dev Cell 8, 365-375.

Ginhoux, F., Greter, M., Leboeuf, M., Nandi, S., See, P., Gokhan, S., Mehler, M.F., Conway, S.J., Ng, L.G., Stanley, E.R., et al. (2010). Fate mapping analysis reveals that adult microglia derive from primitive macrophages. Science 330, 841-845.

Kissa, K., and Herbomel, P. (2010). Blood stem cells emerge from aortic endothelium by a novel type of cell transition. Nature 464, 112-115.

Lam, E.Y., Hall, C.J., Crosier, P.S., Crosier, K.E., and Flores, M.V. (2010). Live imaging of Runx1 expression in the dorsal aorta tracks the emergence of blood progenitors from endothelial cells. Blood 116, 909-914.

Medvinsky, A., and Dzierzak, E. (1996). Definitive hematopoiesis is autonomously initiated by the AGM region. Cell 86, 897-906.

Morrison, S.J., Hemmati, H.D., Wandycz, A.M., and Weissman, I.L. (1995). The purification and characteriza-

tion of fetal liver hematopoietic stem cells. Proc Natl Acad Sci U S A 92, 10302-10306.

Muller, A.M., Medvinsky, A., Strouboulis, J., Grosveld, F., and Dzierzak, E. (1994). Development of hematopoietic stem cell activity in the mouse embryo. Immunity 1, 291-301.

North, T.E., de Bruijn, M.F., Stacy, T., Talebian, L., Lind, E., Robin, C., Binder, M., Dzierzak, E., and Speck, N.A. (2002). Runx1 expression marks long-term repopulating hematopoietic stem cells in the midgestation mouse embryo. Immunity 16, 661-672.

North, T.E., Stacy, T., Matheny, C.J., Speck, N.A., and de Bruijn, M.F. (2004). Runx1 is expressed in adult mouse hematopoietic stem cells and differentiating myeloid and lymphoid cells, but not in maturing erythroid cells. Stem Cells 22, 158-168.

Schulz, C., Gomez Perdiguero, E., Chorro, L., Szabo-Rogers, H., Cagnard, N., Kierdorf, K., Prinz, M., Wu, B., Jacobsen, S.E., Pollard, J.W., et al. (2012). A lineage of myeloid cells independent of Myb and hematopoietic stem cells. Science 336, 86-90.

Slack, J.M. (2008). Origin of stem cells in organogenesis. Science 322, 1498-1501.

Yoder, M.C., Hiatt, K., Dutt, P., Mukherjee, P., Bodine, D.M., and Orlic, D. (1997). Characterization of definitive lymphohematopoietic stem cells in the day 9 murine yolk sac. Immunity 7, 335-344.

Yokomizo, T., and Dzierzak, E. (2010). Three-dimensional cartography of hematopoietic clusters in the vasculature of whole mouse embryos. Development 137, 3651-3661.

Yoshimoto, M., Montecino-Rodriguez, E., Ferkowicz, M.J., Porayette, P., Shelley, W.C., Conway, S.J., Dorshkind, K., and Yoder, M.C. (2011). Embryonic day 9 yolk sac and intra-embryonic hemogenic endothelium independently generate a B-1 and marginal zone progenitor lacking B-2 potential. Proc Natl Acad Sci U S A 108, 1468-1473.

Yoshimoto, M., Porayette, P., Glosson, N.L., Conway, S.J., Carlesso, N., Cardoso, A.A., Kaplan, M.H., and Yoder, M.C. (2012). Autonomous murine T-cell progenitor production in the extra-embryonic yolk sac before HSC emergence. Blood 119, 5706-5714.

SUMMARY

Hematopoietic Stem Cells (HSCs) are at the foundation of the whole blood system. A single HSC can give rise to all different blood cell lineages while constantly renewing its own pool. These properties (multi-lineage and self-renewal) allow HSCs to sustain blood production during the complete life of an organism. The only reliable method to identify HSCs is to perform transplantation in a conditioned mouse recipient. HSCs will reveal their potential by repopulating at long-term the complete blood system of the transplanted mouse. Although HSCs mainly reside in the Bone Marrow (BM) during adult life, they are not initially generated there. HSCs are first detected in the aorta of the Aorta-Gonad-Mesonephros (AGM) region at embryonic day (E)10.5 of mouse development. Afterward, they are also found in other hematopoietic organs: the Yolk-Sac (YS), placenta and Fetal Liver (FL). HSCs will finally migrate to the BM before birth.

The formation of the first HSCs is – more than ever – an outstanding question that remains in most part unresolved. A century ago it was hypothesized that HSCs are derived from the vessel endothelium. Groups of blood cells (since called Intra-Aortic Hematopoietic Clusters, IAHCs) were observed in different vertebrate embryos attached to the endothelium of the aorta, and they looked as they were budding from it. Recently, abundant and elegant studies gave credit to the hypothesis of a hemogenic endothelium (*i.e.* endothelium capable of giving rise to blood). However, the mechanism of IAHC emergence and the location of the hemogenic endothelial cells remain elusive. The most straightforward approach one could undertake is to directly observe the transition of an endothelial cell toward a hematopoietic cell. Because the mouse embryo is opaque, we developed a method to achieve direct observation of the embryonic aorta in thick transversal non-fixed embryo slices (Chapter 2). The aortic endothelium was specifically labelled after injection of antibodies directly inside the aorta before performing time-lapse confocal microscopy imaging. We used *Ly6A-GFP* embryos to trace HSCs, and $CD41^{YFP}$ expression as a marker of hematopoietic lineage commitment. With this approach, we witnessed hematopoietic cells emerging toward the lumen and coming directly from the underlying aortic endothelium (Chapter 3). These cells expressed Ly6A-GFP, c-kit and CD41, all being markers of Hematopoietic Stem and Progenitor Cells (HSPCs). Therefore, we proved that the aortic embryonic endothelium is hemogenic, as it was hypothesized a century ago.

Expression of αIIb (CD41) is a landmark of the commitment to blood. We asked whether this integrin sub-unit could thus be useful to enrich for HSCs throughout development. We found that only the first AGM HSCs express

αIIb (Chapter 4). Moreover, the expression of the associated integrin sub-unit β3 (CD61) and another integrin sub-unit αv (CD51) can be used to enrich HSCs at different time points of development and in different hematopoietic organs (Chapter 5). Besides, we uncovered the critical role of αIIb for normal development of the first HSCs found in the AGM. In fact, E11 AGM cells from αIIb deficient embryos had a significant decrease in HSC activity in comparison to normal embryos. Strikingly, HSC activity was normal in the YS and even higher in the FL.

HSCs derive from the hemogenic endothelium and, according to the consensus, reside at first in the IAHCs. Indeed, as stated above, we directly observed the emergence of HSPCs from the aortic endothelium. However, the time of appearance and the number of IAHCs and HSCs greatly differ. We show that IAHCs isolated before any HSC can be detected yet contain few hematopoietic progenitors but cells capable of reconstituting immunodeficient newborn recipients (therefore referred as pre-HSCs) (Chapter 6). We performed successful secondary transplantations in normal adult recipients, showing that pre-HSCs located in IAHCs are able to generate HSCs in vivo. We also observed phenotypic maturation of IAHC cells toward Ly6A-GFP^{+} HSCs in the aortic environment.

Taken together, we conclude that the aortic endothelium produces blood cells during a precise developmental period. We also conclude that these blood cells are stem cells, but require further maturation steps to be able to engraft into an adult environment. Finally, we highlight the role of the integrin αIIb in the first steps of HSC production.

SAMENVATTING

Hematopoietische stamcellen (afkorting in het Engels: HSCs) liggen aan de basis van het gehele bloedvormende systeem aangezien een enkele stamcel de potentie heeft om alle verschillende soorten bloedcellen in grote hoeveelheden aan te maken terwijl tegelijkertijd het aantal stamcellen niet verminderd. Deze twee eigenschappen (omni-bloedcelvorming-potentie en zelf-vernieuwing) stellen HSCs in staat om gedurende het gehele leven van een organisme alle bloedcellen in constante hoeveelheden te produceren. De enige betrouwbare methode om HSC activiteit te meten is door een transplantatie te doen : het overzetten van cellen van een donor naar een acceptor. Vaak worden deze experimenten in muizen gedaan. Acceptor muizen zijn dusdanig gekozen en geconditioneerd dat de getransplanteerde cellen alle kans krijgen om bij te dragen aan bloedvorming en hun afstammelingen goed te detecteren zijn. Getransplanteerde HSCs verraden hun aanwezigheid doordat ze in de ontvangende muis gedurende het hele leven alle bloedcellen kunnen maken. Alhoewel in volwassen muizen de HSCs met name in het beenmerg gevonden worden is dat niet hun oorspronkelijke plek van afkomst. In muizenembryo's worden HSCs voor het eerst waargenomen op dag 10.5 (E10.5) in de aorta van het Aorta-Gonad-Mesonephros (AGM) gebied. Daarna worden ze ook gevonden in andere hematopoietische organen van het embryo: de dooierzak, placenta en de lever. Net voor de geboorte van de muis verplaatsen HSCs zich naar het beenmerg.

Men weet nog steeds niet goed hoe de eerste HSCs gevormd worden, dit is een onderzoeksgebied dat zich – meer dan ooit – in het centrum van wetenschappelijke en klinische belangstelling bevindt. Ongeveer een eeuw geleden werd de hypothese geopperd dat HSCs afkomstig zijn van het bloedvatendotheel: dit endotheel zou dus "hemogene" eigenschappen bezitten. Groepjes bloedcellen, vastzittend aan het endotheel van de aorta (die Intra-Aortische Hematopoietische Clusters (afkorting in het Engels: IAHCs) worden genoemd), zijn inderdaad waargenomen in embryo's van verschillende vertebraten. Hun vorm en ligging deden vermoeden dat deze IAHC klonters zich van het endotheel aan het afscheiden zijn. Pas recentelijk hebben een aantal elegante experimenten echte ondersteuning gegeven aan de hypothese van een "hemogeen" endotheel. Hoe IAHCs precies ontstaan en de embryonale ligging van "hemogene" endotheliale cellen bleven echter onopgehelderde vragen. De meest directe manier om dit probleem aan te pakken is door in levende embryo's met een microscoop te kijken of men de overgang van een endotheliale naar een hematopoietische cel kan waarnemen. Omdat het muizenembryo ondoorzichtig is hebben we een methode ontwikkeld waarmee we levende, relatief dikke, transversaal gesneden plakken van de embryonale aorta konden bekijken (Hoofdstuk 2). We gebruikten een confocale microscoop om gedurende een aantal uren op bepaalde tijdstippen plaatjes te maken van fluorescente cellen. Het aorta endotheel was specifiek gemarkeerd met fluorescente antilichamen, die in de aorta waren geïnjecteerd voordat we opnames van de plakken maakten. Bovendien gebruikten we transgene Ly6A-GFP embryo's om fluorescente HSCs te onderscheiden en CD41YFP expressie om cellen te kunnen zien die zich gecommitteerd hadden aan differentiatie

in de hematopoietische richting. Met deze methode konden we het ontstaan van hematopoietische cellen in het aorta endotheel waarnemen en het bewegen van deze cellen naar, alsmede hun uitstulpen in, het lumen van de aorta op microscopische plaatjes in de tijd vastleggen (Hoofdstuk 3). Deze cellen maken Ly6A-GFP, c-kit en CD41, drie eiwitten die karakteristiek zijn voor hematopoietische stam en voorloper cellen (afkorting in het Engels: HSPCs). Hierdoor bewezen we, zoals ongeveer een eeuw geleden was geponeerd, dat het aorta endotheel inderdaad "hemogeen" is.

De expressie van αIIb (CD41) is, in volwassen muizen, een kenmerk van cellen die de bloedceldifferentiatie zullen doorlopen. We vroegen ons daarom af of deze integrine subeenheid ook gebruikt kon worden om gedurende de embryonale ontwikkeling HSCs uit bepaalde celpopulaties te verrijken. We vonden echter dat alleen de eerste HSCs (uit het AGM gebied) αIIb tot expressie brengen (Hoofdstuk 4). Bovendien vonden we dat de integrine sub-eenheid β3 (CD61), die normaliter met CD41 associeert, alsmede een andere integrine sub-eenheid, αv (CD51), gebruikt konden worden om HSCs te verrijken uit verschillende hematopoietische organen gedurende de embryonale ontwikkeling van de muis (Hoofdstuk 5). Daarnaast ontdekten we dat αIIb een belangrijke rol speelt in de ontwikkeling van de eerste HSCs in het AGM gebied. We vonden namelijk dat E11 AGM cellen van muizen die geen αIIb kunnen maken veel minder HSC activiteit hadden dan normale E11 AGM cellen. De HSC activiteit van αIIb-deficiënte cellen die we isoleerden uit de dooierzak was verassenderwijs normaal, terwijl de activiteit van αIIb-deficiënte cellen uit de foetale lever zelfs hoger was dan van normale cellen.

HSCs stammen af van het "hemogene" endotheel en de algemeen heersende opvatting is dat ze eerst in IAHCs gaan zitten. Inderdaad hebben wij, zoals hierboven beschreven, de totstandkoming van HSPCs uit het aorta endotheel middels confocale microscopie direct waargenomen. Nochtans verschillen HSCs en IAHCs behoorlijk, zowel in het tijdpunt waarin ze voor het eerst worden gevonden als in aantallen cellen die gedurende de embryonale ontwikkeling voorkomen. Wij konden aantonen dat IAHCs, die gezuiverd waren voordat er enige HSC activiteit waarneembaar is, bijna geen hematopoietische voorloper cellen bevatten, maar dat deze cellen wel in staat zijn om alle bloedceltypen te vormen in pasgeboren immunodeficiënte muizen; daarom hebben we deze cellen pre-HSCs genoemd (Hoofdstuk 6). We hebben deze cellen bovendien succesvol getransplanteerd uit immunodeficiënte donoren naar normale volwassen (secundaire) acceptoren en konden hierdoor laten zien dat de pre-HSCs die in IAHCs zitten *in vivo* in HSCs kunnen worden omgezet. We hebben ook de phenotypische rijping van IAHCs naar Ly6A-GFP$^+$ HSCs in het milieu van de aorta waargenomen.

Samenvattend komen we tot de conclusie dat het endotheel van de aorta gedurende een specifieke tijd in de embryonale ontwikkeling bloedcellen aanmaakt. Dit zijn stamcellen maar deze cellen moeten nog een aantal rijpingsstappen ondergaan voordat ze in staat zijn om in volwassen muizen in het mileu van het beenmerg aan te slaan. Tot slot hebben we nadrukkelijk een functie voor αIIb integrine beschreven gedurende de eerste periode van HSC ontwikkeling.

ABBREVIATIONS

7-AAD	7-Aminoactinomycine D
Ac	Acetylated
AGM	Aorta-Gonad-Mesonephros region
APC	Allophycocyanin
BABB	Benzylalcohol/Benzylbezoate
bFGF	Basic Fibroblast Growth Factor
BL-CFC	Blast Colony-Forming Cells
BM	Bone Marrow
BMP4	Bone morphogenic protein 4
BSA	Bovine Serum Albumine
CAR	CXCL12-Abundant Reticular cells
CD	Cluster of Differentiation
CFU-C	Colony forming unit in culture
CFU-E	Colony forming unit-erythrocyte
CFU-G	Colony forming unit-granulocyte
CFU-GEMM	Colony forming unit-granulocyte, erythrocyte, macrophage, megakaryocyte
CFU-GM	Colony forming unit-granulocyte, macrophage
CFU-M	Colony forming unit-macrophage
CFU-S	Colony forming unit in the spleen
c-Kit	Cellular Kit
DLP	Dorsal Lateral Plate
E	Embryonic day
ECM	Extra-cellular Matrix
ee	embryo equivalent
e.g.	example given
EGF	Epidermal Growth Factor
EHT	Endothelial to Hematopoietic Transition
EMP	Erythro-Myeloid Progenitor
ESC	Embryonic Stem Cells
FACS	Fluorescence-Activated Cell Sorting
FCS	Fetal Calf Serum
FL	Fetal Liver
Flk-1	Fetal liver kinase -1
GFP	Green Fluorescent Protein
Gr-1	Granulocyte antigen 1
HC	Hydrocortisone
Hh	Hedgehog
HSC	Hematopoietic Stem Cell
HSPC	Hematopoietic Stem and Progenitor Cell
IAHC	Intra-Aortic Hematopoietic Cluster
i.e.	id est “that is”
IL	Interleukin
IP	Intra-Peritoneal
iPS cells	induced Pluripotent Stem Cells
L	Lymphoid lineage
LDL	Low-Density Lipoprotein
Lin	Lineage markers
LN	Lymph Node
LSK	$Lin^{-}Sca\text{-}1^{+}c\text{-}Kit^{+}$
LT-HSC	Long-term HSC
Ly6A	Lymphocyte Antigen 6A
M	Myeloid lineage
Mac-1	Macrophage antigen-1
MHC	Major Histocompatibility Complex
NK	Natural Killer
NO	Nitric Oxyde
NOG	Nonobese diabetic/Severe Combined Immunodeficiency/IL-2R
PE	Phycoerythrin

PB	Peripheral Blood
PBS	Phoshate Buffered Saline
PCR	Polymerase Chain Reaction
PGC	Primordial Germ Cell
PHH3	Phospho histone H 3
PL	Placenta
PS	Penicillin Streptomycin
P-Sp	Para-aortic Splanchnopleure
RAG-2 γc	Recombination Activating Gene-interleukin-2 receptor subunit γ
RB	Retinoblastoma
Rho	Rhodamine 123
RT	Room Temperature
RT-PCR	Real-time polymerase chain reaction
Sca-1	Stem Cell antigen-1
SCF	Stem Cell Factor
SCL	Stem Cell Leukemia
SDF-1	Stromal cell-derived factor-1
SLAM	Signaling Lymphocyte Activation Molecule
s.p.	Somite pair
TGF α/β	Transforming Growth Factor α/β
TH	Thymus
TK	Thymidine Kinase
TPO	Thrombopoietin
Thy	Thy antigen
UA	Umbilical Artery
VA	Vitelline Artery
VBI	Ventral Blood Island
VCAM	Vascular Cell Adhesion Molecule
VE-cadherin	Vascular Endothelial Cadherin
VEGF	Vascular Endothelial Growth Factor
WT	Wild-type
YS	Yolk sac

CURRICULUM VITAE

Name: Jean-Charles BOISSET

Address: Bas Jungeriusstraat 40A1
3081VE, Rotterdam, NL
Tel: 00316 14653865

Date of birth: 27th Nov 1985

Nationality: French

EDUCATION

Present	PhD student Erasmus University Medical Center, Rotterdam, The Netherlands
2008	Master of Physiopathology. Paul Sabatier University, Toulouse, France
2006	"Licence" of Molecular biology and biochemistry (three years university degree), obtained with honors. Paul Sabatier University, Toulouse, France
2005	"DEUG" of Molecular biology and biochemistry (two years university degree), obtained with honors. Paul Sabatier University, Toulouse, France
2003	Science based "Baccalauréat". Bourdelle high school, Montauban, France

TRAINING

2008-2012	PhD student under supervision of Dr. Catherine Robin (Erasmus Stem Cell Institute, Department of Cell Biology, Erasmus University Medical Center, Rotterdam, The Netherlands) "Identification and characterization of hematopoietic stem cells during mouse embryonic development".
2007-2008 Oct-Jul	Internship under supervision of Dr. Anne-Catherine Prats (INSERM U858/I2MR, Toulouse, France). "MicroRNAs regulation of FGF-1"
2007 jun-aug	Internship under supervision of Dr. Mervin C. Yoder (Herman B Wells Center for Pediatric research, Indiana University School of Medicine, Indianapolis IN 46202, USA). "Compared observation of Aorta-Gonad-Mesonephros region – Hematopoietic Intra-Aortic Clusters & Sub-Aortic Patches – in wild type and NCX1 null mouse embryos".
2006-2007 Oct-Jan	Internship under supervision of Dr. Michel Simon (Université Paul Sabatier – CNRS, UMR5165, Toulouse, France). "Expression and immunolocalization of Plasma Membrane Ca2+ ATPase in normal human epidermis".
2006 jun-aug	Internship under supervision of Dr. Mervin C. Yoder (Herman B Wells Center for Pediatric research, Indiana University School of Medicine, Indianapolis IN 46202, USA). "Isolation and identification of endothelial colonies forming cells from porcine peripheral blood mononuclear cells".

PUBLICATIONS

Boisset, J.C., and Robin, C. (2012). On the origin of hematopoietic stem cells: Progress and controversy. Stem Cell Research 8, 1–13.

Boisset, J.C., Andrieu-Soler, C., van Cappellen, W., Clapes, T., and Robin, C. (2011). Ex vivo time-lapse confocal imaging of the mouse embryo aorta. Nature Protocols 6, 1792-1805.

Boisset, J.C., and Robin, C. (2011). Endothelial origin of hematopoietic stem cells: the proof in image. [Origine endothéliale des cellules souches hématopoïétiques: la preuve en image]. Médecine/sciences 27, 875-81.

Robin, C.*, Ottersbach, K.*, Boisset, J.C., Oziemlak, A., and Dzierzak, E. (2011). CD41 is developmentally regulated and differentially expressed on mouse hematopoietic stem cells. Blood 117, 5088-5091. *equal contribution.

Boisset, J.C., and Robin, C. (2010). Imaging the founder of adult hematopoiesis in the mouse embryo aorta. Cell Cycle 9, 2489-2490.

Boisset, J.C., van Cappellen, W., Andrieu-Soler, C., Galjart, N., Dzierzak, E., and Robin, C. (2010). In vivo imaging of haematopoietic cells emerging from the mouse aortic endothelium. Nature 464, 116-120.

ORAL PRESENTATIONS

2011	Stem cells in development and disease, Berlin, DE.
2010	ISSCR 8th annual meeting, Poster teaser presentation (2min), San Francisco, USA.

POSTER PRESENTATIONS

2012	ISEH 40th annual meeting, Amsterdam, NL
	ISSCR 10th annual meeting, Yokohama, Japan.
2011	Advances in stem cell research, EMBO meeting, Paris, FR.
2010	Stem cells in development and disease, Amsterdam, NL.
	ISEH 38th annual meeting, Melbourne, Australia.
	ISSCR 8th annual meeting, San Francisco, USA.
	Erasmus Stem Cell institute inauguration meeting, Rotterdam, NL.

MISCELLANEOUS

Supplementary movie 5 from the 2010 Nature article was exposed as part of two independent temporary art exhibition : « Beauty in science », 2011, Museum Boijmans van Beuningen, Rotterdam, NL, and « Rollercoster, pictures in the 21st century », 2012, Museum of the Image (MOTI), Breda, NL.

PhD PORTFOLIO

Name PhD student:	Jean-Charles BOISSET
Erasmus MC department	Cell Biology
Research school	Molecular Genetic Center
PhD period	Sept 2008 – Aug 2012
Promoter	Prof. Elaine Dzierzak
Co-promoter	Dr. Catherine Robin

PhD TRAINING	YEAR
Course	
In vivo Imaging: from molecule to organism	2008
Laboratory animal science (Art. 9)	2008
Development, Stem Cells and Disease	2009
Molecular and Cell Biology	2008-2009
Safety working in laboratory	2010
Radiation safety course (Level 5b)	2010
Literature training course	2011
Workshop	
MGC workshop Brugge, BE	2009
MGC workshop Maastricht, NL (oral presentation)	2011
Erasmus Stem Cell Institute retreat, Nijverdal, NL (oral presentation)	2011
National conferences	
MGC, Rotterdam	2008, 2009
Dutch Society for Stem Cell Research (DSSCR), Rotterdam	2009
Erasmus Stem Cell Institute Inaugural meeting (poster presentation)	2010
DSSCR, Utrecht	2010
Dutch Society for Developmental Biology (DSDB), Utrecht	2011, 2012
International conferences	
Stem cell congress UPMC, Paris, FR	2008
Stem Cell in Development and Diseases (SCDD), Amsterdam, NL	2008
International Society for Experimental Hematology (ISEH), Athens, GR	2009
SCDD, Amsterdam, NL	2009
International Society for Stem Cell Research (ISSCR), San Francisco, USA (oral for “Poster teaser” and poster presentation)	2010
ISEH, Melbourne, AU (poster presentation)	2010
Nederland Institute of Regenerative Medicine (NIRM), Amsterdam (poster presentation)	2010
Advance in stem cell research, Paris, FR (poster presentation)	2011
SCDD, Berlin, DE (oral presentation)	2011
ISSCR, Yokohama, JP (poster presentation)	2012
ISEH, Amsterdam, NL (poster presentation)	2012

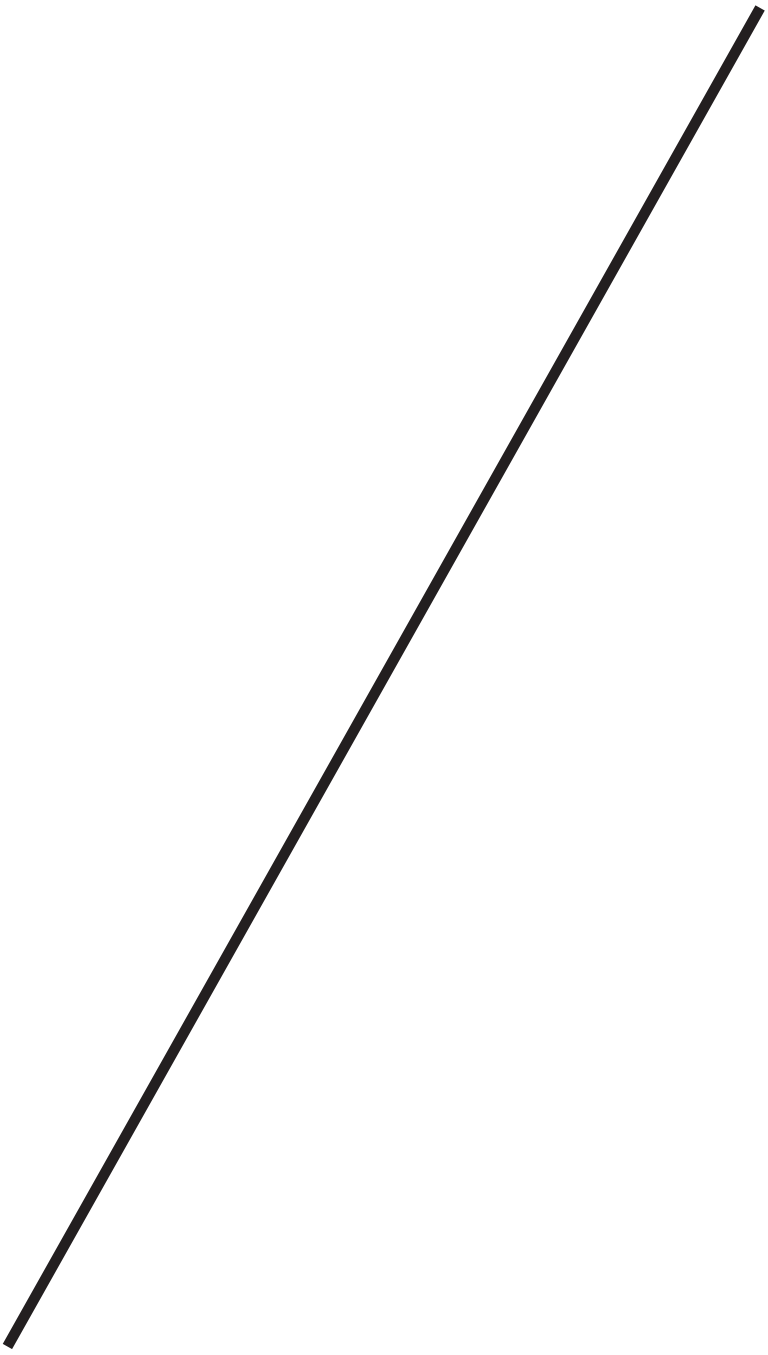

Acknowledgments

The acknowledgments part is the first thing I read when a thesis is handed out to me. Though I hope you reader will check the other chapters too...

Only my name appears on the cover page, but 4 years of work summed up in this thesis is certainly not the effort of one. Therefore I would like to thank some people.

Thank you Catherine for the exceptional and passionate mentorship you dispensed during the PhD period. The goal is achieved -> providing PhD student J-C BOISSET the tools for being a good scientist. I very much appreciated your open mind on the projects, the freedom of work and the trust I was given. I am aware this is quite exceptional to be working on the projects one could only dreams of. Besides, thank you for keeping the atmosphere friendly, yet serious. Perhaps your most awesome quality is your generosity, and is surely what I will remember in the long-term. But above all, I will certainly not forget the Nature story. I can still remember on my first interview day: the live embryo slices were coincidentally mounted in gel. I was inside like whoa, this is mad. You said "this will go to Cell", but 'yeah, right' that's usually to attract the naïve student. Time showed that optimism was not deceived; only after many hurdles though, which were also a good lesson...

Thank you Elaine for the positive answer you gave to my candidature. It was quite a privilege to work in the environment you provided, with such a background in developmental hematopoiesis. I learnt a lot during these 4 years, notably through giving me the opportunity to review some papers. I did really appreciate that trust.

Thank you Frank for being insightful during the occasional meetings, for your inspiring vision of science, for accepting to be part of the inner committee – and for keeping my bike from being stolen thank to your son's story (you probably don't remember that, but I do).

Thank you Niels for so not taking yourself seriously. You do have great jokes and a fine sense of humor. But that would be irrelevant without mentioning your contagious love of research, and your bold mac/apple attitude.

Thank you Thomas for being the funniest workmate ever. Be sure I do say that in a positive way. Thank you for your easiness, friendliness, boldness, and, ah... your Michael Jackson moves. Thanks for accepting to be the stylyest paranymph. True story.

Thank you Fanny for that too. *

It was cool to have you around, to chat about the nostalgic somehow common past, the present hurdles, and many other things during

* I hereby apologize for you and potential attendant at my thesis defense for having only southwestern French people as paranymphs.

these 4 years far from sunny home.
Thank you Anna for your kindness, your quick repartee and your cleverness leading to interesting discussions. Berlin calling.
Thank you Chloé for having the coolest hyperactivity disorder. E.g. for the reader to understand: you don't have time to figure out that your tip box is empty that she already filled it and autoclaved it, ready to use again...
I shall here thank all the people in the lab. Thank you to Polynikis (clown, strange/cool music and guide in Athens), Parisa (who kindly allowed me access to the hood), Parham (always relax), Chris (shared good taste for gastronomy and music: although still miss one → [illegible], Tomoko (O genki desu ka?), Mihaela (speaks French more than French), Emma (also likes some Michael Jackson moves) Gerben (pluk de dag tik een eitje), Alvin (Foin!), Reinier (there are no beads in the tube, could you make a new one?), Danielle (you're not made of sugar, you're not going to melt), Nesrin (likes to find new unused word in the English dictionary), Melodie (Could I borrow the connector?/appreciate the XX), Derek (postdoc tips/the clock is ticking), Mernaz (travel tips), Davide (I don't like the FC Bayern), Undine (Ach'so!), Tracy (iPS master), and the old team: Francesco, Yoko, Ester. I shall also thank people around the lab. Thank you Martine (buffers/tempers supervisor), Gert van Cappelen (knows microscope inside-out), Eric (j'avalise), Charlotte (là, il est excité...), Stephan (STOP IT Jean-Charles!) and Shane (sensible gentleman). Thank you to the ones that made impossible experiments possible: Tom and Natalie (puppies magic masters!), Jos and Mieke (Best photographs ever: I owe you the cover), Klazina and Nico (my ultrasound dreams came ah... true!) and John Kong a San (stiches/nothing can go wrong here). Thank you Thierry Jaffredo and Philippe Herbomel for coming all the way from Paris to chilly Rotterdam to participate in the defense of my thesis.
Thank you to the many people that provided ideas/ help/ encouragements, which I'm sure I injudiciously forgot here.
I am profoundly grateful to the Yoder's lab (even if the odds are low that they ever read this). Thank you Merv for giving me the opportunity to have my first lab experience ever. The fact that I am now writing a thesis on developmental hematopoiesis is in itself a testimony to your inspiring mentorship. The same applies to Momoko (you killed my RNA! Green tea cakes & many more) and Chris Lux (confocal teacher/Sufjan Stevens is kidish/mice sing ultrasonic love songs).
Finally, I cheerfully want to thank my friends and family, especially my parents for their continuous warm and affectionate support.

→ and Dorota (generous cookie provider)

Jaap! Thank you for that too...